TEXTILE RESEARCH JOURNAL

Publication of

TEXTILE RESEARCH INSTITUTE

VOLUME XXIX NOVEMBER 1959 NUMBER 11

Textile Research Center
School of Textiles
North Carolina State College

For Expanding Research Program . . .

Positions in basic and applied research in polymers and in textile materials, chemicals, and processes are open for qualified persons. Inquiries are especially solicited from men interested in participating in developing research and graduate-education programs leading to doctoral degrees in chemistry and physics. Location in developing North Carolina Research Triangle area offers excellent cultural and residential facilities and intellectual atmosphere for professional development. Present programs include studies in nuclear radiation effects and applications, and computer technology. New facilities will be occupied in the near future.

Specific needs exist for:

PHYSICAL CHEMIST OR CHEMICAL ENGINEER to participate in research on polymerization by radiation, including kinetics and mechanisms of reactions.

FABRIC DEVELOPMENT ENGINEER OR PHYSICIST to conduct research on mechanical properties of fabrics, and studies on preparatory processes.

HEAD, PHYSICAL TESTING SECTION, for supervision of physical testing laboratory and for exploratory research in physics of testing and development of test methods and instruments.

NUCLEAR PHYSICIST to participate in research on applications of nuclear radiation to textile materials and processes, with initial emphasis on activation-analysis techniques.

CHEMISTS OR PHYSICISTS with interest in fiber technology, physics, structure-performance relationships, X-ray and infra-red studies of polymer structure, and mechanical properties of fibers, yarns, or fabrics.

Ph.D's preferred, but applicants of any educational level considered. All replies treated in confidence. Send resume of education, experience, and publications to:

Director, Textile Research Center
School of Textiles
North Carolina State College
Raleigh, North Carolina

TEXTILE RESEARCH JOURNAL

VOL. XXIX *November 1959* NUMBER 11

Editor: **Richard K. Toner**

Production Editor: **Candida Frenking**

Advisory Board

Herbert J. Ball
Earl E. Berkley
John Boulton
C. H. Fisher
Walter J. Hamburger
Milton Harris
R. M. Hoffman
Harold P. Lundgren
Herman Mark
Edward R. Schwarz
George Switlyk
Helmut Zahn

TEXTILE RESEARCH JOURNAL, published monthly at Prince and Lemon Streets, Lancaster, Pa., is devoted to the interest of research in textile and allied industries. It is published by Textile Research Institute.

Manuscripts and communications should be sent to the Publications Department, P.O. Box 625, Princeton, N. J.

Second-class postage paid at Lancaster, Pa.

Subscription rates: $25.00 per year; additional for postage, 50 cents to Canada, $1.00 to all other countries. Single copies, $2.50 each.

Contents copyrighted © 1959 by Textile Research Institute Advertising rates supplied on request.

IN THIS ISSUE

The Effect of Certain Variables in Warp Sizing on Weavability. *Henry W. Saffer, Henry A. Rutherford, and David M. Cates* 849

A Measure of Cotton Fiber Development. *L. E. Hessler* ... 858

Influence of $Na_5P_3O_{10}$-$CaCl_2$-H_2O Phase Equilibrium on Laundering of Cotton Fabric. *W. J. Diamond and J. E. Grove* 863

A Rheological Interpretation of the Hottenroth Index Method for Viscose. *Shigeharu Onogi and Yoshiki Hayashi* 873

The Nature of Tenaciously Bound Soil on Cotton. *William C. Powe* 879

The Preparation and Properties of Partially Phosphonomethylated Cotton. *Stanley R. Hobart, George L. Drake, Jr., and John D. Guthrie* 884

Cord Stresses in Inflated Tires. *Herbert G. Lauterbach and William F. Ames* 890

Some Effects of Sheep Nutrition on the Mechanical Constants of Wool. *V. D. Burgmann* 901

Spectrophotometric Measurements of Color in Wool Fabrics. *F. G. Lennox* 906

A New Replica Technique for the Study of Fabrics and Other Surfaces. *W. Rhett Berry* 912

Reaction of Epoxides with Cotton Cellulose in the Presence of Sodium Hydroxide. *John B. McKelvey, Beverly G. Webre, and Elias Klein* 918

Stress Relaxation and the Transition Temperature of Wool. *B. J. Rigby* 926

REPRINT REQUESTS SHOULD BE DIRECTED TO THE AUTHORS
SEE ARTICLES FOR ADDRESSES

NOVEMBER 1959
VOL. XXIX NO. 11

TEXTILE RESEARCH JOURNAL

The Effect of Certain Variables in Warp Sizing on Weavability[1]

Henry W. Saffer,[2] Henry A. Rutherford, and David M. Cates

The Textile Research Center, North Carolina State College, Raleigh, North Carolina

Abstract

The effect of certain variables (size add-on, degree of polymerization of size, and temperature of application) in sizing was determined in relation to simulated weaving for a cotton yarn sized with poly(ethylene oxide).

Increasing the size add-on decreased the tendency of the sized yarns to shed fibers and size. The effect of resin DP varied with size add-on. At low add-ons an increase in DP was accompanied by an improvement in weavability which was attributed to the concomitant increase in toughness of the resin; after very high values of DP were reached, however, weaving became unsatisfactory, apparently because of poor anchoring of resin to yarn. At high add-ons an increase in resin DP resulted in improved weaving performance for all ranges of DP, and this effect was attributed both to the increase in toughness of the resin film and to the increase in film coverage of the yarn surface and in film thickness achieved at high add-ons. As the temperature of application was raised, penetration of size through yarn increased. This resulted in poor weavability at low DP's; at high DP's, however, weavability was improved, apparently because the increase in temperature permitted better anchoring of size to yarn.

Introduction

The object of the present work was to isolate and relate the effect of certain variables in the sizing of cotton, i.e., size add-on, degree of polymerization of the size (DP), and temperature of application, to weaving performance. It was desirable to select a system in which the effect of these variables could be isolated and easily measured. Evaluation of the usual starch formulations is difficult because these mixtures contain additives that complicate the interpretation. To avoid this complication, poly(ethylene oxide)[3] (PEO), an experimental, water-soluble resin, was selected as the sizing agent because it can be applied as a one-component size.

The best method of evaluating the effect of a particular variable in the warp sizing treatment is to carry out large-scale loom tests, but this is time-consuming and costly. Much effort has been made to find a more expedient laboratory method. One

[1] Taken in part from a thesis submitted by H. W. Saffer to the Department of Textile Chemistry, School of Textiles, North Carolina State College, in partial fulfillment of the requirements for the degree of Master of Science in Textile Chemistry. This work was done under a fellowship sponsored by Union Carbide Chemicals Company.

[2] Present address: Textile Research Institute, Princeton, New Jersey.

[3] Available as "Polyox" (a trademark of Union Carbide Chemicals Company).

approach has been to make use of miniature looms that simulate the essential motions of a loom [3, 4, 5]. In this work the warp shed tester [1, 5] was used. The shed tester is simpler to operate than the loom and has fewer adjustments.

The shed, defined as the mass of fibers and size abraded from the yarn during weaving, was the dependent variable in the experiments and was taken as a convenient measure of weavability. Shed is produced in the weaving process by the abrasion of yarn against yarn and yarn against metal. It poses a housekeeping problem in the mill and may also cause yarn ruptures if a sufficient number of fibers are rubbed off the yarn. Often these short fibers collect on the yarn in the form of small, tangled aggregates that become lodged in the metal parts of the loom and cause end breakage. Finally, they may wrap around adjacent yarns and reduce the opening of the shed. This places excess tension on the yarns and may cause them to break.

A section of the paper is devoted to size distribution and "fiber lay." Fiber lay refers to the ability of the size to cement surface fuzz fibers to the compact main body of the yarn. Both size distribution and fiber lay have an obvious effect on shed and are believed to be important determinants of weavability.

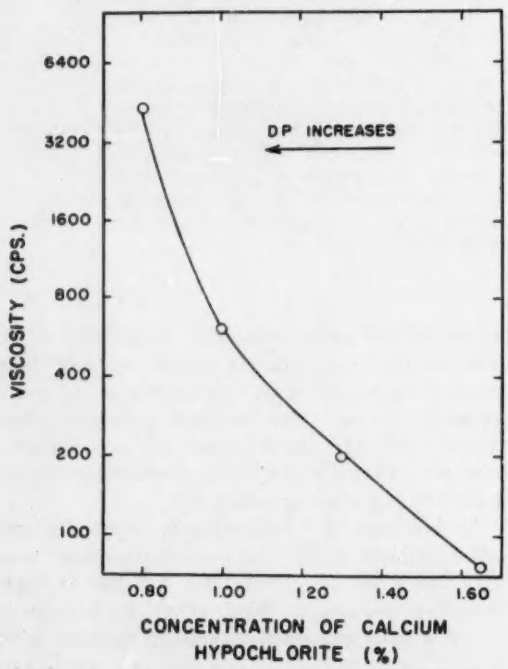

Fig. 1. Effect of concentration of calcium hypochlorite on viscosity of 4% PEO solution measured at 25° C.

Experimental

Materials

A carded 30/1 cotton yarn with a 4.3 twist multiplier was sized with PEO. The viscosity of a 1% solution of the original PEO was 3,100 cps. measured on a Brookfield Viscometer operating at 2 r.p.m. and 25° C. In order to obtain solutions of suitable viscosities for warp sizing, the molecular weight was reduced by calcium hypochlorite oxidation, following the procedure given later.

The effect of calcium hypochlorite on the viscosity of PEO solution is shown in Figure 1, where the concentration of oxidizing agent refers to percent of hypochlorite on the weight of the resin. Calcium hypochlorite attacks the PEO molecule by an oxidation mechanism, presumably at the ether linkage, which is the most labile position in the polymer [2].

The viscosity of PEO in solution can also be varied by diluting and by raising the temperature, as shown in Figures 2 and 3.

Methods

Mixing. Solutions were mixed at room temperature by dispersing the calcium hypochlorite in water and stirring for approximately 5 min. with a variable-speed mixer. The size was then sprinkled into the dispersion to the desired concentration and the whole solution was mixed 1–2 hr. and allowed to stand overnight. Slow addition of PEO was necessary to prevent the formation of aggregates which are very difficult to dissolve. The viscosities of the solutions were measured with a Brookfield Viscometer operating at 30 r.p.m. using the appropriate spindle.

Sizing. Ends of 30/1 cotton (100) were slashed on the Callaway Sample Slasher (open model) for each experimental run. The yarns were dipped in the size box and squeezed between a rubber roll and a stainless steel roll. Size was applied at room temperature (near 25° C.) except in the case of the temperature-of-application studies. The load on the rolls was held constant at 200 lb. (100 lb. hanging vertically from each side). The sized warp was dried on a series of four drying cans thermostatically controlled at 93° C. and then split by two lease rods and collected on a small beam. The length of each warp was 40 yd. and the speed of the slasher was 7–9 yd./min.

Weaving. The sized warps were drawn in on a modified Southern Research Institute Warp Shed Tester [5]. Essentially this device simulates the action of drop wires, harnesses, and reed on the loom. A schematic diagram of the modified instrument is shown in Figure 4. Yarn on beam (A) was drawn through drop wires (B) and then through two sets of double-bar harnesses (C). The cams (F) that control the harnesses were arranged to simulate a plain weave on a loom. The yarn, after leaving the harnesses, was drawn through a 30-dent reed at 3 ends/dent to give a sley of 90 ends/in. Although no filling was present, the beat up by the reed (D) was comparable to inserting 170 picks/min. The take-up roll (E) operated at 5 yd./hr. and the test was run for 4 hr. Tension was applied to the yarn by means of weights suspended from a pulley and attached to the let-off roll. The shed tester was operated in a room controlled at 75° F. and about 75% relative humidity. Occasional measurements indicated that relative humidity ranged as high as 80% and as low as 70%.

Desizing. Three grams of each sized sample before being shed tested were desized in the following manner. Duplicate yarn samples were dried in weighing bottles overnight in an oven at 85–90° C. This low temperature was used to avoid discoloration of wet cotton. The samples were cooled to room temperature in a desiccator and weighed on an analytical balance. The water-soluble resin was removed by treating the sample in 250 ml. of water for 30 min. at room temperature and then rinsing in running water for 5 min. The squeezed, desized sample was dried overnight at 85–90° C., cooled in a desiccator, and weighed. An unsized cotton control was run along with the yarn as a correction for water-soluble impurities in the yarn and for relative humidity and temperature differences that occurred between weighings. Size add-on was calculated on the weight of the desized yarn.

The shed was separated into water-soluble and fibrous components by extracting it by the same procedure used for sized yarn. Following the water extraction, the suspension was filtered through a sintered glass filter; the retained fibers were rinsed and dried. The control used was approximately 0.5 g. of cotton shed collected when a sample of unsized yarn was tested on the shed tester.

Staining techniques. All solutions were tinted

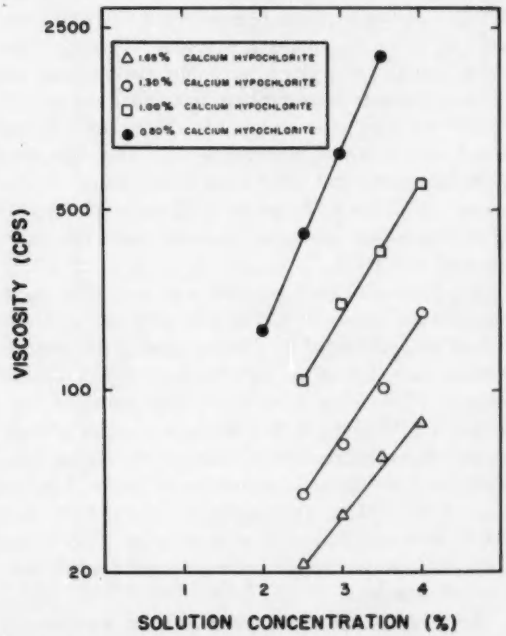

Fig. 2. Effect of PEO concentration on viscosity measured at 25° C.

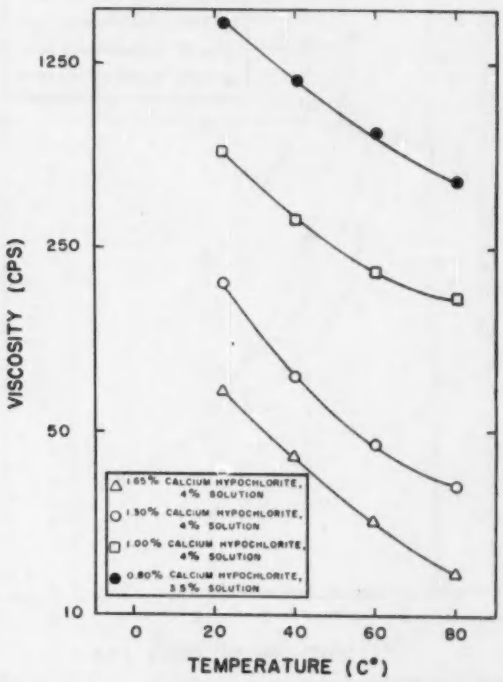

Fig. 3. Effect of temperature on viscosity of PEO solutions.

with 1% (on the weight of the resin) of Calcocid Rhodamine B, a fluorescent acid dye (CI 45100). Preliminary tests showed that the dye distributed itself evenly through a PEO film cast from a resin-dye-water system.

Film casting and testing. Films were cast on a glass plate from PEO solutions similar to those used for the sizing operation. The thickness was controlled by running a spatula mounted on brass templates over the glass which had been coated with sizing solution to give a dry film depth of 0.9–1.2 mils. The dried films were removed from the glass by hand and heated in an oven at 90° C. for 1 min. to remove imperfections in the films.

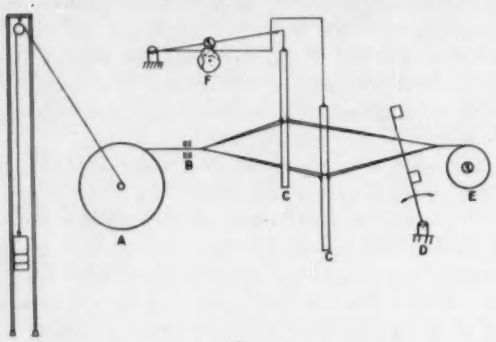

Fig. 4. Schematic diagram of warp shed tester.

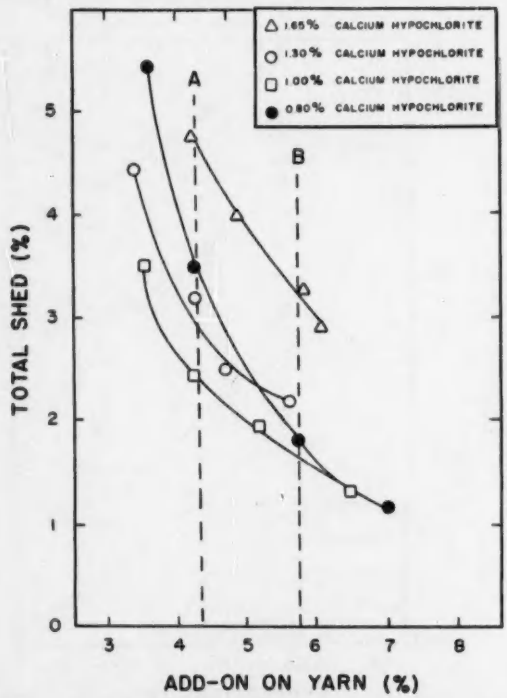

Fig. 5. Effect of add-on on total shed; temperature of application, 25° C.

The initial modulus, maximum strength, and elongation and energy to break at beginning of rupture were calculated from measurements made on 4 × 1 in. strips with an Instron tester using 0.5 in./min. crosshead speed and 1 in. gauge length. The calculations for modulus, strength, and energy to break were corrected for thickness differences between films by dividing the calculated value by the average film depth.

All films were cast and tested at 70° F. and 65% relative humidity.

Results and Discussion

Four solutions of PEO resin were prepared with 1.65%, 1.30%, 1.00% and 0.80% calcium hypochlorite, respectively, on the weight of the resin. The mixture containing the greatest amount of hypochlorite represented the resin with the lowest DP. The concentration of each solution was 4% PEO by weight, except in the case of the one containing 0.80% calcium hypochlorite, where 3.5% PEO was used in order to obtain a practical viscosity. Because actual DP values were not determined, the percent calcium hypochlorite was taken as a convenient measure of this property. Each solution was tinted with Calcocid Rhodamine B. The viscosities of the solutions that were used in the sizing experiments varied from 75 cps. to 1912 cps. The higher figure represents an upper viscosity limit for slashing with PEO [2].

One portion of each solution was applied at room temperature (near 25° C.) at four different add-ons; add-on was controlled by diluting part of the original portion (see *Effect of Add-On* and *Effect of DP* below). The other portions of the solutions containing 1.30% and 1.00% calcium hypochlorite were applied from the slasher at successively higher temperatures (see *Effect of Temperature* below); in the case of the DP's represented by the 1.65% and 0.80% solutions, however, new solutions (4.0% and 3.5% PEO respectively) were prepared for the temperature studies.

The sized warps were tested on the shed tester, and the shed was collected, weighed, and analyzed. Longitudinal mounts of the sized samples before

shed testing were inspected under the microscope to observe fiber lay. In addition, cross sections of the yarn were observed to determine the extent of penetration by the size into the yarn.

The shed-tester results are shown in Figures 5–7.

Effect of Add-On

The discussion here is limited to the relationship, at a constant DP of resin, between size add-on on yarn and total shed, PEO shed, and add-on shed. This relationship is shown by any single curve in Figures 5, 6, and 7, respectively. Size was applied at room temperature, and add-on was controlled by diluting the original solution. The following terms, expressed in percent on an oven-dry basis, are used.

Size add-on on yarn = (wt. PEO/wt. desized yarn) × 100

Total shed = (wt. of shed/wt. tested yarn) × 100

PEO shed = (wt. PEO in shed/wt. tested yarn) × 100

Size add-on on shed = (wt. PEO in shed/wt. desized shed) × 100

As the amount of resin (at constant DP) applied to yarn is increased, the total shed (Figure 5) and PEO shed (Figure 6) decrease, while the relative amount of PEO in the shed (Figure 7) increases.

In general, when the concentration of a sizing solution is raised to obtain higher add-ons, penetration of the size into the yarn may be expected to decrease as a result of higher solution viscosities. Where penetration is not extensive, add-on may also affect the continuity and thickness of the film of size on the yarn surface, and these properties in turn are important in their effect on fiber lay.

Microscopic examination indicated that the penetration of PEO resins applied at room temperature in the present range of add-ons was limited to the outer fibers of the yarn bundle. In the case of the two higher molecular weight resins, fiber lay improved markedly with increasing add-on. Although differences in hairiness of yarn were difficult to distinguish at add-ons close to one another, the differences at the extremes were obvious. Cross sections of the tinted yarn revealed that as add-on was in-

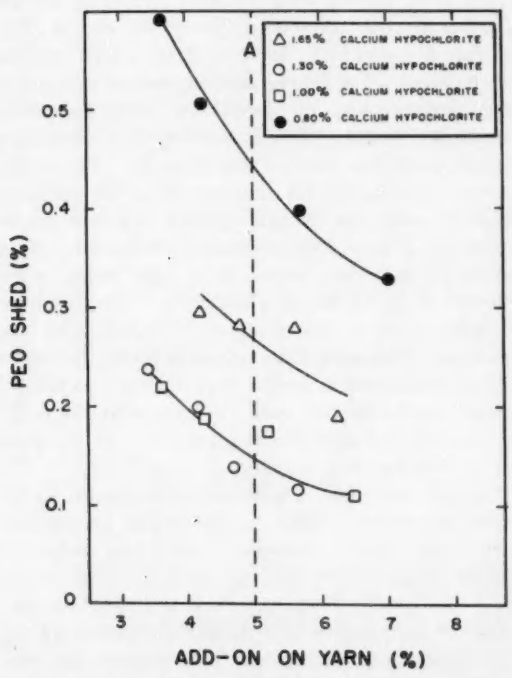

Fig. 6. Effect of add-on on PEO shed; temperature of application, 25° C.

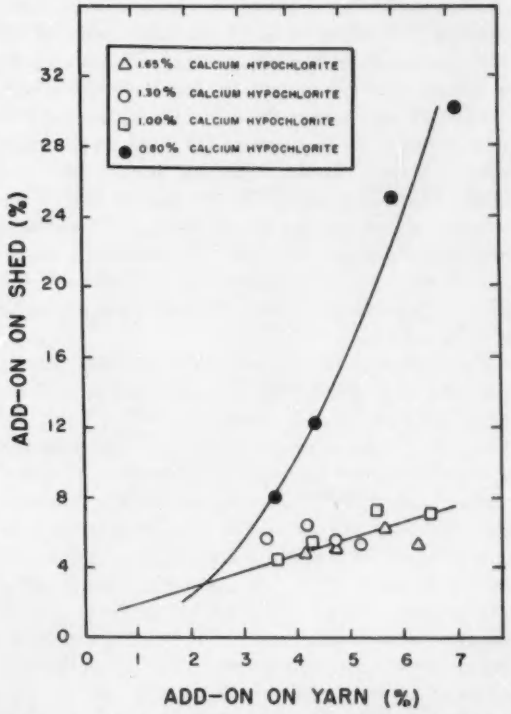

Fig. 7. Effect of add-on on yarn on add-on on shed; temperature of application, 25° C.

TABLE I. Film Properties of PEO

Calcium hypochlorite, %	Thickness, mils	Initial modulus, g./cm. mil	Maximum strength, g./mil	Elongation, %	Energy to break, g. cm./mil
1.65	1.28	430	415	16.7	7.21
1.30	1.05	476	354	38.8	15.80
1.00	0.98	449	388	64.5	30.40
0.80	1.24	426	378	95.5	41.40

creased, the thickness of the band of size around each individual yarn increased, affording more protection to the yarn. Presumably the transition from high shed values at low add-ons to low shed values at high add-ons shown in Figures 5 and 6 is related to the continuity and thickness of this band of size.

It is clear from Figure 6 that PEO resin adheres strongly to cellulose. Although size add-ons range from 3.5% to 7%, the amount of size abraded from the yarn is only of the order of a few tenths of a percent.

Effect of DP

Film properties. Tensile properties were measured on PEO films in which the same range of DP was covered as in the sizing work. The films prior to testing were translucent, the low-molecular-weight resins forming cloudier films than the high-molecular-weight resins. The range of DP used was comparable to passing from a relatively brittle solid to a tough, flexible material. This is evident from Table I, which shows that energy to break, i.e., toughness, increases markedly with DP. Toughness is important on the warp shed tester and loom, where resistance to flex, abrasion, and shock is brought under test.

Penetration of size. The degree of penetration by size into yarn is dependent on the viscosity of the sizing solution, and therefore on DP. Thus, for solutions of equal concentration, a change from low to high DP would be expected to produce a relative change from high to low penetration. The inference from the data, however, is that the change in penetration is appreciable only in the region of high DP values, represented in this work by the material treated with 0.80% hypochlorite. Microscopic observation showed that none of the resins had penetrated into the core of the yarn. The high-DP resin appeared to be located chiefly on top of the protruding fuzz fibers, however, rather than on the main body of the yarn, whereas with the other materials of lower DP, relatively more of the resin was observed to have penetrated to the main body of the yarn. The results pictured in Figure 6, in which PEO shed is presented as a function of yarn-add-on, show that the highest DP material is shed more readily at all add-ons than any of the other materials. Finally, the behavior of the resin of high DP with respect to the add-on on shed is very different from that of the other materials, as shown by Figure 7; the ratio of add-on on shed to add-on on yarn is greater and increases at a faster rate than is the case with the other resins. These qualitative observations have led to the opinion that the high DP resin is poorly "anchored" to the yarn.

Weaving results. The effect on weavability of the molecular weight of resin is shown in Figures 8A and 8B, which relate the DP of the resin (in terms of percent calcium hypochlorite) to total shed at constant add-on. The curves correspond to the add-ons indicated by lines A and B of Figure 5. In general, Figure 8A is meant to represent low add-ons, to the left of line A in Figure 5, and Figure 8B to represent high add-ons, to the right of line B in Figure 5.

At low add-ons (Figure 8A), where a discontinuous or thin, continuous film of size on the yarn surface is assumed to be favored, the curve exhibits a minimum. The falling portion denotes a progressive improvement in weavability with increasing molecular weight. This is attributed to increasing toughness of the resins (see Table I). The rising portion of Figure 8A indicates that the resin of highest molecular weight (0.80% calcium hypochlorite) affords less protection to the yarn than some of the lower-molecular-weight resins, even though it forms the toughest film. This behavior is believed to be related to the distribution of size on yarn. Following the discussion above, the highest molecular weight resin apparently was "anchored" much less firmly than was the case with the other resins and was more easily removed from the yarn surface during shed testing.

At high add-ons (Figure 8B), the picture is altered somewhat. There is the initial progressive reduction in shed with resins of increasing molecular weight, as in Figure 8A, but then the shed essentially levels off. Thus, the increase in surface coverage of yarn and in film thickness achieved by the size at high add-ons appears to overcome the poor anchoring ability that has been attributed to the high-molecular-weight resin.

We applied the same reasoning to Figure 9 (corresponding to add-on indicated by line A in Figure 6); yarn sized with the lowest DP resin sheds PEO more readily than yarn sized with the two intermediate molecular weights, because of the brittle nature of the resin, but less readily than yarn sized with the highest DP resin, because the latter resin is less firmly anchored.

Microscopic observations. The two highest molecular weight resins pasted nearly all the fuzz fibers to the main body of the yarn at the high add-ons. On the other hand, yarns sized with the two lowest molecular weight materials were characterized by many fuzzy areas where small fibers projected from the main body of the yarn, even at high add-ons. At low add-ons all samples were rather hairy, regardless of DP, and no distinct differences were apparent.

The resin of highest molecular weight at low add-ons was distributed unevenly along the yarn, and occasionally lumps of resin were discernible on the fuzz fibers; at high add-ons a continuous sheath of size appeared to coat the yarn. By comparison, the low-molecular-weight resin seemed to be more uniformly distributed along the yarn surface at all add-ons, and there was resin located on the main body of the yarn.

Cross sections of the tinted yarns viewed under the microscope permitted the determination of size location. In all cases a continuous band of size was observed around each individual yarn. As the size add-on increased at constant DP or as DP increased

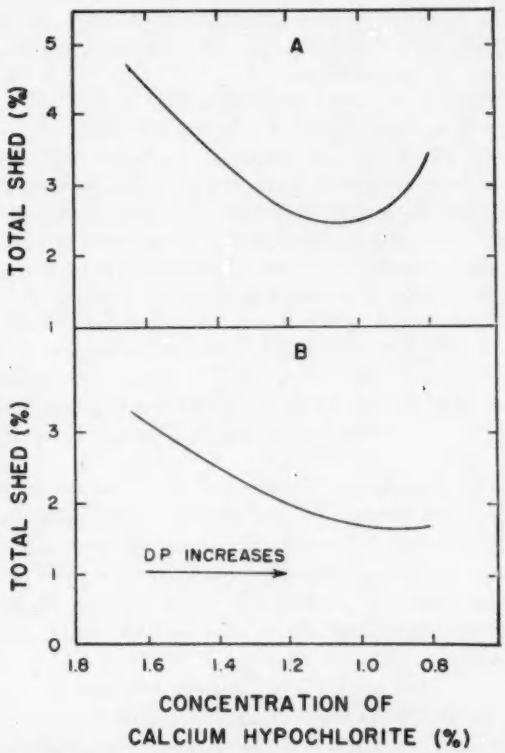

Fig. 8. A, effect of DP on total shed at low add-on; B, effect of DP on total shed at high add-on.

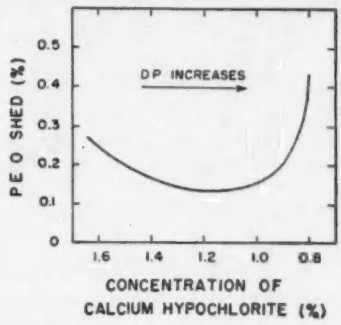

Fig. 9. Effect of DP on PEO shed at any add-on.

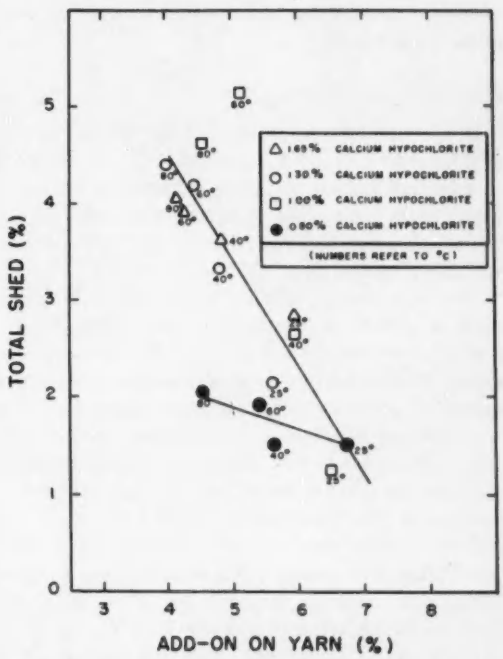

Fig. 10. Effect of add-on on total shed for different molecular weights and temperatures of application.

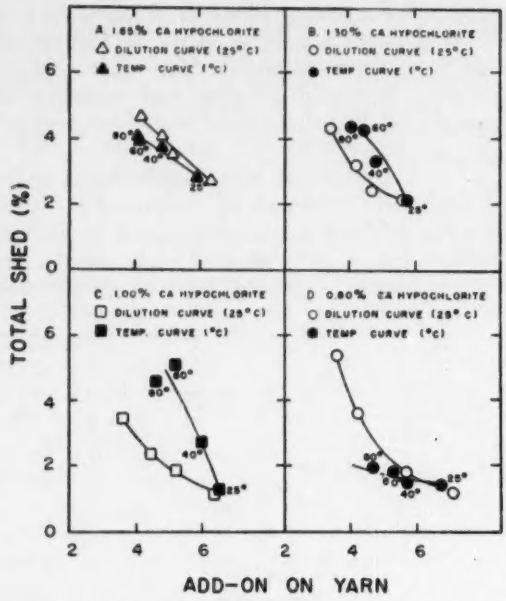

Fig. 11. Dilution effects compared with temperature effects.

at constant add-on, the thickness of the band increased. Penetration was limited to the periphery of the yarn bundle.

Effect of Temperature

PEO solutions were applied to cotton yarn at 25° C., 40° C., 60° C., and 80° C. Increases in temperature caused decreases in solution viscosities which were responsible for lower add-ons. A similar relationship between size uptake and viscosity was also observed by Zilahi and Kelen [6].

The relationship between yarn add-on and total shed is shown in Figure 10. Although the DP studies demonstrated the effect of DP on total shed among the three lower molecular weight resins when applied at room temperature, these differences were not observed at elevated temperatures. The probable explanation is that increasing the temperature increases the penetration of size through yarn. Differences in film properties probably are much less important when there is extensive size penetration rather than size coating. Figure 10 shows that the highest DP material produces better weaving performance at higher temperatures than the materials of lower DP. Evidently such penetration as is achieved is particularly effective with the high-molecular-weight resin and results in improved anchoring of the size to the yarn. This effect is discussed in greater detail below.

A comparison of dilution effects and temperature effects with respect to total shed and size uptake at each DP is given in Figures 11A–D. The temperature curve for the lowest DP material falls below the dilution curve (Figure 11A), indicating that better weavability is obtained when size uptake is controlled by elevating the temperature than by dilution methods. This is contrary to what might be expected for low-molecular-weight materials. The point of view adopted here presumes that the size improves weavability by altering the surface of the yarn and that size on the outside affords more protection to the yarn than that located in the core of the yarn. In any case the lowest DP material appears to be unsuitable as a size because of its poor mechanical properties.

For the two intermediate values of DP (Figures 11B and C) the temperature curves fall above the dilution curves. This is consistent with the belief expressed above that increasing the temperature increases penetration of size into the yarn, resulting in poor weavability.

For the highest molecular weight resin, the temperature curve lies slightly below the dilution curve (Figure 11D). A previous conclusion was that much of the high DP material is located on the outside of the surface fuzz fibers. Increasing the temperature permits the resin to position itself to a greater extent on the main body of the yarn, resulting in better anchoring and improved weaving.

Microscopic observations of longitudinal mounts showed better fiber lay at the low temperatures of application than at the high. It is not known whether this was caused by differences in penetration or by differences in size uptake, although both may be contributing factors.

Cross sections of the sized yarn gave some indication that penetration was increased by raising the temperature. Because the ultraviolet light source was not bright enough, or the cross sections not thick enough, to adequately show up color in the areas between the fibers composing the yarn, this observation is not unequivocal.

No relationships were apparent between size uptake and PEO shed or add-on on shed, probably because penetration of size through yarn obscured any differences.

Summary

Increasing the add-on of resin (at constant DP and temperature of application) decreases the tendency of the sized yarn to shed fibers, although the relative amount of size in the shed increases. The shed is composed mostly of cotton fibers regardless of yarn add-on, DP of resin, or temperature of application.

Increasing the DP of the resin (at constant yarn add-on and temperature of application) up to a certain molecular weight is accompanied by an improvement in weavability, apparently as a result of the improvement in mechanical properties of PEO. After high DP values are reached, however, weaving becomes less satisfactory, presumably because the resin is poorly anchored to the yarn, thus negating the excellent film properties. The condition of poor anchoring appears to be more serious in the range of low add-ons than in the range of high add-ons. The explanation was advanced that the increase in surface coverage of yarn and in film thickness achieved at high add-ons counteracts the poor anchoring ability that was attributed to high molecular weight resins.

Increase in temperature of application (at constant add-on and DP) increases the penetration of size through the yarn. In the range of low values of DP, increase in temperature of application results in poorer weavability, apparently because relatively more of the resin is distributed through the body of the yarn rather than on the yarn surface. In the range of high values of DP, increase in temperature of application results in better weavability because of better anchoring of size to yarn.

Although the present results are reported specifically for PEO resin, there appears to be no reason why they may not also be generally applicable to other synthetic sizes; this conclusion must of course await experimental confirmation.

Literature Cited

1. Abrams, E., Rougeux, C. W., and Coker, J. N., TEXTILE RESEARCH JOURNAL **26**, 875 (1956).
2. Martin, W. R. and Bailey, F. E., Union Carbide Chemicals Co., private communication.
3. Radhakrishnan, T., Mehta, P. C., and Shelat, B. R., TEXTILE RESEARCH JOURNAL **27**, 439 (1957).
4. Ramierez, R. P. and Vidosic, J. P., *Textile World* **106**, 104 (1956).
5. Southern Research Institute, U. S. Patent No. 2,556,012.
6. Zilahi, M. and Kelen, I., *Acta Tech. Acad. Sci. Hung.* **18**, 37 (1957).

Manuscript received April 3, 1959.

A Measure of Cotton Fiber Development

L. E. Hessler

Textile Research Laboratories, Texas Technological College, Lubbock, Texas

CUT swollen cotton fibers have been used to study mercerization and fiber damage in European countries for a number of years. In studying mercerizing, Willows and Alexander [7] noticed cut fibers showed a pronounced "dumbbell" shaped extrusion. Later, Markert [6] made extensive use of the technique in determining chemical damage in fabrics. Chemically damaged cotton which had been cut and swollen did not form the typical "dumbbell" pattern because the retaining cuticle no longer prevented swelling. Hummelreich [4] studied bleach damage in rayon–cotton mixtures with little success, since synthetics do not have the retaining surface, consequently on swelling show no protrusion. Herzog [3] used the method to determine HCl damage on fibers of different degrees of maturity. Koch [5] made an extensive cotton fiber study of the method for both biologically and chemically damaged cotton fiber.

The work reported here was undertaken to determine to what extent the cut fiber method can be used to evaluate cotton fiber development and utility.

Materials and Methods

Cotton samples used were of known boll age of development or with Micronaire readings to show development characteristics. The boll samples were 21, 28, and 35 days from blooming date and from the same field experiment. The Micronaire samples range was 3.0, 4.0, and 5.0 in Micronaire units. Two varieties of cotton, one determinant (fast developing) and the other indeterminant (slow developing) were used to study cotton fiber development by the cut swollen fiber method. The sample received no pretreatment prior to sectioning, other than a cold solution red dye to add contrast to the photographs. Boiling in solutions softened the cuticle and affected ballooning of the cut fibers.

The fibers were prepared for sectioning by combing; a tuft of the fiber was placed at midsection in a Mico Cross Section Device. In sectioning the fiber no imbedding material was used. Adjustments were made after the first cut to give fibers around 50 μ in length. The cut fibers were placed on a micro slide in a clump and a drop of 15% NaOH was incorporated into the sample. A cover glass was placed on the sample. After a few minutes the results are ready for viewing in a microscope.

Photographs can be taken with any number of photomicrography instruments available. The present work was photographed with a regular microscope and Silge and Kuhne Orthophot equipment, using Kodak Pan X high contrast film.

The areolometer was used to determine the dimensional properties in Table I [1]. The determination of cellulose and crystallinity has been previously described [2].

Results

The cut swollen fibers in Figure 1 show, reading clockwise from the fiber tip, a graduation of development as measured from swelling and ballooning from highly underdeveloped to fully developed cotton. The configurations in this figure may be

Fig. 1. Cut and swollen cotton fibers showing degree of development from fiber tip in clockwise direction.

used to judge the degree of development in subsequent photographs. The 21-day-old bolls from the indeterminant type are largely primary wall fibers which show no ballooning or even a slight protrusion at the ends to indicate wall thickening (Figure 2A). The lumen is not very pronounced in the photograph, indicating a thin wall and a large underdeveloped central cavity. A week older fiber (28 days) shows lumen and the start of protrusion at the ends of some fibers (Figure 2B). Swelling has begun to close the lumen of some fibers, but not enough to balloon the fibers. The 35-day-old bolls from the same type show considerable wall thickening with very little visible lumen and various amounts of ballooning by about a third of the fibers (Figure 2C). Other fibers are showing the beginning of ballooning. In about 50 days most of the 35-day-old fibers would be fully developed.

Micronaired fibers of 3.0, 4.0, and 5.0 units are shown for the indeterminant cotton (Figure 3). Micronaire sample 3.0 (Figure 3A) shows very little ballooning or "dumbbell" forms. The lumen is visible in a large percentage of the fibers. By the cut swollen fiber method this would have to be considered a highly underdeveloped fiber or perhaps the equivalent of a slightly more than 35-day-old boll (Figure 2C). The cotton with a Micronaire of 4.0 shows further development with more dumbbell

TABLE I. Chemical and Physical Properties of Two Types of Cotton with Different Degrees of Development

Cotton type	Age of bolls, days	Cellulose, %	Crystallinity, %	Fiber fineness		Perimeter, μ	Wall thickness, μ	Diameter, μ	Maturity, %		Immaturity ratio	Shape factor
				Micronaire	Areolometer				NaOH	Areolometer		
Indeterminant	21	77.4	66.8	−2.4	—*	—	—	—	10	—	—	—
	28	85.0	70.0	−2.4	—	—	—	—	24	—	—	—
	35	92.6	72.1	2.9	2.6	63	2.0	19.9	57	46	2.75	94
	Open	91.2	83.1	3.0	2.8	60	2.0	19.1	40	48	2.69	89
	Open	92.7	86.3	4.0	3.9	53	2.7	16.8	59	76	1.88	40
	Open	95.2	89.1	5.0	4.8	40	3.3	12.3	80	97	1.31	10
Determinant	21	86.9	65.6	−2.4	—	—	—	—	23	—	—	—
	28	92.3	72.4	2.9	2.4	60	1.8	19.1	42	40	2.94	109
	35	94.6	73.2	3.5	2.8	64	2.1	22.2	67	49	2.67	88
	Open	93.4	84.5	3.0	3.0	53	2.2	17.0	41	64	2.22	63
	Open	94.6	87.1	4.0	4.2	44	2.8	14.1	64	86	1.59	22
	Open	95.1	91.0	5.0	4.7	48	3.1	15.3	84	87	1.55	20

−2.4 indicates below scale.

* Blank spaces were out of range of the areolometer.

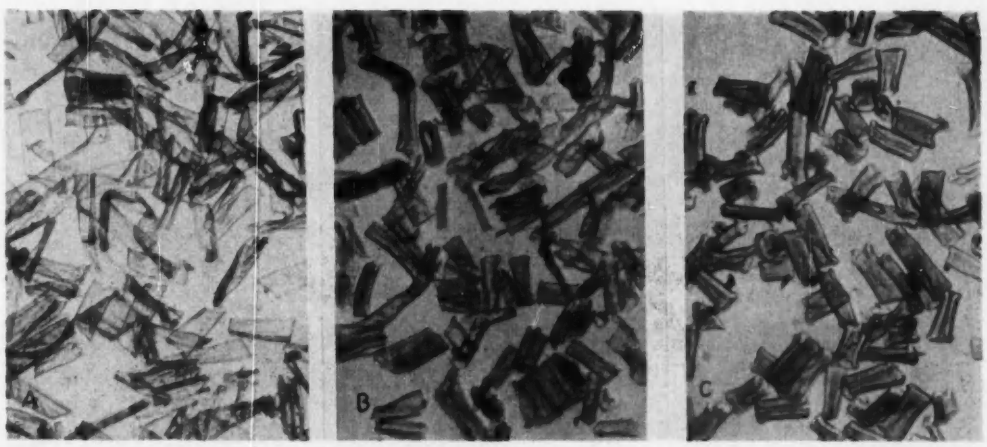

Fig. 2. Cut and swollen cotton fibers from: (A) 21-day, (B) 28-day, and (C) 35-day-old cotton bolls, indeterminant type.

forms and less visible lumen (Figure 3B). The last sample (Figure 3C), with a Micronaire reading of 5.0, shows increased fiber development as measured by fewer visible lumens and more dumbbell forms with increased development.

The cut swollen fibers for the determinant type of cotton show more development for the cotton from bolls of known age (Figures 4A, B, and C). Because of its faster growth, this cotton is perhaps a week further advanced in fiber development. The samples of known Micronaire fineness for the determinant type show nearly the same degree of dumbbell formation for each Micronaire reading that was shown by the indeterminant cotton (Figures 5A, B, and C).

The data in Table I for a determinant and indeterminant type cotton of various boll ages and Micronaire finenesses correspond to the photographs of cut swollen fibers in Figures 2, 3, 4, and 5. Chemically, increasing cellulose and crystallinity characterize the fibers as to development. The physical properties such as fiber fineness, maturity, immaturity ratio, shape factor, and wall thickness are visually seen in the photographs. The low Micronaire values with very little swelling and thin walls show no dumbbell formation. Increasing de-

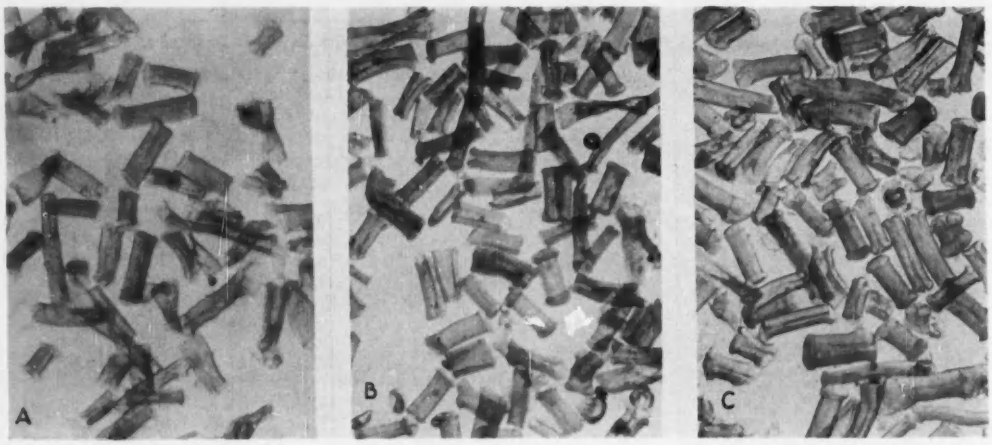

Fig. 3. Cut and swollen cotton fibers from sample of (A) Micronaire 3.0, (B) Micronaire 4.0, and (C) Micronaire 5.0, indeterminant type.

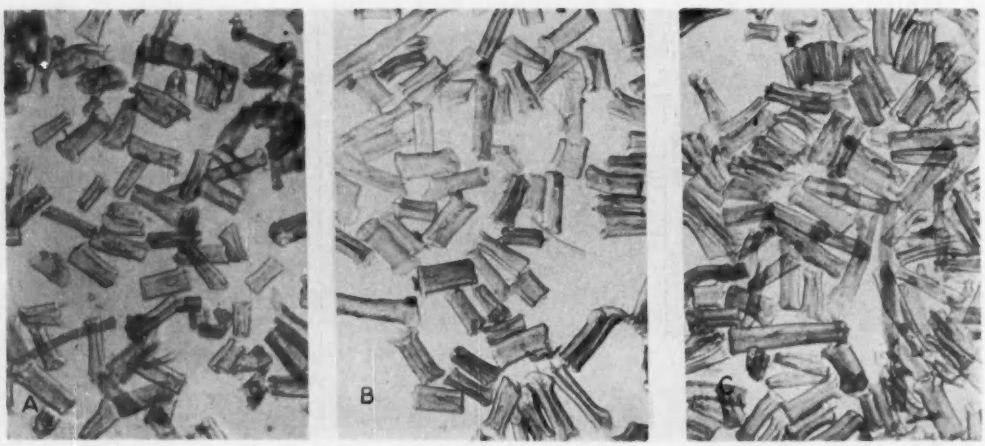

Fig. 4. Cut and swollen cotton fibers from (A) 21-day, (B) 28-day, and (C) 35-day-old cotton bolls, determinant type.

velopment as measured by fineness shows increasing wall thickness and increasing dumbbell formation. Maturity values based on two different methods while not in too good agreement increase with dumbbell formation (Table I). High shape factors are associated with low wall thickness or the ability of a fiber to collapse. This property is clearly visible for the underdeveloped fibers.

In order to establish a more quantitative approach to cotton development, fibers of different degree of fineness were counted with ballooning and designated mature fibers. A comparison with the conventional NaOH maturity is shown in Figure 8. Correlations between fiber fineness and the two maturity methods are high and considered significant.

Discussion

Besides fiber development, cut fibers can give considerable information on a sample of cotton. Damage from microorganisms can be detected by lack of ballooning of cut swollen fibers. Fibers that have the cuticle damaged will not balloon but will appear rough on the surface.

Many finishing operations affect the ballooning of cut swollen cotton fibers. Kiering, souring, and bleaching, depending on the concentration of the chemical and the extent of boiling, destroy or soften the fiber cuticle to prevent ballooning or modify it to the extent that ballooning no longer takes place. If the cuticle is altered by chemical treatment, swelling outwardly of the fiber gives a modified type of ballooning with a larger lumen. Finishing by resin treatment, which requires considerable heat, prevents ballooning. High heat (above 200° C.) for a period of time was shown by Koch [5] to alter or prevent ballooning of raw cotton. Thus, the test

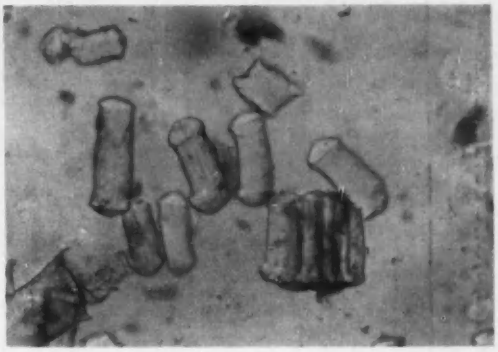

Fig. 6. Cut and swollen bast fiber flax.

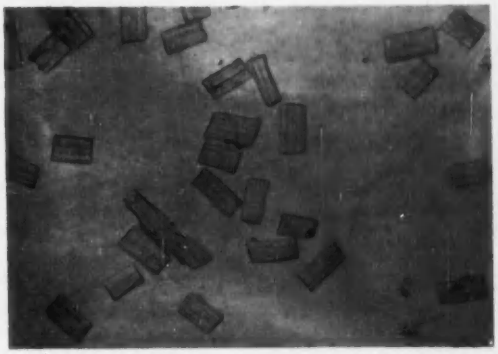

Fig. 7. Cut and swollen synthetic fiber rayon.

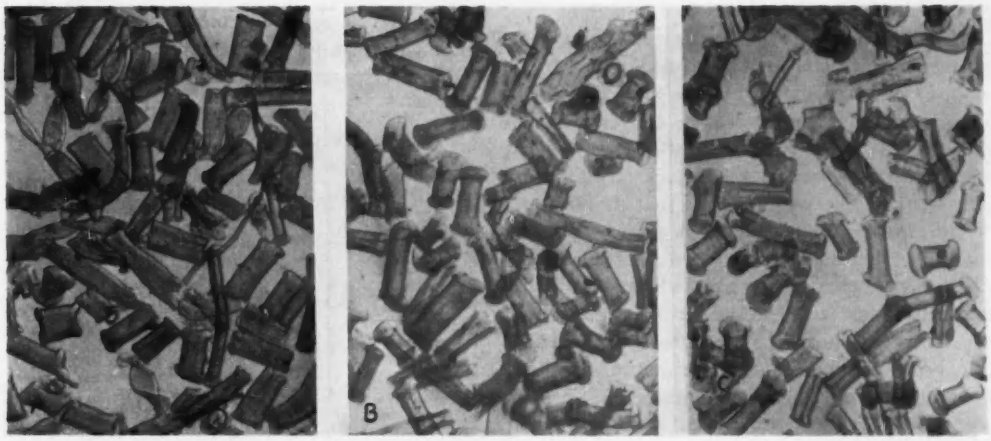

Fig. 5. Cut and swollen fibers from (A) Micronaire 3.0, (B) Micronaire 4.0, and (C) Micronaire 5.0, determinant type.

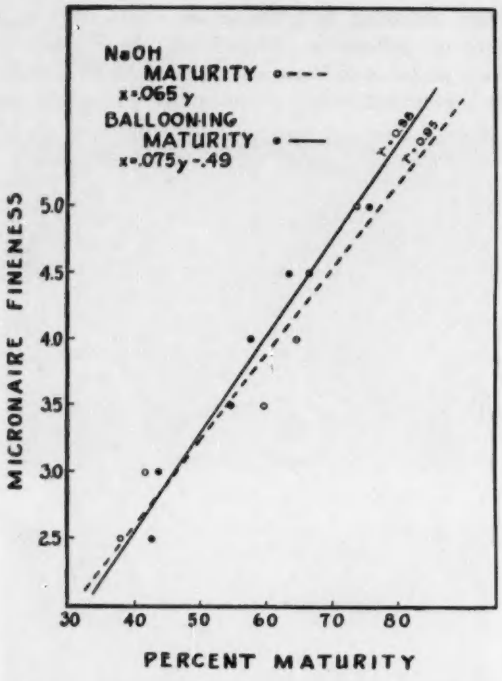

Fig. 8. The relation between Micronaire fineness of cotton and two maturity methods; one by the ballooning method and the other by the conventional NaOH method.

may have a place in cotton finishing as a control measure to study damage.

The underdeveloped fibers show a several-fold difference in diameter. Since these fibers were in the process of development and perhaps under adverse environment, the growth of the fiber in certain areas of the boll and seed may be retarded. In some samples, fiber diameter may be a function of variety. In either case, information of this kind could be of value to the cotton breeder. How this lack of uniformity of the fiber will affect the utility of the cotton is open to speculation. A lack of uniformity in diameter could very well mean a lack of uniformity in length, and spinning properties may be affected adversely. There is some reason to believe that low perimeter cottons may have advantages in development in low temperature areas, consequently better utility in spinning. The method should be advantageous in studies of this kind.

Cotton fiber development becomes increasingly important in adverse environmental areas. Whether earliness should be defined as the ability of a cotton to develop rapidly, early in the season, by producing early blooms or the ability of a cotton to lay down cellulose at a rapid rate is questionable. The rate of fiber development between two cottons which vary in determinancy is well demonstrated in the photographs. The more determinant cotton is, perhaps, a week or more further advanced in development. The dimensional and chemical properties in Table I confirm the visual findings for the two cottons.

Only a few vegetable fibers give ballooning on cut fibers, and they are distinguishable from cotton in shape. Flax and ramie can be distinguished from cotton in mixtures by the cut fiber method [5] (Figure 6). Also, synthetic fibers do not have the same retaining cuticle as cotton; therefore, they may be recognized by no ballooning when cut and swollen with 15% NaOH (Figure 7).

The cut fibers swollen on a slide may be observed under a microscope for routine work. However, for research a photograph has many advantages for a permanent record and future reference.

Summary

Cut swollen cotton fibers can be used to study cotton fiber development and determine cotton maturity. The method can be used to identify biological and chemical damage in a raw cotton sample. Cotton may be distinguished from other natural and synthetic fibers in mixtures.

Acknowledgment

This work is a part of a program sponsored by the Cotton Research Committee of Texas. Acknowledgment is made to Dr. Harry Lane, Texas Agricultural Experiment Station, for cotton samples.

Literature Cited

1. Hertel, K. L. and Cravens, C. J., TEXTILE RESEARCH JOURNAL **21**, 765 (1951).
2. Hessler, L. E., Simmons, C. R., and Lane, H. C., TEXTILE RESEARCH JOURNAL **27**, 412 (1957).
3. Herzog, A., *Aufl. Textteil* **5**, 210 (1955).
4. Hummelreich, W., *Textil u. Faserstofftechn* **5**, 623 (1955).
5. Koch, P. A. and Hefti, H., *Textil-Rundschau* **11**, 512, 645 (1956).
6. Markert, H., *Textile Forschung* **15**, 1 (1933).
7. Willows, R. S. and Alexander, A. C., *J. Textile Inst.* **13**, 237 (1922).

Manuscript received June 8, 1959.

Influence of $Na_5P_3O_{10}$-$CaCl_2$-H_2O Phase Equilibrium on Laundering of Cotton Fabric

W. J. Diamond[1] and J. E. Grove[2]

Abstract

Study of the phase equilibrium diagram for the $CaCl_2$-$Na_5P_3O_{10}$-H_2O system suggested that washing phenomena would depend on the phase region as well as specific $CaCl_2$ or $Na_5P_3O_{10}$ concentration.

Radioactive zirconyl phosphate was used as a redeposition soil, and tagged sodium alkyl aryl sulfonate was used for determination of detergent adsorption on cotton fabric. Ca^{++} concentrations from 0 to 5.5 mmoles/l. were reacted with sodium tripolyphosphate concentrations from 0 to 3.2 mmoles/l.

The quantity of radioactive ingredients deposited was measured after a 10-min. wash cycle in a Turg-O-Tometer. Desorption by a 5-min. rinse cycle was also evaluated.

Both redeposition and rinsability depend upon the $CaCl_2$-$Na_5P_3O_{10}$ phase region in which washing is performed.

Higher tripolyphosphate concentrations in the wash cycle retard redeposition and promote the rinsing of detergent from cotton fabrics. Hardness of water definitely influences both redeposition and rinsability. The influence of tripolyphosphate on redeposition is most pronounced at low soil loads.

Introduction

In 1954, Quimby [9] reported the phase boundary for the $CaCl_2$-$Na_5P_3O_{10}$ system in aqueous solution as determined by J. A. Gray and K. E. Lemmerman. The regions were labeled precipitate and no precipitate. Duplication of their experiments in this laboratory [2] generally confirmed their results, but indicated that a more proper labeling of the regions would be heterogeneous and homogeneous (as suggested in the text by Quimby) or two-phase region and single-phase region. Further, examination of the heterogeneous material revealed that it was essentially a suspension of very small particulates, approaching colloidal size.

From these observations, it was predicted that washing phenomena such as redeposition and rinsability would be governed by different laws in each region. In the single-phase region, amount of active detergent adsorbed on fabric should depend upon ionic strength [1, 7, 8]. In the two-phase region, the active ingredient should be adsorbed by both fabric and the $Ca_5P_3O_{10}$ and other precipitates [3]. Adsorption of these precipitates on fabric should also occur, and will be recorded as detergent adsorption. At constant sodium tripolyphosphate concentration, increasing $CaCl_2$ concentrations in a detergent bath should result in a regular change in detergent adsorption until the concentration of the phase boundary is reached. Further increases in $CaCl_2$ concentration should result in a sharp change in detergent adsorption. Similar behavior was predicted for redeposition. Since Quimby's work was performed in the absence of surfactant and since sodium dodecyl benzene sulfonate is also precipitated by Ca^{++} [10], some shifting of the phase boundary should occur.

This paper describes the influence of the phases of the $CaCl_2$-$Na_5P_3O_{10}$-H_2O system on deposition of sodium dodecylbenzenesulfonate and a particulate redeposition soil (zirconyl phosphate) on cotton fabrics and the removal of these deposits by rinsing.

Experimental

Materials

Fresh 0.008 *M* sodium tripolyphosphate solution was prepared daily using distilled water and recrystallized sodium tripolyphosphate (96.24% $Na_5P_3O_{10}$) [6] supplied by the Westvaco Mineral Products Division of Food Machinery and Chemical Company.

[1] Present address: Brunswick-Balke-Collender Company, Muskegon, Michigan.

[2] Present address: Post Division, General Foods Company, Battle Creek, Michigan.

Zirconyl phosphate redeposition soil was prepared by reacting 50 ml. of 0.033 *M* zirconyl chloride with 50 ml. of 0.02 *M* Na_3PO_4 containing approximately 0.04 millicuries of radioactive P^{32}. HCl was added until the solution was 0.01 *N* with respect to acid and then heat treated at 190° F. for 30 min. The pH was then adjusted to 7 with 1 *N* NaOH and the solution diluted to 250 ml. A 10-ml. aliquot of this mixture was used per test (approximately 0.01 g. of soil/test).

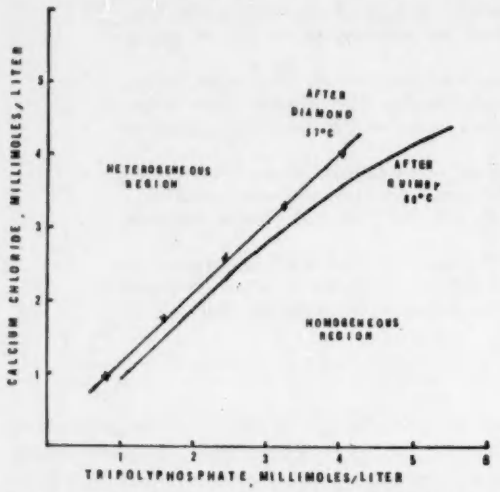

Fig. 1. Phase diagram for $Na_5P_3O_{10}$-$CaCl_2$-H_2O system.

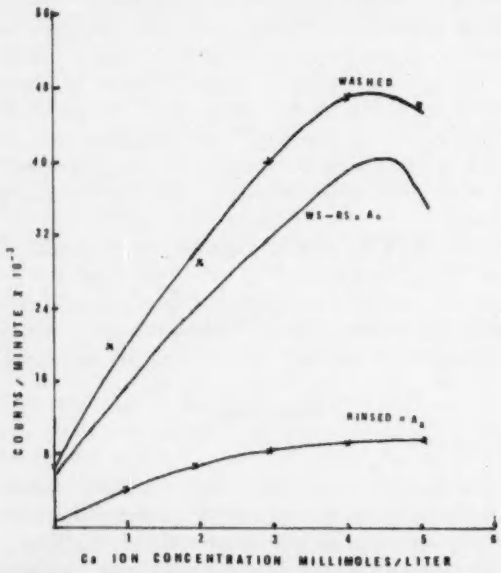

Fig. 2. Detergent adsorption at zero tripolyphosphate concentration.

The detergent used in the redeposition experiments was Siponate DS-10 (98% sodium dodecylbenzenesulfonate) supplied by American Alcolac Corporation. For detergent adsorption experiments, a 98% sodium dodecylbenzenesulfonate was synthesized in these laboratories using radioactive $H_2S^{35}O_4$.

Stock solutions of 0.01 *M* Ca^{++} were made from Fisher USP $CaCl_2 \cdot 2H_2O$ and distilled water.

Procedure

Standard cotton sheeting, boiled off, bleached and calandered, no added finish, 64 × 64 weave, weight 5 oz./yd. (North Carolina Finishing Company) was washed three times in 160° F. deionized water, spun damp dry, and ironed dry. It was then cut to swatch size, 3 × 5 in., and stored in a dry box at room temperature.

For each experiment, 1200 ml. of solution was prepared. Sodium tripolyphosphate solution was measured into a stainless steel beaker and heated to 59° C. In a second 2-l. stainless steel beaker, $CaCl_2$ solution and distilled water were heated to temperature. Tripolyphosphate solution was then added to the calcium solution, mixed for 1 min. and the mixture divided into two 600-ml. portions, one each for particulate redeposition and detergent adsorption experiments.

For the particulate redeposition experiment, 10 ml. of redeposition soil and 0.3 g. of the Siponate were added to 600 ml. of the above solution and agitated for 3 min. in a Terg-O-Tometer (U. S. Testing Company) operating at 59° ± 1.5° C. and 68 cycles /min. After mixing, 100 ml. of the solution was withdrawn for measurement of conductivity (L & N #4866 conductivity bridge and dip cell), turbidity (Fisher Nefluorophotometer), and radioactivity. Seventeen swatches were added to the remaining 500 ml. of solution and washed for 10 min. in the Terg-O-Tometer. After being washed, the swatches were damp dried by inserting between blotting paper which was passed through the rolls of a wringer washer. Seven of these swatches were immediately placed in an oven and dried at 120° F. for a minimum of 15 min. The other 10 swatches were placed in 240 ml. of distilled water at 59° C. and rinsed for 5 min. in the Terg-O-Tometer. After the rinse cycle, they were damp dried and oven dried as above.

For the detergent adsorption experiments, 10 ml. of radioactive detergent solution, containing 0.3 g. of

active detergent, was added to 600 ml. of $Na_5P_3O_{10}$-$CaCl_2$ solution and mixed for 6 min. A sample of 100 ml. was withdrawn for physical measurements. To the remaining 500 ml., 17 swatches were added and processed in the same manner as the redeposition swatches.

Equipment and procedure for counting of the radioactivity on the swatches were as previously described [4].

Calculations

The damp drying process reduced the moisture content of the swatches to 57 ± 1% by weight based on the dry weight of the swatch. Since concentration of this absorbed solution was the same as the concentration of the bath from which it is removed

WS (count on washed swatches)
$$= A_a + A_o + (C_w V_w)k \quad (1)$$

RS (count on rinsed swatches)
$$= A_a + (C_{w_1} V_w)k \quad (2)$$

$$\text{Difference } (WS - RS) = A_o + kV_w(C_w - C_{w_1}) \quad (3)$$

where A_a = count of adsorbed detergent or particulate remaining after rinse, A_o = count of adsorbed detergent or particulate desorbed by rinse, C_w = count of wash bath at end of cycle (~ concentration), C_{w_1} = count of rinse bath at end of cycle (~ concentration), V_w = volume of adsorbed solution after damp drying, and k = constant to correct for difference in counting geometry between the swatches and planchets. For these experiments, C_w was approximately constant, V_w was a constant equal to 13, and volume of rinse solution was a constant equal to 240 ml. The concentration of the absorbed solution after rinsing and damp drying was

$$C_{w_1} = 13/235\ C_w = 0.05\ C_w \quad (4)$$

and

$$WS = A_a + A_o + k_1 \quad (5)$$

$$RS = A_a + 0.05\ k_1 \quad (6)$$

$$\text{Difference } (WS - RS) = A_o + 0.95\ k_1 \quad (7)$$

where $k_1 = kV_wC_w$.

An attempt was made to experimentally determine k_1 for alkyl aryl sulfonate by restricting the washing cycle to 30 sec. with no agitation. It was presumed that little or no adsorption would occur under such conditions at zero calcium concentration. Then from Equation 6,

$$k_1 = RS/0.05 \quad (8)$$

and from Equation 5,

$$A_o = WS - RS/0.05 = WS - k_1 \quad (9)$$

Results of 4384 and 456 were obtained for the washed and rinsed swatches respectively. By substitution in Equations 8 and 9, $k_1 = 9120$ and A_o had a negative value, which was obviously impossible. Therefore, substantial adsorption must have occurred within 30 sec. even without agitation.

The order of magnitude of k was calculated empirically from the values of the washed and the rinsed swatches at zero Ca^{++} concentration and Equations 6 and 7. A_a could not be greater than RS nor could A_o be greater than the difference between WS and RS. By successive substitution of values, it was determined that A_a must be between 830 and 700 at zero Ca^{++} concentration. Using the mean value of 765 for A_a, $k_1 = 1300$, and $A_o = 4770$. Using these values, $1/k$ was calculated as 11.6, which is 4 times the value determined by the empirical method of Fava and Eyring [5].

From the above, A_a has approximately the same numerical value as the rinsed swatch and will vary directly with RS. A_o has a value substantially less than the difference between WS and RS, but varies directly with this difference. Therefore, evaluation of the difference $(WS - RS)$ within the limits of these experiments is a measure of desorption (A_o). Similar reasoning can be applied to the particulate deposition experiments. In Figures 2–11, three values are reported. The washed value is the total quantity of detergent or particulate deposited on the fabric during the washing cycle; the rinsed value, designated as A_a, is the amount of adsorbed material remaining after rinsing; the difference between the washed and rinsed swatch is designated as A_o and is proportional to the quantity of material desorbed by rinsing.

Discussion

Detergent Adsorption and Desorption

In the absence of tripolyphosphate, deposition of detergent on fabric increases with increasing Ca^{++} concentration (Figure 2) until an optimum is obtained at 4 mmoles/l. There is some indication of decreasing deposition at Ca^{++} concentrations greater

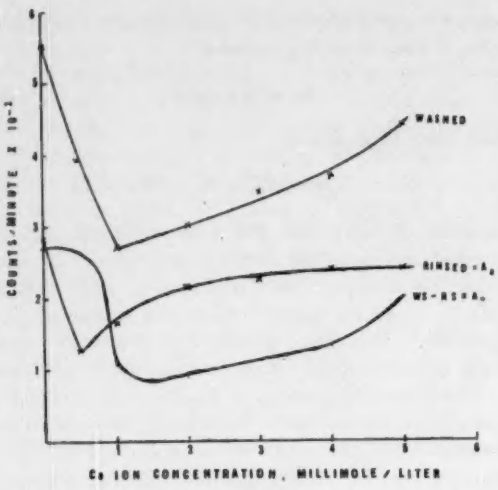

Fig. 3. Particulate adsorption at zero tripolyphosphate concentration.

than 4.5 mmoles/l., but this was not confirmed, as such hardness concentrations generally are not encountered in practice. The curve is drawn as a least square line from 0 to 4.0 mmoles/l. It is possible, however, that the value at 2.0 mmoles/l. is a real deviation from linearity rather than experimental error. Phase equilibrium considerations of the alkyl aryl sulfonate–calcium chloride–water system certainly do not preclude such behavior at this concentration. In any case, the effect is small and it would seem likely that this system would have little influence on detergent adsorption in the $CaCl_2$-$Na_5P_3O_{10}$-H_2O system.

A constant 19.5 ± 0.5% of the adsorbed detergent was retained when the swatches were rinsed (exception: 23% retained at 2 mmoles/l.). The physical-chemical significance of this constant partition value is not readily apparent. It could be only a manifestation of the difference in Ca^{++} concentrations in the wash and rinse baths. On the other hand, it could be a function of adsorption sites on the fabric and/or mode of deposition of the detergent.

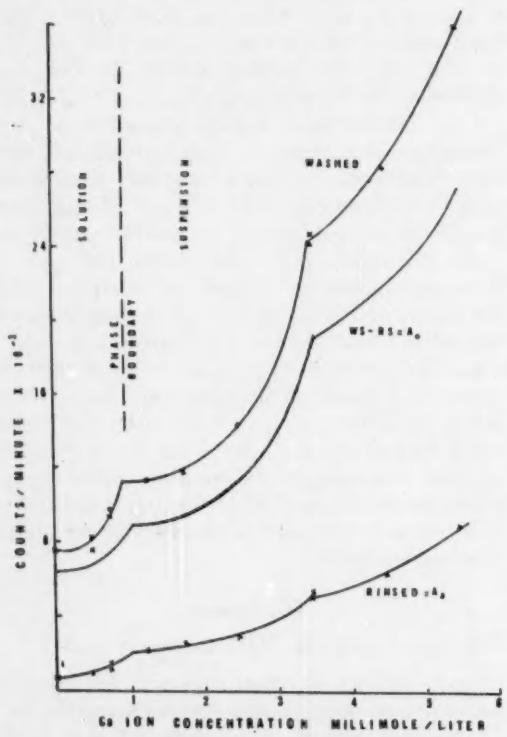

Fig. 4. Detergent adsorption at 0.8 mmoles/l. of tripolyphosphate.

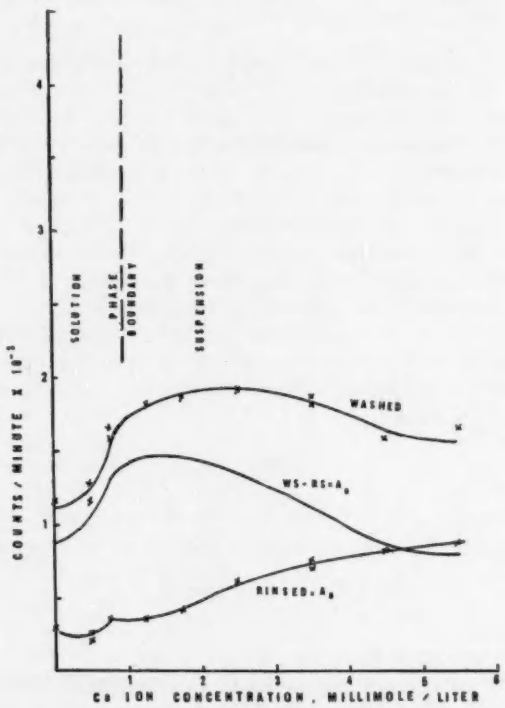

Fig. 5. Particulate adsorption at 0.8 mmoles/l. of tripolyphosphate.

The amount of adsorbed detergent which is retained on rinsing asymptotically approaches the 9000 count/min. grid. At first glance this would seem to indicate saturation of a limited number of available adsorption sites on the fabric. If this is so, however, the number of available sites or the tenacity of fiber–detergent complex would seem to depend upon the Ca^{++} concentrations of the detergent bath and the rinse bath. This would follow from the fact that a high level of true adsorption occurs in the detergent bath while the asymptotical value in the rinse bath is substantially lower. Further, the order of magnitude of the absorbed detergent is substantially less than the maximum adsorption values on swatches from both the rinse and wash baths.

Addition of tripolyphosphate to the detergent bath substantially reduces both the amount of detergent deposited in the wash bath and the quantity retained after rinsing (Figures 4, 6, 8, and 10). The shape of the adsorption vs. Ca^{++} concentration curves with tripolyphosphate are substantially different from the tripolyphosphate free curves. Also, there is substantial difference in shape of the curves at different tripolyphosphate concentrations. In every case, however, there is a break in the curves at the phase boundary concentration.

With 0.8 mmoles/l. of sodium tripolyphosphate there are two breaks in the curves. The first at approximately 1 mmole/l. of Ca^{++} was the expected break due to initial formation of the solid phase of the $Na_5P_3O_{10}$-$CaCl_2$-H_2O system. The excellent duplication of data substantiates the validity of the break at 3.5 mmoles/l. of Ca^{++} for which no physical explanation has been derived.

At Ca^{++} concentrations between the two break points in the curve, 1–3.5 mmoles/l., the percentage of deposited detergent retained on rinsing is approximately the same as when no tripolyphosphate was present, 20.5%. At Ca^{++} concentration above 3.5 mmoles/l., percent retention increases with Ca^{++} concentration (25% at 5.5 mmoles/l. of Ca^{++}). At Ca^{++} concentration below 1 mmole/l., percent retention decreases with decreasing Ca^{++} concentration (9% at

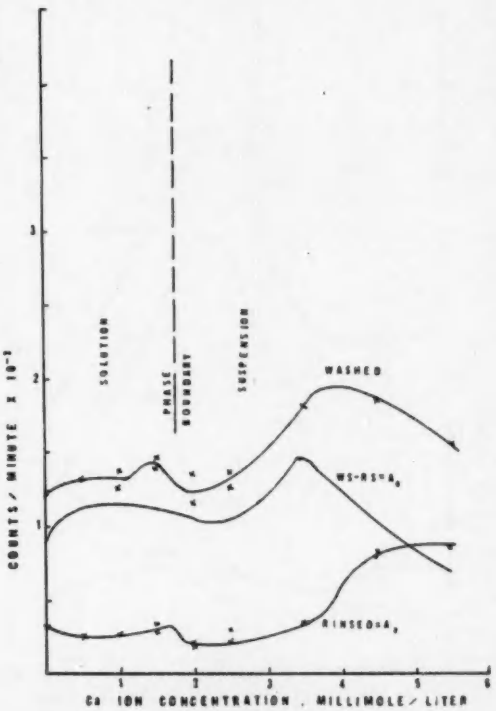

Fig. 6. Detergent adsorption at 1.6 mmoles/l. of tripolyphosphate.

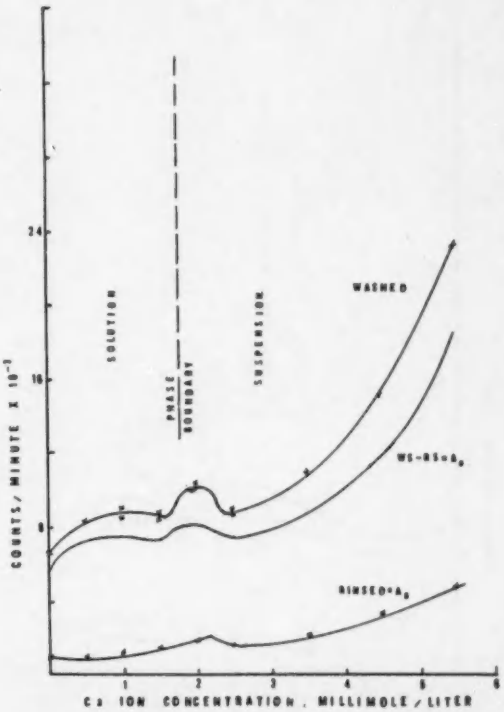

Fig. 7. Particulate adsorption at 1.6 mmoles/l. of tripolyphosphate.

zero Ca^{++}). Neither the washed nor rinsed swatch curves show signs of reaching an optimum in the range studied. In fact, at 5.5 mmoles/l. of Ca^{++}, the quantity of detergent retained after rinsing is the same as that retained when no tripolyphosphate was present. The indications are that at still higher Ca^{++} concentrations, a greater quantity of adsorbed detergent would be retained in the presence of 0.8 mmoles/l. of tripolyphosphate than in the absence of tripolyphosphate.

When 1.6 mmoles/l. of tripolyphosphate is reacted with varying quantities of Ca^{++} (Figure 6), the curve for the washed swatches breaks at 1.75 mmoles/l. of Ca^{++}, which is the phase boundary. A small but distinct maximum deposition occurs at 2.0 mmoles/l. of Ca^{++}, followed by a minimum at 2.5 mmoles/l. This maximum appears to be a superimposed phenomenon upon a more basic phenomenon. Validity of the observation is enhanced by the excellent duplicate values obtained. There is some evidence in Figures 8 and 10 of maxima occurring at Ca^{++} concentration slightly in excess of the phase boundary concentration.

As in the previous cases, there is one range of Ca^{++} concentrations (3.5–5.5 mmoles/l.) in which the percent retention of deposited detergent is 19.5 At Ca^{++} concentration between 1.5 and 2.5 mmoles/l., 17% of the deposited detergent is retained on rinsing. At Ca^{++} concentrations less than 1.5 mmoles/l., lesser quantities of detergent are retained on rinsing.

When 2.4 mmoles/l. of tripolyphosphate is reacted with varying quantities of Ca^{++}, the shape of the detergent adsorption and desorption curves are radically different from those with lesser quantities of tripolyphosphate. The shape of the curve for retention of detergent on rinsing is the same as with lower concentrations. Amount of detergent deposited and retained on rinsing is substantially lower at the higher Ca^{++} concentrations.

Breaks occur in both the deposition and retention curves at approximately 2.6 mmoles/l. of Ca^{++}, which is the concentration of the phase boundary. A maxi-

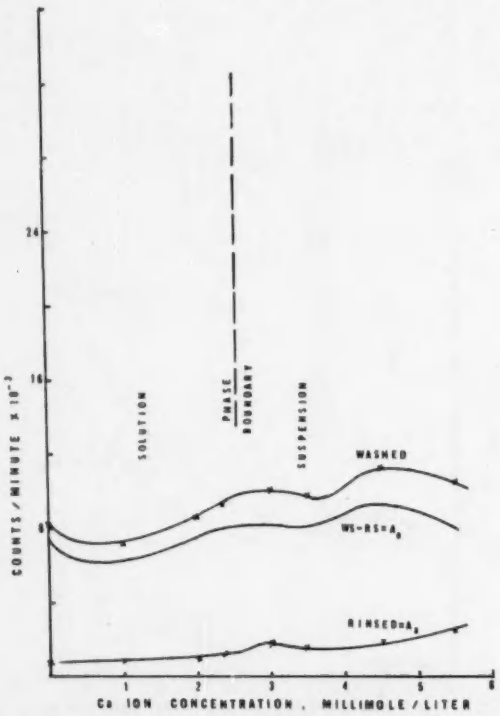

Fig. 8. Detergent adsorption at 2.4 mmoles/l. of tripolyphosphate.

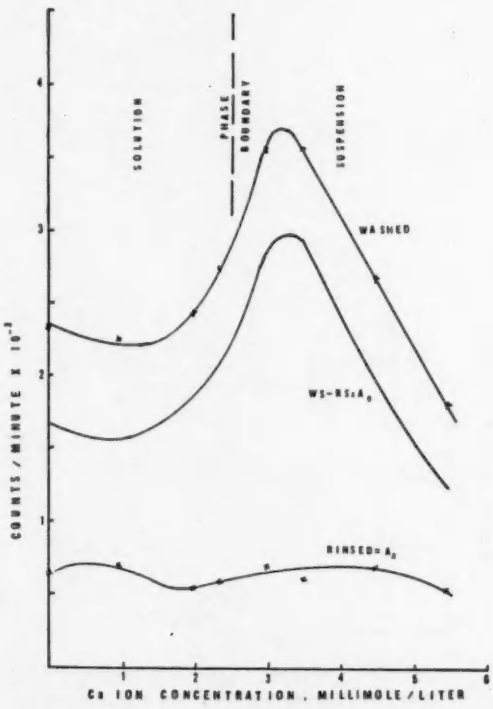

Fig. 9. Particulate adsorption at 2.4 mmoles/l. of tripolyphosphate.

mum occurs in the deposition curve at approximately 4.5 mmoles/l. of Ca^{++}. The ratio of Ca^{++} to $P_3O_{10}^{-5}$ at this maximum corresponds to the concentration ratio for maximum quantity of precipitate [3]. At greater or lesser concentrations of Ca^{++}, the quantity of precipitate will be smaller. Since the amount of deposition is also smaller at these concentrations, this would appear to be evidence that in this particular range of Ca^{++} concentrations, the amount of deposition is a function of the quantity of particulates formed by the reaction of Ca^{++} with $P_3O_{10}^{-5}$. The lack of this maximum in the previous curves could indicate that a certain minimum quantity of precipitate is required before the phenomenon becomes apparent.

At Ca^{++} concentrations between 3 and 4.5 mmoles/l. the percent retention of deposited soil after rinsing is 18.7. With this datum, a relationship between percent retention and tripolyphosphate concentration becomes apparent (Table I). At Ca^{++} concentrations less than 3 mmoles/l., percent retention decreases with decreasing Ca^{++} concentrations. At Ca^{++} concentrations above 4.5 mmoles/l., percent retention increases with increased Ca^{++} concentration.

Increasing the tripolyphosphate concentration from 2.4 to 3.2 mmoles/l. increases the amount of detergent which is deposited if the Ca^{++} concentration is greater than that of the phase boundary. The amounts retained on rinsing are, however, comparable. The optimum at 4.5 moles/l. of Ca^{++} and 3.2 mmoles/l. of $P_2O_5^{-5}$ is comparable with that at 3 mmoles/l. of Ca^{++} and 2.4 mmoles/l. of tripolyphosphate. It is predicted that a second maximum would occur in the deposition curve at approximately 6.4

TABLE I

TPP concentrations	% Retention	Range of Ca^{++} conc., mmoles/l.
0	19.5	1.0–5.0
0.8	20.5	1.0–3.5
1.6	19.3	3.0–5.5
2.4	18.7	3.0–4.5
3.2	17.7	3.5–4.0

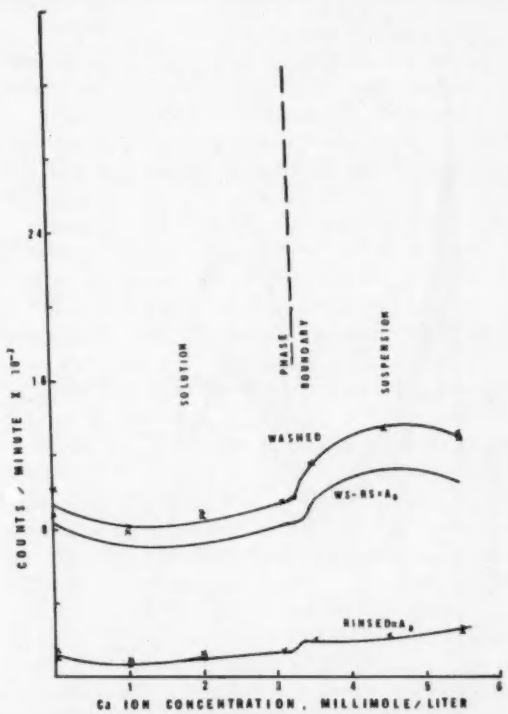

Fig. 10. Detergent adsorption at 3.2 mmoles/l. of tripolyphosphate.

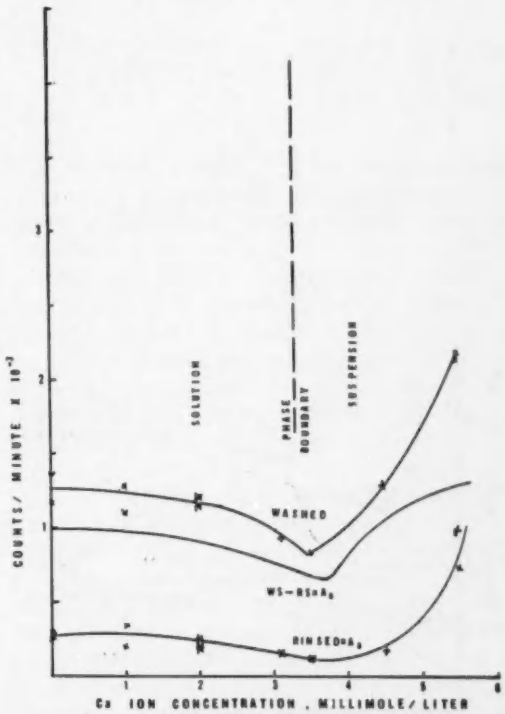

Fig. 11. Particulate adsorption at 3.2 mmoles/l. of tripolyphosphate.

mmoles/l. of Ca^{++} and 3.2 mmoles/l. of tripolyphosphate corresponding to the maximum deposition with 4.5 mmoles/l. of Ca^{++} and 2.4 mmoles/l. of tripolyphosphate.

When all the detergent adsorption and desorption data are reviewed *in toto,* some incontroversial conclusions are reached. On the other hand, however, many questions remain unanswered. Why is the shape of the deposition curves at tripolyphosphate concentrations below 2.0 mmoles/l. different from those above 2 mmoles/l.? Why is there an increase in deposition at a Ca^{++} concentration of 5 mmoles/l. when the tripolyphosphate concentration is increased from 2.4 to 3.2 mmoles/l.? Why are there maxima in the deposition curves at Ca^{++} concentrations slightly higher than the phase boundary concentrations when the tripolyphosphate concentration is 1.6 mmoles/l. or greater? Why are the rinsed curves for tripolyphosphate concentrations of 2.4 and 3.2 almost exactly comparable though the deposition curves are quite different in magnitude?

Particulate Adsorption and Desorption

In the absence of tripolyphosphate, maximum deposition occurred quite unexpectedly at zero Ca^{++} concentration. This was apparently contrary to the finding of Vitale [11] and Ross, et al. [10] with an Aquadag soil. Actually, there is but little disagreement between the results. Ross et al. based their conclusion on data at 0, 1, and 3.6 mmoles/l. of Ca^{++} with rinsed swatches. In Figure 3, the rinsed swatch data for Ca^{++} concentrations between 0.5 and 5.0 mmoles/l. agree completely with the Aquadag results. The results at zero Ca^{++} concentrations are, however, in complete disagreement.

The divergence of data is possibly explainable by the many differences in testing conditions: soil load, detergent concentration, temperature, detergent used, and processing of the swatches before test and during the test. However, the question of validity of the two soils (Aquadag vs. zirconyl phosphate) and the methods of measurement (reflectometer vs. radioactivity) cannot be ignored.

In the absence of tripolyphosphate, the particulate

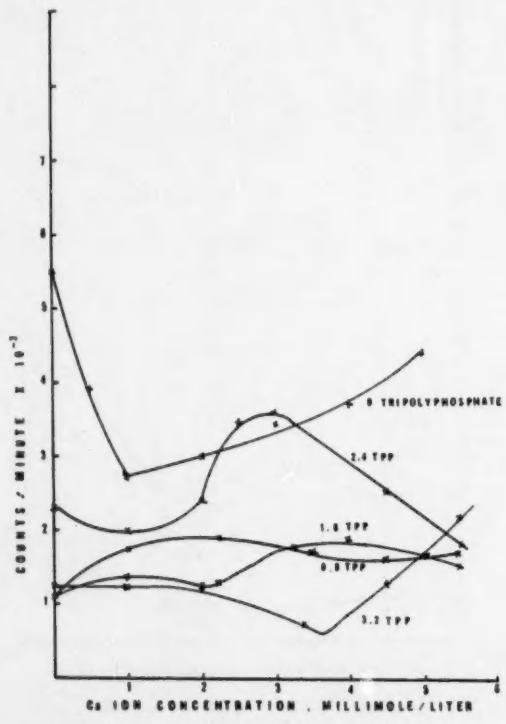

Fig. 12. Summary of particulate deposition data.

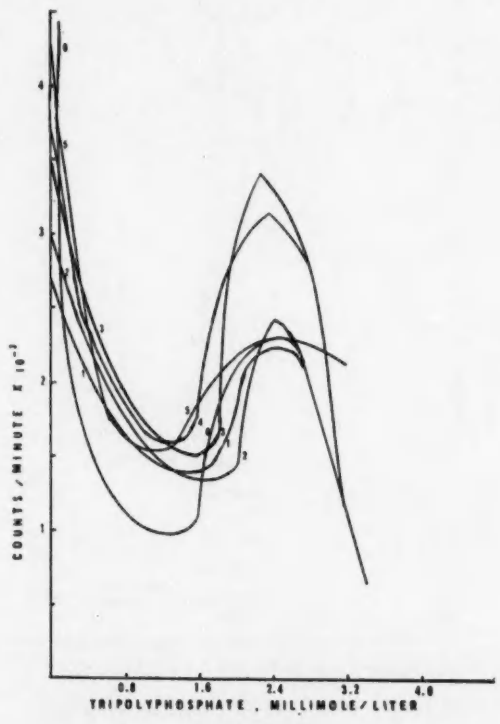

Fig. 13. Summary of particulate deposition data.

retention curve is very similar to the detergent retention curve except at zero Ca^{++} concentration. With increasing Ca^{++} concentrations, both approach an asymptotical value. Optimum retention is attained at a Ca^{++} concentration of approximately 4 mmoles/l. in both cases.

When tripolyphosphate is present, sharp breaks occur in the absorption and desorption curves (Figures 5, 7, 9, and 11) at phase boundary concentrations. Several unexpected results are apparent. In Figure 5, deposition and desorption decrease with increasing Ca^{++} concentration in excess of the phase boundary concentration, but retention increases with Ca^{++} concentration. Thus, less soil is being deposited but more of it is being retained through the rinsing cycle. A comparable condition is observed at all tripolyphosphate concentrations (except at 3.2 mmoles/l.).

Comparison of Figure 7 with Figure 6 reveals a sharp minimum in particulate deposition as compared to a sharp maximum in detergent deposition at Ca^{++} concentrations slightly higher than that of the phase boundary.

From Figures 3, 5, 7, 9, and 11, at any Ca^{++} concentration, as the tripolyphosphate concentration is increased, the quantity of particulate deposited in the wash cycle and retained through the rinse cycles decrease, with the notable exceptions at 2.4 mmoles/l. and Ca^{++} concentrations less than that of the phase boundary.

The deposition of particulates as a function of Ca^{++} concentration has been summarized in Figure 12. These curves emphasize the hazards inherent in detergent investigations. Several investigators could evaluate the effect of tripolyphosphate on redeposition and correctly report completely contradictory behavior depending upon the Ca^{++} concentration used by each investigation.

Except for the influence of the phase boundary, the data of Figure 12 appear to have little systemization. Replotting the data (Figure 13) with tripolyphosphate concentration as the variable at constant Ca^{++} concentrations results in a clear definition of the system. With increasing tripolyphosphate concentration, there are minima in all the deposition curves between 1.6 and 1.8 mmoles/l. An optimum deposition occurs at approximately 2.4 mmoles/l. of tripolyphosphate. Though magnitude of deposition varies with Ca^{++} concentration, approximate location of the minima and maxima appear to be a function only of the tripolyphosphate concentration. Ross

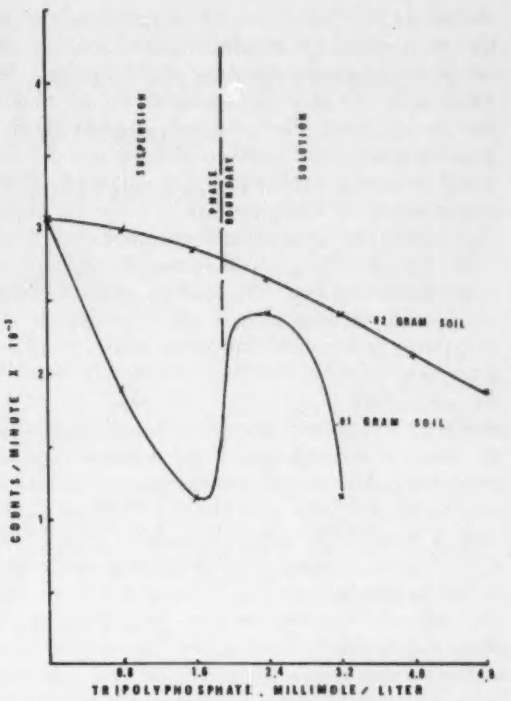

Fig. 14. Effect of soil load on deposition of particulates at 2 mmoles/l. of $CaCl_2$.

et al. [11] found a minimum in their deposition curve at a Ca^{++} concentration of approximately 1.7 mmoles/l. but their results show no maximum at 2.4 mmoles/l.

Before attempting an explanation of the phenomena in Figure 13, it was necessary to determine if the minima at 1.6–1.8 mmoles/l. of tripolyphosphate were related in any manner to the quantity of cloth or the quantity of soil. A test series with 2.0 mmoles/l. of Ca^{++}, varying quantities of tripolyphosphate, 22.7 g. of swatch material (same as previous test) but twice the weight of soil was evaluated.

It is evident from Figure 14 that the minimum at 1.6 mmoles/l. of tripolyphosphate is a direct manifestation of quantity of soil but independent of the quantity of fabric, except as the quantity of fabric and soil might be interrelated. The concept of a direct chemical reaction between the tripolyphosphate and the zirconyl phosphate redeposition soil can be eliminated, since such a stoichiometric reaction would require a minimum at 2.8 mmoles/l. of tripolyphosphate when twice as much soil was present. Furthermore, since a minimum deposition is also obtained in the

absence of Ca^{++}, any concept of interaction of the Ca^{++} with either the tripolyphosphate, soil, or cloth can be disregarded as the cause of the minima. The influence of the alkyl aryl sulfonate on the minima was not explored. Suffice to say, it could not be a direct stoichiometric reaction with the soil, for this would require a minimum at 1.4 mmoles/l. of tripolyphosphate of either one half or twice the magnitude when twice as much soil was used.

We can, therefore, conclude that the $P_3O_{10}^{-5}$ ion either directly or indirectly causes a physical change on a small quantity of soil which renders it less susceptible to deposition on cotton fabric. Furthermore, this resistance to being deposited increases as the concentration of $P_3O_{10}^{-5}$ increases up to 1.4 mmoles/l. Whatever the mechanism of the process, its effect is then progressively weakened and increased deposition results from an increase in $P_3O_{10}^{-5}$ concentration. Since it is rather difficult to picture such a reversal by direct interaction of soil and $P_3O_{10}^{-5}$, it is proposed that the minima result from an interaction between the soil and a $P_3O_{10}^{-5}$–alkyl aryl sulfonate reaction product. As the polyphosphate concentration is increased, the concentration of the reaction product is increased, and it in turn influences the deposition tendencies of the soil by charge reversal or some other change in surface properties. At 1.4 mmoles/l., a maximum quantity of the reaction product is formed and a minimum deposition results. As the tripolyphosphate concentration is increased beyond 1.4 mmoles/l. the reaction product is progressively decomposed, there is less of the product to influence the soil, and deposition increases. At 2.4 mmoles/l., the entire quantity of reaction product has been decomposed. The lack of a minimum in the data for twice the quantity of soil requires the supposition that the reaction product be uniformly distributed among all the soil particles and that a certain minimum concentration on the particle be required for any effect on deposition.

Conclusion

Redeposition of soil in cotton fabric and rinsing of detergent from cotton fabrics are substantially influenced by the phase region of the Ca^{++}-$Na_5P_3O_{10}$ system in which washing and rinsing takes place. Rinsing of detergent is improved as the concentration of tripolyphosphate is increased or as the Ca^{++} concentration is decreased in the detergent bath.

Particulate deposition is at a minimum with approximately 1.7 mmoles/l. of tripolyphosphate and all concentration of Ca^{++} from 0 to 5.5 mmoles/l. with small soil loads. Maximum deposition with small soil loads occurs at a tripolyphosphate concentration of 2.4 mmoles/l. These maxima and minima are not present at larger soil loads.

Desorption of detergent or particulate soil from cotton fabric is directly proportional to the amount deposited over a substantial range of concentrations.

There are inflections in the detergent and particulate deposition, desorption, and retention curves at the concentration of the phase boundary of the Ca^{++}-$Na_5P_3O_{10}$-H_2O system.

Since particulate and detergent removal is enhanced at high tripolyphosphate concentrations in the wash bath, it can be inferred that high tripolyphosphate concentrations would be advisable in the rinse bath.

Literature Cited

1. Camp, M. and Durham, K., *J. Phys. Chem.* **59**, 993–997 (1955).
2. Diamond, W. J., *J. Phys. Chem.* **63**, 123 (1959).
3. Diamond, W. J., *J. Phys. Chem.* **63**, 1528 (1959).
4. Diamond, W. J. and Levin, H., TEXTILE RESEARCH JOURNAL **27**, 787–795 (1957).
5. Fava, A. and Eyring, H., *J. Phys. Chem.* **60**, 890–898 (1956).
6. Netherton, L. E., Wreath, A. R., and Bernhard, D. N., *Anal. Chem.* **27**, 860 (1955).
7. Palmer, R. C., *J. Soc. Chem. Ind., London* **60**, 56–60 (1941).
8. Pawney, J. and Noad, R. W., *J. Textile Inst.* **30**, T157–171 (1939).
9. Quimby, O. T., *J. Phys. Chem.* **58**, 603–618 (1954).
10. Ross, J., Vitale, P. T., and Schwartz, A. M., *J. Am. Oil Chem. Soc.* **32**, 200–204 (1955).
11. Vitale, P. T., *J. Am. Oil Chem. Soc.* **31**, 341 (1954).

Manuscript received March 13, 1959.

A Rheological Interpretation of the Hottenroth Index Method for Viscose

Shigeharu Onogi and Yoshiki Hayashi[1]

Department of Textile Chemistry, Kyoto University, Kyoto, Japan

Abstract

Some rheological properties of viscose during titration with various salt solutions, especially ammonium chloride, have been studied by employing a new automatic tester. The principle of the tester is to record automatically the change in viscosity of the viscose sample during titration with salt solution; the change in torque required for stirring the sample at constant velocity is converted into the change in electrical potential by means of a linear variable differential transformer device. From the experimental results it is concluded that the conventional Hottenroth index method for determining the degree of ripeness of viscose does not always determine a volume of 10% NH_4Cl solution by which coagulation of the viscose sample just sets in. On the other hand, it has been found that viscose with ammonium chloride solution added manifests a thixotropic nature, and a new rheological interpretation has been put on the Hottenroth index method; it measures a volume of 10% NH_4Cl solution by which a viscose sample becomes notably thixotropic.

Introduction

In a previous paper [4], a change in viscoelastic behavior of viscose during its ripening was studied by means of an electromagnetic transducer, and it was concluded that the most suitable degree of ripeness for spinning deduced from a viscoelastic standpoint agreed well with that which had been decided by conventional industrial control methods such as falling-ball viscosity and Hottenroth index methods. The latter is a colloidal method to determine the degree of ripeness of viscose [5, 6] and is used extensively in industry, since it is more practical and simpler than chemical methods. In this method, the Hottenroth index is defined as the exact volume (ml.) of 10% NH_4Cl solution needed to cause coagulation of a viscose sample. As shown below, however, it is not always true, and the principle on which the Hottenroth index method is based has not yet been understood clearly.

The present paper is concerned with the rheological behavior of viscose with salt solutions added, especially with thixotropy observed in viscose with ammonium chloride solution added, the purpose being to put a rheological interpretation on the Hottenroth index method and to contribute to a plan of a new automatic tester for determining the degree of ripeness of viscose.

[1] Present address: Nagoya Mill, Dainihon Transparent Paper Mfg. Co., Ltd., Nagoya, Japan.

Experimental

Apparatus

The principle of the apparatus employed in this study consists in recording automatically a change in the torque caused by stirring a viscose sample in a vessel at a constant velocity. By means of this apparatus, we can follow a change in viscosity of viscose during titration with a salt solution. The apparatus is somewhat similar in its principle and structure to that of Boenig and Beniers [2], which is the only automatic tester so far as we know, but the operating mechanisms are quite different. The stirring velocity of our apparatus is constant during a titration. Thus we can always measure viscosities at a constant rate of shear and can be free from complicated rate of shear dependence of the viscosity of viscose, a typical non-Newtonian liquid. In Figures 1 and 2, a block diagram and an electrical circuit for the apparatus are shown.

In Figure 1, a cylindrical vessel made of plastic molding is mounted on a rotator. The upper part of the rotator forms a disk capable of fixing the

vessel, while its lower part forms a hollow cylinder. In the center of the cylinder, the rotator is suspended with a torsion wire hung from an arm fixed to the base to the bottom of this cylinder, and is also supported by a couple of frictionless pivots at its top and bottom in order to avoid transverse motion. When the sample in the vessel is stirred by a stirrer connected with a synchronous motor at a constant velocity, the vessel and the rotator are twisted to an equilibrium position at which the torque in the wire balances with that causing the sample to shear. Since the angle of the twist is proportional to the torque, we can convert a change of this torque into a change of electrical potential by employing a linear variable differential transformer device, whose top view is shown in Figure 3. There are two transformers (one at the left and at the right side of the cylinder); their cores are connected to sufficiently long arms united with the cylinder and can shift in proportion to the twist of the cylinder. The output from the transformers is recorded automatically by a recorder or indicated by a voltmeter after being amplified.

The relation between the torque and the reading of the recorder was determined by using a standard spring of known stiffness; it was found to be linear except for the first part, as shown in Figure 4. By using this relation, a reading of the recorder in milliamperes can directly be converted into a torque in gram-centimeters. The apparatus is also provided with a special pump to keep a constant flow rate of salt solution from the burette and with a device to stop the flow at any appointed torque.

As in a usual procedure, the viscose sample, undiluted or diluted, is put into the vessel, stirred, and then titrated with a salt solution at a constant rate of about 2 ml./min. A change in torque is recorded automatically. Two examples of the recording obtained by this apparatus with young and old viscose [2] diluted with water at the ratio of 2:3 in weight are shown in Figures 5 and 6. The salt solution employed here is 10% NH_4Cl solution, as in the usual Hottenroth index method. The ordinate and abscissa of the figures represent the torque in milliamperes and the volume of the solution in milliliters, respectively, and arrows on the curves indicate the Hotten-

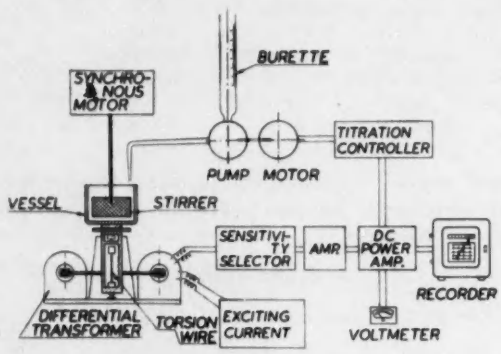

Fig. 1

[2] It is our custom to call viscose having low degree of ripeness (or large Hottenroth index) young viscose, and one having high degree of ripeness old viscose.

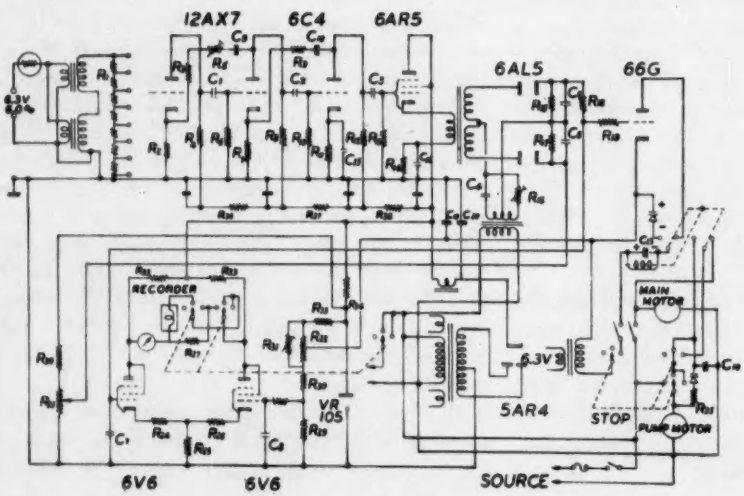

Fig. 2

roth index determined independently by the usual procedure [3] with the same viscose. The two curves in the figures are very different in shape from each other, suggesting that the old viscose is more sensitive to the salt than the young. Such a curve of torque drawn against the volume of salt solution will be designated as a coagulating curve hereafter.

The accuracy and reproducibility of our apparatus are very satisfactory. The error due to the apparatus itself is less than 1% and is small enough as compared with some other experimental errors. Thus, successive titrations with the same viscose sample under the same conditions always give practically the same results. Furthermore, we could not find any appreciable fluctuation of the zero point during continuous usage for several months.

Sample

The sample viscose used in this study was that for a regenerated cellulose film industry and was not very different from that for a rayon industry. The total alkali content of the viscose was about 5.8% and its cellulose content was about 8.0% independent of time of sampling.

In some cases, the viscose was used in an undiluted state; in other cases, it was used after being diluted with water as in the conventional Hottenroth index method (viscose 20 g.; water 30 ml.).

The measurements were always carried out in an air-conditioned room at 23° C.

Results and Discussion

Coagulating Curves Obtained with Various Salt Solutions

In order to compare the coagulating effect of various salt solutions, coagulating curves were obtained with viscose having a Hottenroth index as low as 4.8, since older viscose would give a sharper coagulating curve than the young. The results are summarized in Figure 7. The choice of the salt solution is not only arbitrary but also rather restricted.

The coagulating curve of 10% NH_4Cl solution was obtained with diluted viscose. The torque increases gradually up to around 6 ml. of the salt solution, and then increases very rapidly to give a comparatively sharp bending. The curve of 20% $ZnSO_4$ solution obtained with diluted viscose is rather monotonous in its shape, except for a hump in the neighborhood of 4 ml. of solution. This hump is attributable to the fact that the coagulation of a viscose sample by $ZnSO_4$ solution does not occur uniformly due to the very great coagulating power of this salt; as soon as the solution drops on the viscose sample, a local coagulation takes place, and a coagulate of zinc xanthate, like half-boiled egg, adheres to the stirrer.

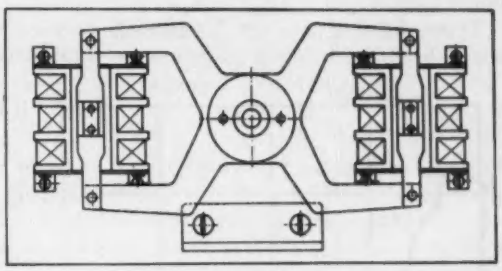

Fig. 3

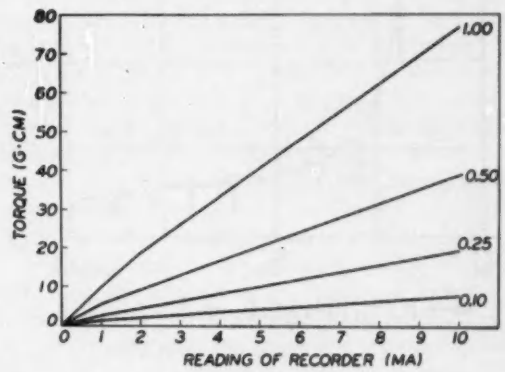

Fig. 4

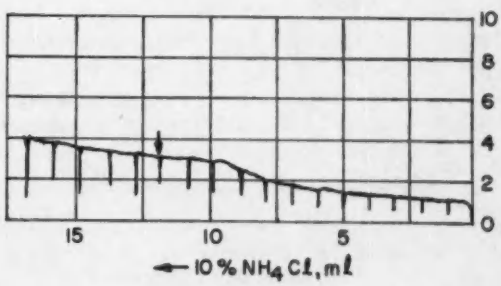

Fig. 5

[3] In the usual procedure employed by us, a sample of 20 g. of viscose, diluted with 30 ml. of water, is titrated with 10% NH_4Cl solution under vigorous stirring with a glass rod. When the glass rod is temporarily raised from the solution during the titration, a small amount of solution adhering to the rod flows down very quickly at the beginning of the titration, and then more and more slowly as the titration proceeds until it reaches a point where no viscose drips. This point is regarded by us as the end point of the titration.

Hence, the original recording has many fine jags and is not so smooth as the curve shown in the figure, which is reproduced by neglecting such jags.

On the other hand, the coagulating curves of 20% NaCl and 15% KCl solutions were obtained with 20 g. of undiluted viscose. The coagulating powers of these salts are so weak as compared with those of the above two salts that the coagulating curves decrease in the early stage of the titration due to a predominant diluting effect of the solutions, notwithstanding their higher concentration. A rapid increase of the torque takes place only after much solution is added.

Three different types of coagulating curves obtained here are naturally expected by considering different coagulating effects of these salts upon viscose. Sodium and potassium chlorides coagulate viscose by a purely electrolytic action, i.e., by increasing the ionic strength to the point where the xanthate ions are sufficiently shielded from each other to permit coagulation. On the other hand, ammonium chloride, in addition to its effect as an electrolyte, also decreases the alkalinity of the solution by reacting with alkali in the solution. This leads to a reduction of the stability of viscose to coagulation just as in the case of aqueous solution of purified xanthate [3]. The strong coagulating effect of zinc sulfate mentioned above is due to these two mechanisms plus the third factor, that of the formation of slightly soluble zinc xanthate. This formation of

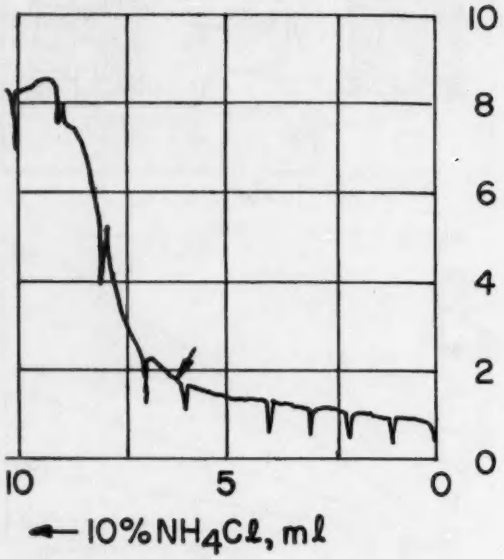

Fig. 6

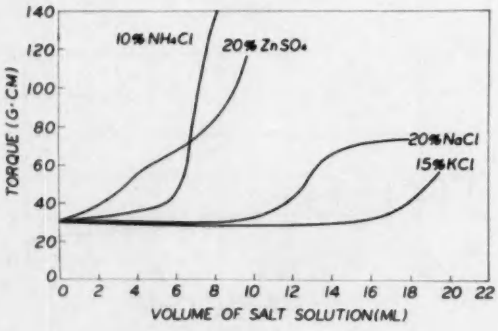

Fig. 7

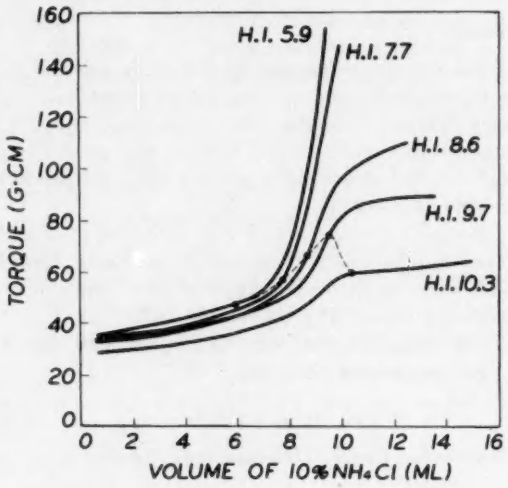

Fig. 8

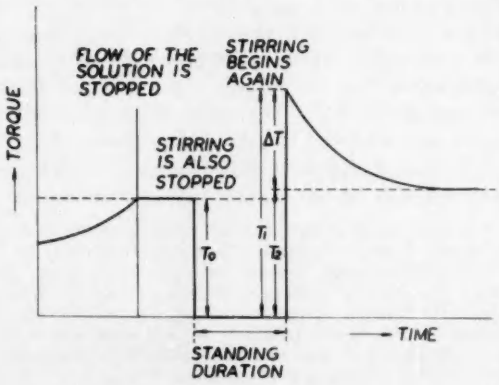

Fig. 9

zinc xanthate occurs very quickly and locally at the place where $ZnSO_4$ solution drops, and strong floccules of zinc xanthate are imbedded in the rest of the solution, which is now of low viscosity. Therefore, the viscosity of the over-all solution does not increase so rapidly despite the very strong coagulating power of this salt.

As seen from these results, ammonium chloride solution gives the sharpest coagulating curve, and appears to be the most suitable for determining the degree of ripeness. It will be noticed here, however, that the Hottenroth index determined by the usual method does not always coincide with the break point of the coagulating curve. For example, the coagulating curves are shown in Figure 8 for various viscose samples differing only in their degrees of ripeness from one another. The solid circles on the curves show the Hottenroth index determined independently by the usual procedure for the same viscose samples. It is clear from the figure that the value of the torque corresponding to the Hottenroth index increases in the early stage of ripening and then inversely decreases after passing a maximum. It is very difficult, therefore, to find a simple relation between the Hottenroth index and corresponding torque or viscosity. In other words, the Hottenroth index cannot be determined by only following the change in torque or viscosity. The Hottenroth index is defined as a volume of a 10% NH_4Cl solution which just causes the coagulation of the sample viscose, but it is obvious from the above results that the coagulation does not set in abruptly but rather gradually, and that the Hottenroth index does not always coincide with a volume of 10% NH_4Cl solution by which a comparatively abrupt change in torque or a comparatively abrupt coagulation takes place.

Thixotropy in Viscose with Ammonium Chloride Solution Added

As mentioned above, the usual method for determining the Hottenroth index does not always determine the volume of 10% NH_4Cl solution by which an abrupt change in torque or coagulation takes place. Nevertheless, it will always afford reproducible results with considerably high accuracy, though appreciable personal errors are inevitable. This fact is suggestive of the existence of an unknown peculiar behavior in viscose with ammonium chloride solution added. We presumed this behavior to be thixotropy, and have been able to confirm it experimentally as described below.

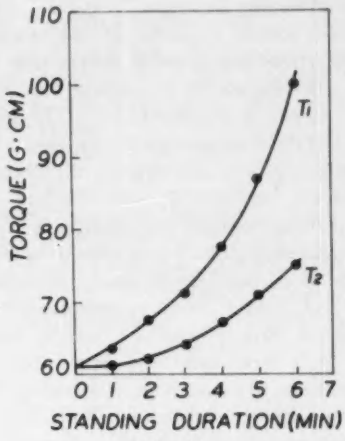

Fig. 10

Both the empirical fact that the velocity of a ball falling through viscose in a falling-ball viscometer is the lowest at the first measurement and the experimental result [1] that the viscosity of viscose decreases after filtration suggest that viscose itself has thixotropic nature. However, this thixotropy is rather slight, and it takes a long time for the recovery of thixotropic structure broken under shear. In other words, the thixotropy of viscose itself can be observed only by long time-scale experiments. It has been observed, on the other hand, that viscose with ammonium chloride solution added manifests very remarkable thixotropy even in a short time.

By employment of our apparatus, when a titration with 10% NH_4Cl solution is stopped suddenly in the neighborhood of the Hottenroth index of a sample viscose and only the stirring is continued, the torque attains an equilibrium value T_0 at once, and keeps it for a while.[4] In this stage, the stirring also ceases abruptly and the sample is allowed to stand for several minutes. After this standing duration, the stirring is begun again. The torque instantaneously attains a value T_1 much larger than T_0, then decreases almost exponentially with time until it reaches a somewhat higher equilibrium value T_2 than

[4] Since the coagulation of viscose with added salt solution proceeds more rapidly than with the pure viscose, the torque increases a few minutes after the stirring is ceased. The more solution is added, the more rapidly the torque increases, and when the solution is added near the Hottenroth index level, the torque increases even if the stirring is continued.

T_0. The difference between T_2 and T_1, ΔT, corresponds to a torque required for the disruption of thixotropic structure formed during the standing duration. In Figure 9 the change in torque just described is shown schematically. The longer the standing duration, of course, the stronger the thixotropic structure, and the greater the increment of torque, ΔT.

As an actual example, the change of T_1 and T_2 with the standing duration is shown in Figure 10 for a diluted viscose sample having the Hottenroth index 7.7. T_1 and T_2 were measured after addition of 8.2 ml. of 10% NH_4Cl solution to the sample viscose. It is clear from the figure that both T_1 and T_2 increase with increasing standing duration, and that the former does so more rapidly. Therefore, ΔT also increases with the increasing standing duration, as is shown in Figure 11. Thus, the longer the standing duration, the more remarkable the thixotropy.

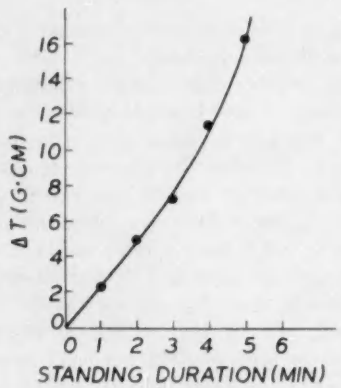

Fig. 11

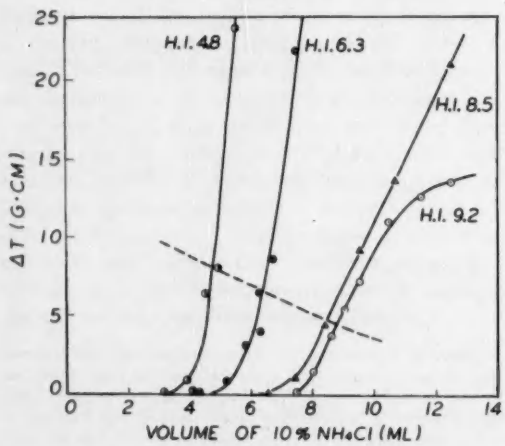

Fig. 12

From the standpoint that the usual procedure for determining the Hottenroth index probably utilizes this thixotropic nature ingeniously, the relation between ΔT and the volume of 10% NH_4Cl solution added to viscose was examined with four viscose samples ripened to different extents. In this experiment, the standing duration was chosen arbitrarily as 1 min.; the results are shown in Figure 12. The figures on the curves represent the Hottenroth index by the usual method, varying from 9.2 to 4.8. As seen from the figure, ΔT is not measurable unless the ammonium chloride solution is added to a volume near the Hottenroth index of each sample. In other words, thixotropy develops only after the titration progresses near the Hottenroth index. Furthermore, the older the viscose, the more rapidly ΔT increases. This shows that older viscose becomes more remarkably thixotropic than the younger by addition of a small amount of the salt solution, and agrees very well with an empirical fact that the accurate determination of the Hottenroth index by the usual procedure is very easy for older viscose, while it is very difficult for the younger.

It follows from the above results that the usual procedure for determining the Hottenroth index measures a volume of 10% NH_4Cl solution by which viscose becomes notably thixotropic. It is very interesting that viscose is capable of formation of such a stable thixotropic structure before it coagulates into a very strong gel. Such a phenomenon of thixotropy may be attributed to the decrease in alkalinity of the sample solution as described above. The decrease in alkalinity will lower the solvent power of the aqueous solution, permitting the formation of strong hydrogen bonds between cellulose xanthate molecules. These hydrogen bonds will become increasingly difficult to break instantaneously, but their formation will not occur so quickly as compared with the formation of slightly soluble zinc xanthate. Hence a comparatively strong network structure due to the hydrogen bonds will be built up not locally but uniformly throughout the solution. Such a continuous network structure will gradually be broken by a shear and reformed after disappearance of the shear. This may be a reason why the remarkable thixotropic behavior can be observed in solutions of ammonium chloride. We are now carrying out a

further investigation on the thixotropic nature of viscose and on a practical application of our apparatus to determine the Hottenroth index of viscose in the rayon industry. The results will be published in the near future.

Acknowledgments

The authors wish to express their sincere gratitude to Professor Masao Horio for his kind interest and encouragement. They are indebted to the Iwamoto Manufacturing Co. for helpful cooperation in manufacturing the tester used in this study.

Literature Cited

1. Bergek, T. and Ouchterlong, T., *Svensk Papperstidn.* **49**, 470 (1946).
2. Boenig, H. and Beniers, M., *Melliand Textilber.* **35**, 1119 (1954).
3. Heuser, E., "Cellulose Chemistry," New York, Wiley 359 (1948).
4. Hirai, H., Kondo, T., Terasaki, H., and Onogi, S., *J. Chem. Soc. Japan, Ind. Chem. Sect.* **61**, 596 (1958).
5. Hottenroth, V., *Chem.-Ztg.* **39**, 119 (1915).
6. Mukoyama, T., *Kolloid-Z.* **43**, 349 (1927).

Manuscript received June 23, 1959.

The Nature of Tenaciously Bound Soil on Cotton[1]

William C. Powe

Research Laboratories, Whirlpool Corporation, St. Joseph, Michigan

Abstract

A serious problem in drycleaning and laundering is the progressive deterioration in the appearance of fabrics caused by the gradual accumulation of unremoved and redeposited soil. Electron micrographs of natural soil *in situ* were taken to determine the identity and particle size of this material. These electron micrographs suggest that clay minerals 0.02–1 μ in diameter are the major particulate material causing soil build-up on cotton fibers. Properties of clay minerals which contribute to their forming strong bonds with cotton fibers are discussed.

Introduction

A serious problem in drycleaning and laundering is the progressive deterioration in the appearance of fabrics. They become dull, dingy, and unattractive. This is caused by a gradual accumulation of unremoved and redeposited soil. Electron micrographs of natural soil *in situ* on cotton fibers were made to determine the identity and particle size range of the particulate soil unremoved by normal cleaning procedures.

The literature on soiling and redeposition has been well summarized by both Getchell [1] and Schwartz [8]. The lack of information on the chemical composition and particle size of redeposited soil was noted by both Getchell [1] and Kramer [7]. Some excellent electron micrographs of carbon black, dust, and iron oxide on cotton and wool fibers have been published by Kling and Mahl [6] and Götte, Kling, and Mahl [2]. Most published observations on soiling and redeposition, however, have been based on model systems employing artificial soils such as carbon black, colloidal graphite, ilmenite, iron oxide, or some similar material.

Experimental

Most of the electron micrographs are carbon replicas of the cotton fiber surface. Specimens were shadowed under vacuum with vaporized carbon. The carbon casts were separated from the fiber by soaking the carbon coated cloth in a 50/50 by volume ethanol/water mixture and then dipping in strong

[1] Presented before the Cellulose Division at the 135th National Meeting of the American Chemical Society, Boston, Mass., April 9, 1959.

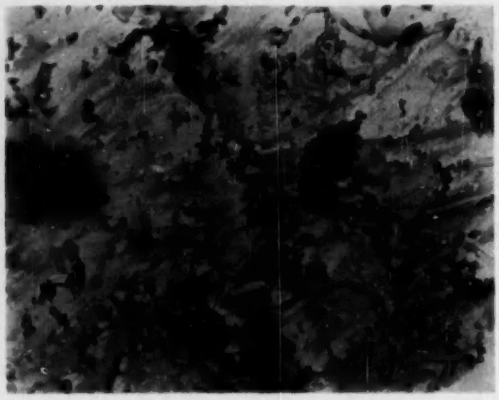

Fig. 1. Electron micrograph of a surface replica of soot on a cotton fiber.

Fig. 3. Electron micrograph of a surface replica of kaolinite particles on a cotton fiber.

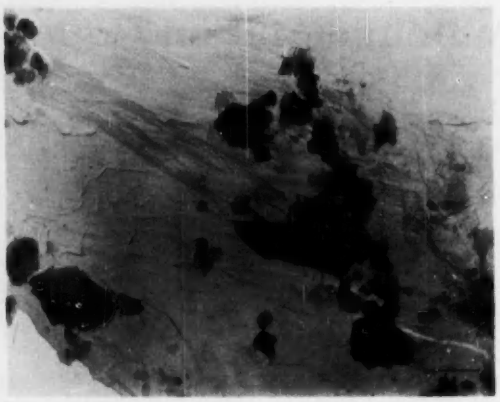

Fig. 2. Electron micrograph of a surface replica of a graphite stain on a cotton fiber.

Fig. 4. Electron micrograph of bentonite. It is composed mostly of the clay mineral montmorillonite, which has very small crystals.

sulfuric acid. The resulting violent exothermic reaction separated the carbon replica from the fiber.

Figure 1 is carbon black, the most common material used in detergency studies. Carbon black can be obtained commercially in a number of particle sizes. This electron micrograph was made to determine the particle size of naturally occurring material that might remain attached to cotton.

The specimen was prepared by rubbing industrial soot into a piece of clean cotton cloth. The soot stain was then soaked with a liquid detergent and rubbed vigorously to remove as much of the soot as possible. The cloth was rinsed free of detergent with distilled water. The remaining stain was only faintly visible to the eye.

However, the electron micrograph shows a heavy concentration of carbon particles which are relatively homogeneous in size. Notice the tendency of this material to form chains; this is typical of carbon black. These particles vary from about 60 to 150 mμ. This particle size range corresponds to the commercial thermal blacks and is larger than most carbon black used in detergency studies.

Figure 2 is a graphite stain from a T-shirt. This stain was quite heavy and had survived numerous washings. The fibers were degreased in carbon tetrachloride before the electron micrograph was taken. The graphite is present as thin plates and the smaller graphite flakes are roughly hexagonal. The interesting thing about this micrograph is the large size of some of the graphite particles that were not removed by laundering. The largest particle

near the center of the field is 2.5 μ at its widest dimension; most of the smaller graphite crystals are about 125–300 mμ.

Figure 3 is the clay mineral kaolinite deposited on a clean cotton fiber. Notice the size of the clay particles in comparison to the fibrils. The fibrils are about 15–30 mμ in diameter, while the clay particles vary from 60 to 600 mμ. This material was applied by dipping the cloth in a dilute slurry of clay and water and rinsing the excess off with distilled water. No attempt was made to remove the clay by washing.

Most clay minerals occur as pseudohexagonal plates. Figure 4 is bentonite. The chief clay mineral occuring in bentonite is montmorillonite, which has very small crystals. However, some clay minerals have other shapes. Figure 5 is the clay mineral attapulgite; it has a lathlike structure. Attapulgite is not widely distributed, but is found mainly in Georgia and Florida and is used extensively as fullers earth. A common clay mineral which is rod-shaped is halloysite. Actually, halloysite is a thin plate which is curled to form a tube but gives the appearance of being a rod. Figure 6 is an electron micrograph of Ohio glacial till showing typical clay particles that make up soil.

Figure 7 shows a cotton fiber taken from a freshly washed but heavily deposited four-year-old T-shirt. The reflectance of this shirt dropped from an original value of about 91% down to 65% because of soil build-up. The "b" value on the Gardner Color Difference Meter was about +3, which indicates that material is present which is causing yellowing. This fiber is coated with amorphous organic material. A number of particulates are present, but they are obscured by organic material so that their shape or size is not well defined.

Figure 8 is a fiber from the same T-shirt which had the organic material removed with fat solvents. This fiber is heavily deposited with a variety of rod- and plate-shaped particles. They vary in size from about 30 to 750 mμ, but the majority are between 100 and 200 mμ.

Figure 9 is a cotton fiber from an Indianhead towel which was included in ten normal wash loads to study the type of material absorbed by cotton from the wash bath. This material was removed from dirty clothes and then redeposited on the clean cotton surface of the towel. The larger dense gummy

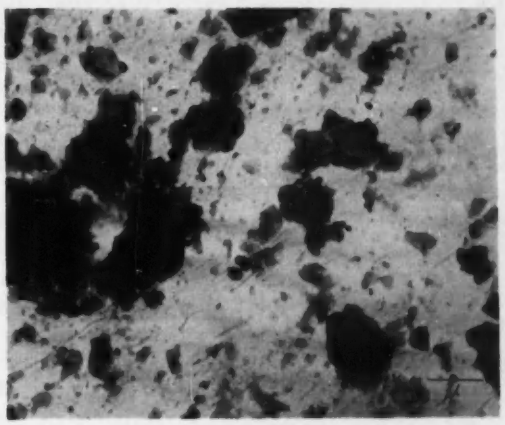

Fig. 6. Electron micrograph of Ohio glacial till showing typical clay particles present in soil.

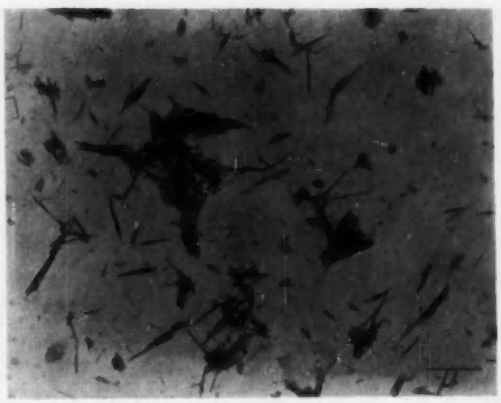

Fig. 5. Electron micrograph of the clay mineral attapulgite showing its lathlike structure.

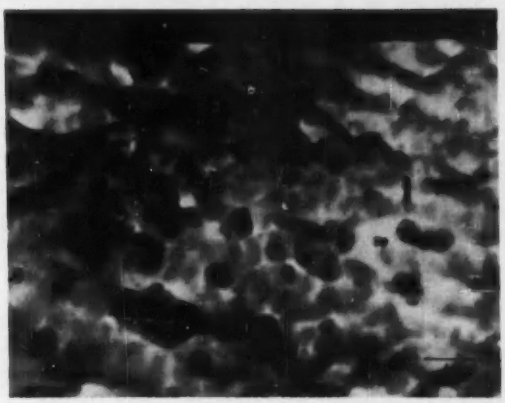

Fig. 7. Electron micrograph of a surface replica of a soiled cotton fiber. The fiber surface and particulate material on the fiber are obscured by amorphous organic material.

areas are pieces of cotton fiber which adhered to the carbon replica. The large particle near the center is clay or graphite and is about 1 μ at its widest dimension. The smaller particles are primarily small clay flakes that average about 100 mμ. Notice that some of these particles are rod shaped.

Figure 10 is a lateral section of a cotton fiber showing that the material causing soil build-up has not penetrated the fiber. The surface of the fiber separated from the main part of the fiber during sectioning.

Discussion

These electron micrographs strongly suggest that under average conditions clay minerals are the major particulate material that contributes to soil build-up on textile fibers. Even without visual proof, clay minerals have a number of properties that make them suspect.

What are the clay minerals? Grim [3] states that the clay minerals are a small group of minerals which are "essentially hydrous aluminum silicate with magnesium or iron proxying wholly or in part for aluminum in some minerals and with alkalies or alkaline earths present or essential constituents in some of them."

These minerals are so named because they compose the major part of clay and contribute most to its properties. Some of the more common clay minerals are kaolinite, halloysite, montmorillonite, and illite. A typical analysis of some clay minerals is given in Table I.

No significance should be placed on minor differences in the analysis of these minerals because their content will vary considerably depending upon where they were obtained. Notice, however, that kaolinite is rich in aluminum, attapulgite in magnesium, and illite in potassium.

Clay minerals are very small. Their upper size limit is about 2 μ; most non-clay minerals do not break down to particles smaller than 1 μ. The lower size limit for discrete particles of the finer clays is about 20 mμ [3].

Clay minerals are thin in at least one dimension; in their maximum dimensions they may be pseudo-hexagonal, lath, or rod-shaped. Some types of montmorillonite are only 2 mμ thick. The ratio of areal diameter to thickness may be as large as 100–

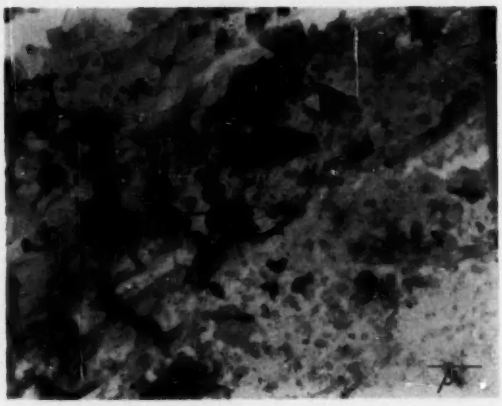

Fig. 9. Electron micrograph of a surface replica of redeposited soil from wash water on a cotton fiber. The dense gummy areas are pieces of cotton fiber which adhered to the carbon replica.

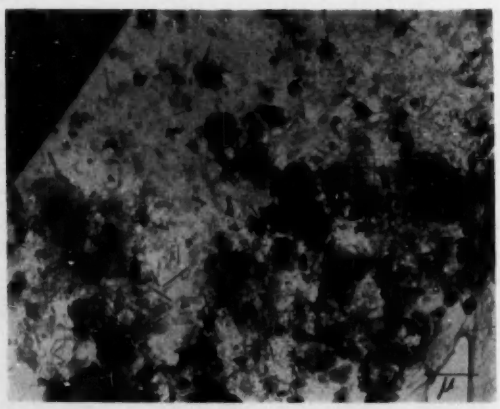

Fig. 8. Electron micrograph of a surface replica of a heavily soiled cotton fiber. Most of the deposited materials are clay minerals.

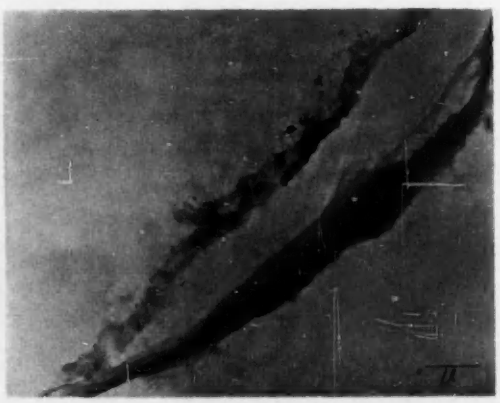

Fig. 10. Lateral section of a cotton fiber showing that the soil has not penetrated the fiber.

300 to 1 [3]. This presents a large surface area per mass, which makes an ideal adsorptive surface.

Typically, clay minerals are referred to as being colloidal, and most clay particles are colloidal in more than one dimension [4]. The colloidal range extends from about 3 to 200 mμ. Discrete clay particles are generally less than 100 mμ thick and if thicker are easily broken down into thin flakes or plates.

Clay minerals have an active surface and are capable of ion exchange. Exchange capacity varies with the type of clay mineral. Kaolinite has relatively low exchange abilities (3–15 meq. cation exchange capacity per 100 g.) and montmorillonite is high (80–150 meq. per 100 g.). The common exchangeable cations are Ca^{++}, Mg^{++}, H^+, NH_4^+, and Na^+; the common exchangeable anions are SO_4^{--}, Cl^-, PO_4^{3-}, and NO_3^- [3].

Clay minerals absorb pigmented organic material to give a gray or black appearance. A very small amount of organic material may have a strong pigmenting effect [3]. Inorganic materials such as iron oxide also color clay. The use of clay to remove color bodies from organic materials is well known.

Clay particles are ideal particles to adhere firmly to textile fibers because they are small, behave as colloids, have an active surface, and probably what is most important, have a large surface area in proportion to their mass.

Because clay minerals are ubiquitous, readily reduced to their ultimate particle size by agitation in water, and are naturally pigmented or can become pigmented by absorbing organic matter, they are suspect as a major cause of soil build-up and redeposition and the resulting deterioration in the appearance of the fabric.

In general, the smaller a particle the stronger it will adsorb to the fiber surface. But the geometry of the particle also has an effect. Carbon black, which has a minimum of surface in contact with the fiber because it is roughly spherical or ellipsoid, will not be as strongly absorbed as a thin plate of clay or graphite of the same mass.

TABLE I. Typical Analyses of Clay Minerals

	Kaolinite	Montmorillonite	Attapulgite	Illite
SiO_2	45.4	51.2	55.0	51.2
Al_2O_3	38.5	19.8	10.3	25.0
Fe_2O_3	0.8	0.8	3.5	4.5
FeO	—	—	—	1.7
MgO	0.1	3.2	10.5	2.8
CaO	0.1	1.6	—	0.2
K_2O	0.1	0.1	0.5	6.1
Na_2O	0.7	trace	—	0.2
TiO_2	0.2	—	—	7.5
H_2O	14.2	24.0	19.3	1.0

Accumulation of soil in the rugosities of the cotton fiber surface does not seem to be an important mechanism in soil retention, since the majority of the soil particles are about 100–200 mμ and the upper limits of the rugosities are about 50 mμ [10]. This agrees with the conclusions of Kling and Mahl [6] and Shuttleworth and Jones [9] for artificially soiled fibers.

Adsorption of the particles to the fiber surface is the chief mechanism of attachment. Whether these forces are Coulombic, Van der Waals, or hydrogen bonds is a matter of speculation; probably all three types of adsorptive bonds are involved.

The amount of organic material that can collect on a fiber is surprising; one would assume *a priori* that most of the fatty material would be removed during washing. This organic material may act as a matrix to entrap and hold particles even bigger than 1 or 2 μ.

Hemmendinger and Lambert [5] state that "The primary cause of degradation of whiteness in detergency is yellowness." One source of this yellowness is probably the natural color of clay minerals and the accumulated organic layer.

Conclusions

Clay minerals are a major cause of soil build-up and redeposition on cotton fibers.

The size of most of the strongly adsorbed particulates varies from 20 mμ to 1 μ. The average particulate is about 100 mμ in diameter.

Soil build-up is a surface adsorption phenomenon and the particulates do not normally penetrate the fiber.

The rugosities of the cotton fiber surface do not seem to be important in holding the soil particles because the particulates in most cases are larger than the upper limits of the rugosities.

A large amount of organic material may accumulate concurrently with the build-up of particulate material on the cotton fiber.

The organic material and the natural color of the clay minerals contribute to the yellowing that accompanies greying in soil build-up on cotton.

Acknowledgment

The author is pleased to acknowledge the assistance of Dr. Albert Vatter, who made the electron micrographs and furnished the clay mineral samples.

Literature Cited

1. Getchell, N. F., TEXTILE RESEARCH JOURNAL **25**, 150–194 (1955).
2. Götte, E., Kling, W., and Mahl, H., *Melliand Textilber.* **35**, 1252–1257 (1954).
3. Grim, R. E., "Clay Mineralogy," New York, McGraw-Hill (1953).
4. Hauser, E. A., "Silicic Science," New York, Van Nostrand (1955).
5. Hemmendinger, H. and Lambert, J. M., *J. Am. Oil Chem. Soc.* **30**, 163–168 (1953).
6. Kling, W. and Mahl, H., *Melliand Textilber.* **35**, 640–645 (1954).
7. Kramer, M. G., Paitchel, H., and Tidridge, W. A., "Bibliographical Abstracts on Redeposition of Soil on Cotton Fabric," ASTM Spec. Tech. Publ. 173 (March 1956).
8. Schwartz, A. M., Perry, J. W., and Berch, J., "Surface Active Agents and Detergents," Vol. II, New York, Interscience (1958).
9. Shuttleworth, T. H. and Jones, T. G., "Proceedings of the Second International Congress on Surface Activity," Vol. IV, New York, Academic Press, 52–59 (1957).
10. Tripp, V. W., Moore, A. T., and Rollins, M. L., TEXTILE RESEARCH JOURNAL **21**, 886–894 (1951).

Manuscript received June 22, 1959.

The Preparation and Properties of Partially Phosphonomethylated Cotton

Stanley R. Hobart, George L. Drake, Jr., and John D. Guthrie

Southern Regional Research Laboratory,[1] New Orleans, Louisiana

CHEMICAL reactions of cotton to produce cellulose esters and ethers are numerous. Until recently, phosphorus-containing compounds which have been chemically reacted with cotton have produced products which have an ester linkage between the phosphorus and the cellulose. Examples of these are phosphorylated cotton [3, 5, 10], produced by curing cotton with a mixture of phosphoric acid and urea, and phosphatoethyl cotton [2], prepared by reacting a mixture of sodium 2-chloroethyl phosphate and sodium hydroxide with cotton.

The preparation of a new phosphorus-containing ether of cotton cellulose, phosphonomethyl cotton, has been described recently [4]. This is a partial ether of cellulose prepared by the reaction of chloromethylphosphonic acid with cotton in the presence of sodium hydroxide. The reaction may be represented as

$$\text{Cell OH} + \text{ClCH}_2\text{P(O)(OH)}_2 + 3\ \text{NaOH} \rightarrow \text{Cell OCH}_2\text{P(O)(ONa)}_2 + \text{NaCl} + 3\text{H}_2\text{O}$$

[1] One of the laboratories of the Southern Utilization Research and Development Division, Agricultural Research Service, U. S. Department of Agriculture.

Inasmuch as the reaction of chloromethylphosphonic acid with cotton took place readily, it was decided to investigate the reaction further, to demonstrate that commercial-scale equipment could be used for the processing, and to evaluate the product.

The degree of substitution may be controlled by varying the concentration of reactants and the reaction conditions. Properly controlled phosphonomethylation produces a permanently starched effect

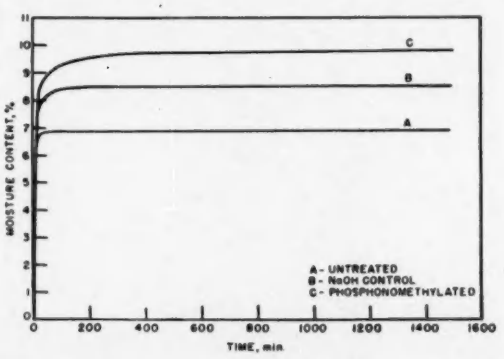

Fig. 1. Moisture regain vs. time for phosphonomethylated 80 × 80 print cloth.

even at moderate degrees of substitution. A high degree of phosphonomethylation brings about radical changes in fabric properties, including water solubility.

New chemical properties obtained are cation exchange and, in the ammonium salt form, flame resistance. The phosphorus introduced into cotton by phosphonomethylation is more firmly bound than in phosphorylated or phosphatoethyl cotton by virtue of the direct phosphorus-to-carbon linkage [7]. Full and uniform dyeings may be obtained with basic dyes. Furthermore, the presence of the acid groups presents an opportunity for further chemical modification of the cotton.

Experimental

Materials and Methods

The fabrics used were standard types 4.8 oz./sq. yd. 48 × 48 cotton sheeting and 3.3 oz./sq. yd. 80 × 80 cotton print cloth which had been desized, scoured, and peroxide-bleached.

The chloromethylphosphonic acid and sodium hydroxide were commercial grade materials.

Preparation of the treating solution consisted of mixing, with cooling, two solutions, A and B. Solution A was made by dissolving 16.25 lb. of NaOH in 30.2 lb. of water and allowing to cool overnight. Solution B was made by dissolving 3.3 lb. of chloromethylphosphonic acid in 8.2 lb. of water and neutralizing by adding a solution of 2 lb. of sodium hydroxide in 5 lb. of water while keeping the temperature below 20° C. Solution A was then added slowly to Solution B while keeping the temperature below 20° C. with cooling. The final solution weight was 65 lb., consisting of 6.8% disodium salt of chloromethylphosphonic acid and 25% NaOH. Fabric was padded through the solution immediately to minimize the possibility of removal of the chlorine atom by hydrolysis prior to use. Commercial scale equipment was used for processing the fabric.

The textile tests were performed under controlled conditioning of 70° F. and 65% RH. Standard methods were employed for the following tests: dry crease recovery angle by the Monsanto method [1a]; tearing strength by the Elmendorf [1b] and tongue [1c] methods; raveled strip breaking strength, elongation at break, weight, thickness, and yarns per inch [1c]; flex abrasion resistance by the Stoll method [1d]; air permeability [1e] using the Permeometer; and stiffness by the Tinius Olsen method [12a]. Flame retardancy was measured both by the standard vertical test [12b] and by the Guthrie strip test method [9]. The latter consists in igniting the end of a 1-cm. wide strip of fabric held by one end with the fabric surface vertical and determining the angular position at which it must be held for the flame to go out. For example, if a strip is held vertically by the bottom and the flame goes out when it is ignited at the top, it is said to have passed the 0° flame test, which requires very little flame resistance; on the other hand, if the same strip is rotated through 180° and the flame goes out when it is ignited at the same end (now the bottom), it is considered to have passed the 180° flame test and has the highest degree of flame resistance. If the flame goes out when the strip is held with the long edge horizontal and the fabric surface vertical it is said to have passed the 90° flame test and to be moderately flame resistant. Strips of the cloth prior to the treatment burned continuously even when held vertically and ignited at the top. Samples which pass the 135° angle test generally pass the standard vertical flame test.

Phosphorus was determined by the colorimetric reduced molybdate method after digestion with sulfuric acid and hydrogen peroxide [8].

The samples were prepared for moisture equilibration from the dry state by drying in a forced draft oven at 110° C. for 40 min. For equilibration from the wet state the samples were soaked in distilled water overnight and passed through the laboratory pad rolls once at number 1 squeeze setting. These samples were then hung in a room conditioned at 65% RH and 70° F. and weighed periodically, thereby determining the rate of moisture equilibration.

Treatment of Fabrics

One hundred yards of 80 × 80 print cloth and 25 yd. of 48 × 48 sheeting were padded through the treating solution twice to obtain a total wet pick-up of 139%. The fabrics were heated on drying cans at 125° C. for 13 min. and washed on the jig. The wash consisted of 6 ends cold running tap water (pH 10) and 6 ends hot tap water (170° F.); the pH of the water from the final wash was then the same as that of the tap water. The wet fabric was passed through squeeze rolls using maximum pressure to remove excess water. This was followed by drying on the tenter frame to a width of 35 in.

Fabric widths for the 80 × 80 print cloth during

the processing were initially 36¾ in., 35 in. after padding and before curing, and 32 in. after washing. The width of the 48 × 48 sheeting was 36¼ in. initially, 34½ in. after padding, 31 in. after curing, and 31¾ in. after washing.

Twenty-two yards of half width phosphonomethylated print cloth and 4.5 yd. of half width phosphonomethylated sheeting were treated together a second time with the same solution, which had aged overnight at 7° C. They were padded through the solution twice on the 20-in. laboratory pad rolls, obtaining a wet pick-up sufficient for the solution to be dripping from the fabric roll. They were then passed over drying cans at 125° C. for 13 min. and washed on a winch. The washing consisted of 4 5-min. cold water washes, 2 10-min. hot water (170° F.) washes, and an additional cold water wash. Excess water was removed by squeezing with the pad rolls and the fabrics dried on the tenter frame.

After washing, the twice treated fabrics were highly swollen and very slick, making them difficult to maneuver on the tenter frame. The drying was very slow, particularly for the sheeting.

For comparative purposes sodium hydroxide control fabrics were also prepared. One hundred yards of 80 ×80 print cloth and 30 yd. of 48 × 48 sheeting were padded twice through 25% NaOH obtaining a total wet pick-up of 135%. They were dried on the cans at 125° C. for 13 min. The washing on the jig consisted of 4 ends in cold running tap water, 4 ends in hot tap water (170° F.), 2 ends in cold running tap water, souring in 0.5% acetic acid, 4 ends in cold running tap water, and 3 ends in hot tap water. The fabrics were dried and pulled out to a width of 35 in. on the tenter frame. The 80 ×80 print cloth was 36¾ in. wide initially and 31 in. wide after washing. The 48 × 48 sheeting was 36¼ in. wide initially and 32 in. wide after washing.

The phosphonomethylated fabrics obtained were largely in the sodium salt forms. Samples were converted to the ammonium and copper salt forms by way of the free acid form. The acids were made by soaking the fabrics in 5% HCl for 1 hr. and then soaking in distilled water for 2 hr. to remove the greater portion of the excess HCl. The ammonium salts were made by soaking the acid form in 5% NH_4OH solution for 1 hr., rinsing in distilled water, and air-drying. The copper salts were made by soaking the acid form in 5% copper acetate solution for 1 hr. and soaking in 3 changes of distilled water over a 1-hr. time, followed by air-drying. Conversion to the copper salts imparted a light blue color to the fabric.

Properties

The phosphorus contents of the 80 × 80 print cloths, phosphonomethylated as described and in the sodium salt forms, are 0.72% for the single treatment and 1.66% for the double treatment; these are degrees of substitution of 0.04 and 0.09, respectively. Phosphorus contents of the 48 ×48 sheetings in the sodium salt forms are 0.95% for the single treatment and 1.83% for the double treatment; 0.05 and 0.10 degrees of substitution, respectively.

The fabric properties of the treated and control fabrics are shown in Table I. Single phosphonomethylation produced only two significant changes in the textile properties. The stiffness of the 80 × 80 print cloth was increased to 7 times that of the untreated control and the stiffness of the 48 × 48 sheeting was increased to 40 times that of its untreated control. Treatment of 48 × 48 sheeting with NaOH alone increased the stiffness by 8 or 9 times. The wet crease recovery of cotton was apparently greatly improved by phosphonomethylation. When a piece of treated fabric was wrinkled thoroughly and then put in water, the wrinkles disappeared.

Several significant changes in the textile properties resulted from a double phosphonomethylation. Stiffness was greatly increased, especially for the 48 × 48 sheeting, for which it was 100 times the untreated control in the filling direction. Tearing strength and dry crease resistance, properties related to stiffness, were greatly reduced, especially for the 48 × 48 fabric, but wet crease resistance was increased. Breaking strength, however, was not greatly altered except for the 48 × 48 material, which was half as strong in the filling direction. Air permeability was increased for a single phosphonomethylation, but was reduced to ⅐ and ½ for the 80 × 80 and 48 × 48 fabrics, respectively, after the double phosphonomethylation. The latter results indicate fiber-to-fiber bonding at the surface, which probably results from the tendency of the fabrics to go into solution at these higher degrees of substitution. An unexplained anomaly was the reduction of flex abrasion resistance of 80 × 80 print cloth to less than half of the untreated control by a double phosphonomethylation, whereas the 48 × 48 sheeting

underwent a small increase in this property over its control by this treatment.

The firm attachment of the phosphorus of these fabrics is shown in Table II for singly phosphonomethylated 80 × 80 print cloth. Three samples of the fabric were boiled for 3 hr. in water, 2% NaOH, and standard soap [11] and soda solution (0.5% standard soap and 0.2% sodium carbonate), respectively, with no attendant lowering of phosphorus content. The slight increases in phosphorus content may be explained by ion exchange of the sodium salt with the cations of the tap water used for washing.

Figures 1 and 2 show the moisture equilibration rates of the sodium salt form of singly phosphonomethylated 80 × 80 print cloth from the bone dry and wet states, respectively, at 70° F. and 65% RH. As shown by the curves, the rate of moisture regain from the dry state is the same for phosphonomethylated cotton as for the untreated and sodium hydroxide controls; however, the former is more hydrophilic and attains a higher final moisture content. The loss of excess water from the wet

TABLE II. Stability of 80 × 80 Phosphonomethylated Print Cloth to Alkaline Boil

	Before boil	After 3-hr. boil in H_2O	After 3-hr. boil in 2% NaOH	After 3-hr. boil in Standard soap and soda
Phosphorus content, %	0.72	0.78	0.76	0.77

TABLE I. Textile Properties of Phosphonomethylated Cotton

		80 × 80 Print cloth				48 × 48 Sheeting			
		Untreated	NaOH control	Phosphonomethylated	Doubly phosphonomethylated	Untreated	NaOH control	Phosphonomethylated	Doubly phosphonomethylated
Phosphorus content sodium salt form, %		—	—	0.72	1.66	—	—	0.95	1.83
Thread count	W	83	89	87	96	54	53	54	60
	F	77	77	79	85	46	48	49	52
Breaking strength, strip, same T.C. as original, lb.	W	47.5	46.3	50.3	52.5	69.2	70.5	73.1	64.8
	F	37.8	36.0	39.8	31.9	41.9	45.1	39.8	22.1
Elongation at break, %	W	9.4	9.5	13.5	19.4	9.3	11.1	16.9	16.5
	F	17.7	22.2	22.3	27.9	23.2	22.8	25.1	24.7
Tearing strength Elmendorf, g.	W	1256	1360	1224	872	2010	1830	1770	928
	F	968	956	796	472	1100	1130	850	376
Tongue, lb.	W	4.1	4.4	4.4	3.3	5.2	5.7	5.3	3.8
	F	4.2	4.0	3.8	2.0	4.1	4.6	3.6	1.8
Abrasion resistance, flex, cycles	W	1735	1451	1458	679	578	559	721	667
	F	1540	1066	1172	390	410	572	728	834
Wrinkle recovery angle, dry, deg.	W	77	92	66	49	85	60	24	26
	F	84	95	74	58	86	79	36	20
Stiffness, bending moment $\times 10^{-4}$, in.-lb.	W	4.8	5.5	37.4	154.5	11.3	108.0	432.0	615.0
	F	2.2	2.3	9.3	38.1	2.6	20.4	107.2	311.6
Weight, oz./yd.^{2}		3.29	3.62	3.79	4.40	4.78	5.04	5.53	5.84
Thickness, in.		0.0073	0.0077	0.0080	0.0093	0.0112	0.0113	0.0126	0.0138
Air permeability, ft.^{3}/min./ft.^{2}		88	123	105	12	73	199	127	37

state occurs at about the same rate for the phosphonomethyl cotton as for the sodium hydroxide control (slightly slower than the untreated cotton); again a higher final moisture content is attained. The well-known phenomenon of attaining a higher moisture content on equilibration from the wet state than when equilibrating from the dry state was observed for all of the fabrics.

The phosphonomethylated fabrics showed some flame retardancy in the sodium salt form, but more in the ammonium salt form. The flame retardancy of the ammonium salts of some phosphonomethylated fabrics is shown in Table III. The ammonium salts of both the singly phosphonomethylated 48 × 48 sheeting and 80 × 80 print cloth failed the standard vertical flame test. Sufficient flame retardancy for passing the standard vertical flame test may be obtained by a single phosphonomethylation by increasing the concentration of chloromethylphosphonic acid in the reaction mixture to introduce more phosphorus [4]. The doubly phosphonomethylated fabrics contained 1.66% phosphorus for the 80 × 80 print cloth and 1.83% phosphorus for the 48 × 48 sheeting: they passed the standard vertical flame test in their ammonium salt forms.

TABLE III. Flame Retardancy of Phosphonomethylated Cotton Fabrics

Description	Phosphorus content,* %	Flame retardancy: Standard vertical char length, in.	Flame retardancy: Strip angle, deg.
80 × 80, phosphonomethylated, NH_4 salt	0.72	B.E.L.†	90
80 × 80, doubly phosphonomethylated, NH_4 salt	1.66	4.0	135
48 × 48, phosphonomethylated, NH_4 salt	0.95	B.E.L.†	145
48 × 48, doubly phosphonomethylated, NH_4 salt	1.83	3.2	160

* In the sodium salt form.
† Burned entire length.

Soil burial tests on the 80 × 80 fabrics showed the copper salt form to be superior in rot resistance to the controls and to the sodium and ammonium salt forms. The degree of rot resistance is not, however, comparable to that imparted by commercial rot resistance treatments. Burial of a limited number of samples of doubly phosphonomethylated 80 × 80 print cloth in the copper salt form was conducted. At the end of 8 weeks, 5.2% of the breaking strength of the treated sample was retained. These results are shown in Table IV.

Weathering of these fabrics is in progress, but the phosphonomethylated fabrics have not shown any advantage over untreated fabric to date.

Cation exchange capacities for some phosphonomethylated 48 × 48 sheetings are shown in Table V. The fabric with 3.95% phosphorus content had a cation exchange capacity of 2.333 meq./g. This is comparable to commercial cation exchange resins. These values are in good agreement with the values calculated on the basis of the phosphorus content of the fabrics. A plot of cation exchange capacities at different pH levels for a fabric containing 2.0% phosphorus is shown in Figure 3. The two breaks in the curve are for the first and second hydrogens of the phosphonic acid. The pH at half capacity for each of these segments of the curve may be taken as an approximation of the pK_a of the acid groups [4, 6]. For example, in the first segment of the curve in Figure 3 the pH at half capacity, and consequently pK_a, are approximately 2.3. Similarly,

TABLE IV. Effect of Soil Burial on the Breaking Strengths of the Copper Salts of Phosphonomethylated Cottons

Description	Warp breaking strength, strip, lb.*: Weeks of burial 0†	1	3	4	8
80 × 80, phosphonomethylated	49.8	45.6	8.1	1.8	0
80 × 80, doubly phosphonomethylated	46.2	47.5‡	—	33.4‡	2.4**

* For same thread count as untreated.
† Untreated breaking strength was 47.5 lb.
‡ Only two breaks.
** Only one break.

TABLE V. Cation Exchange Capacities of 48 × 48 Phosphonomethylated Cottons

Phosphorus content sodium salt, %	Cation exchange capacity, meq./g.: Experimental	Calculated
0.44	0.34	0.28
0.92	0.59	0.59
1.50	1.00	0.97
2.00	1.31	1.29
3.95	2.33	2.55

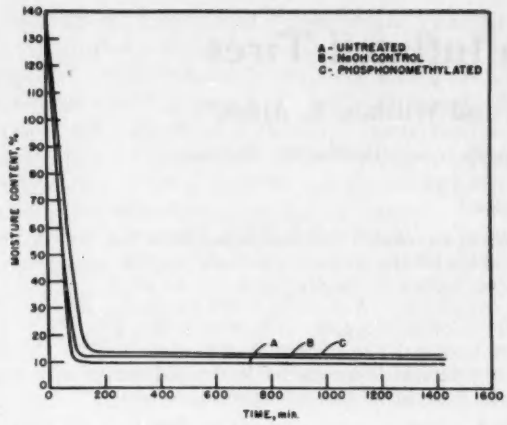

Fig. 2. Moisture loss vs. time for wet phosphonomethylated 80 × 80 print cloth.

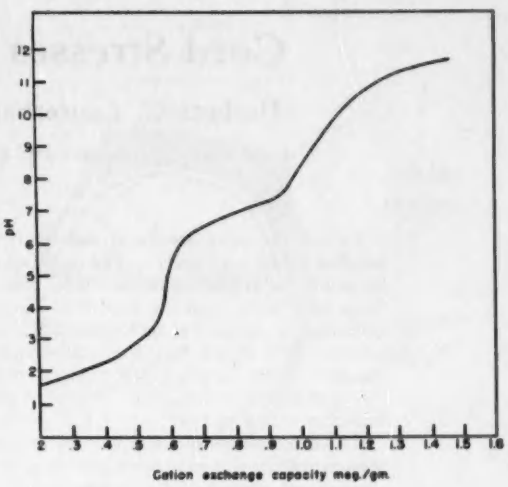

Fig. 3. Cation exchange capacity of phosphonomethylated cotton (2.0% phosphorus, 0.12 degree of substitution).

for the second segment of the curve the pH at half capacity and pK_{a_2} are approximately 7.0.

Summary

Cotton fabrics have been phosphonomethylated on commercial scale textile finishing equipment and the properties of the treated fabrics evaluated. At sufficiently high phosphorus contents the fabrics have a permanently starched feel and improved wet crease resistance. Good flame resistance is observed for the ammonium salt form of the fabrics. The treated fabrics are more hydrophilic than the controls. Stability of the phosphorus content to alkaline treatments is very high. Considerable improvement over untreated cotton is shown by the copper salt form in regard to microbiological deterioration.

Acknowledgments

We wish to thank Mr. James A. Harris and Miss Marian H. Curtis of the Instrumentation and Analysis Laboratory for the phosphorus and cation exchange capacity determinations; also, Misses Emma L. Young, Joycelyn C. Oubre, and Nancy Lee Barlow, Mr. Donald G. McArthur, and their coworkers, also of the Instrumentation and Analysis Laboratory, for the textile evaluations.

Literature Cited

1. ASTM (a) D 1295–53T; (b) D 1424–56T; (c) D 39–49; (d) D 1175–55T, Pt. B; (e) D 737–46T, American Society for Testing Materials, Philadelphia.
2. Chance, L. H., Warren, Jane, and Guthrie, J. D. (to Secretary of Agriculture of the United States), U. S. Patent 2,743,232 (April 24, 1956).
3. Coppick, S. and Hall, W. P., in "Flameproofing Textile Fabrics," edited by R. W. Little (A.C.S. Monograph 104), New York, Reinhold, 179 *ff.* (1947).
4. Drake, G. L., Jr., Reeves, W. A., and Guthrie, J. D., TEXTILE RESEARCH JOURNAL **29**, 270–275 (1959).
5. Ford, F. M. and Hall, W. P. (to Joseph Bancroft & Sons Company), U. S. Patent 2,482,755 (September 27, 1949).
6. Hoffpauir, C. L. and Guthrie, J. D., TEXTILE RESEARCH JOURNAL **20**, 617–620 (1950).
7. Kosolapoff, G. M., "Organophosphorus Compounds," New York, Wiley (1950).
8. Pons, W. A., Jr., Stansbury, M. F., and Hoffpauir, C. L., *J. Assoc. Offic. Agr. Chemists* **36**, 492–504 (1953).
9. Reeves, W. A., McMillan, O. J., Jr., and Guthrie, J. D., TEXTILE RESEARCH JOURNAL **23**, 527–532 (1953).
10. Reid, J. D., and Mazzeno, L. W., Jr., *Ind. Eng. Chem.* **41**, 2828–2831 (1949); Reid, J. D., Mazzeno, L. W., Jr., and Buras, E. M., Jr., *Ind. Eng. Chem.* **41**, 2831–2834 (1949).
11. U. S. Federal Supply Service, "Soap; Chip," Federal Specification P-S-566b (1), U. S. Government Printing Office, Washington, D. C. (1952).
12. U. S. Federal Supply Service, "Textile Test Methods," Federal Specification CCC-T-191b, U. S. Govt. Print. Off., Washington, D. C. (1951), (a) Method 5202; (b) Method 5902.

Manuscript received May 18, 1959.

Cord Stresses in Inflated Tires

Herbert G. Lauterbach[1] and William F. Ames[2]

E. I. du Pont de Nemours and Company, Inc., Wilmington, Delaware

Abstract

In order to calculate the stresses in the cords of an inflated tire, membrane theory is applied to the cord body. The equation describing the tire surface in terms of tire construction parameters and cord properties has been given in the literature, but no solutions have been reported, probably due to its complexity. A solution of this equation, obtained by numerical techniques on a digital electronic computer, is presented in this paper. It is shown how this equation is combined with the equilibrium equations of the surface and how the force components in the principal directions are determined and the cord stresses calculated. The cord stresses in inflated tires are nonuniform, decreasing from crown to bead.

The deformation of a simple cord network is considered, and it is shown how the cord stretch during tire expansion can be determined. It is found that the cord undergoes nonuniform stretch and shrinkage from crown to bead. These calcuations have been confirmed by experimental x-ray measurements on metal-shadowed cord. It is suggested that the calculated and observed nonuniform cord stretch and shrinkage during tire expansion and curing are a direct result of the nonuniform cord tension.

Introduction

Basic Concepts

The pneumatic tire is a composite of rubber, textile cord, and steel, ingeniously combined to provide support of load, transfer of power, maintenance of direction, shock absorption, and riding comfort. The heart of the tire is the carcass, consisting of layers of textile cords interspersed with sufficient rubber to provide a cohesive matrix. The carcass is covered on its outside with a protective layer of rubber. In the sidewall area this rubber layer is of about the same thickness as the carcass. Its function is to protect the carcass from abrasion. The rubber layer may be much thicker than the carcass in the shoulder and tread areas, where is provides bruise protection in addition to abrasion resistance and road grip. The carcass fabric is anchored to two steel hoops called beads which seat firmly against the rim and through the latter provide the necessary connection between the tire and the wheel. The various parts and regions of the tire just mentioned [16] are illustrated in Figure 1.

This paper is concerned principally with the carcass of the tire and with the stresses produced in its component textile cords by the inflation pressure. Since these stresses are influenced by the construction of the tire, the nature of the textile reinforcement of the carcass and the most common present-day method of tire construction will be discussed briefly.

The fabric which makes up the layers or plies of the carcass consists of rather closely spaced parallel cords loosely interwoven with light, widely spaced filling threads. The filling serves only to hold the cords together during early stages of fabrication, while the strength of the carcass is derived from the cords. The cords of modern tires are made up of multiple continuous lengths of either nylon or rayon filaments twisted into cord form. The twisted cord is a flexible structure able to resist fatiguing from the cyclic stresses occurring in running tires. The strength and the resistance to growth or to thermal shrinkage of these cords, particularly of those made from nylon, can be enhanced considerably by subjecting the cords to a hot-stretching and annealing treatment before use. In practice, this treatment is advantageously performed on the cord fabric while it is being coated with the adhesive required to bond it tightly to rubber and prior to the application in a calender of that thin layer of "skim" or matrix rubber which, with the cord, will later form the carcass.

[1] Industrial Products Research Laboratory, Textile Fibers Department.

[2] Engineering Service Division, Engineering Department. Present address: Mechanical Engineering Department, University of Delaware, Newark, Delaware.

Present-day tires are fabricated by the so-called tire expansion process, schematically illustrated in Figure 2. The carcass is built on a cylindrical drum by applying pieces of the fabric described above. The length of each piece equals the circumference of the drum. The piece, also called layer or ply, is cut so that the cords make an angle α with the center line, as shown in Figure 2. The layer next following will be identical to the first except that its cords will make an angle $-\alpha$ with the center line. This process is continued, usually reversing the sign of the angle for each successive layer, until the carcass has been built up. The usual number of layers or plies in a passenger tire is four. The carcass fabric is wrapped around the beads at each end of the drum. The protective sidewall and tread rubber is then applied over the carcass. The process which follows is designed to bring the tire from its present cylindrical shape into its final toroidal shape by expanding it either by vacuum or pressure in the manner shown in Figure 2. One may visualize the expansion process by the simplified picture of the beads being pushed together while the center is pulled out. In this expansion process the cord angle α changes to the angle β, as illustrated in Figure 2. While the cord angle α of the cylindrical (or "green") tire is constant, the angle β of the toroidal or expanded tire is not constant but changes from point to point. Since the cord stresses in the tire are determined by the values of β, it is important to know the relationship between α and β as a function of the expansion process. This knowledge is also required to determine the performance characteristics of the tire which are governed by the cord angle. Stability and softness are examples of such characteristics. In order to construct the tire, the width of the drum (also called drum distance or drum setting) must be specified in addition to the angle α. These construction concepts will be used in this paper, but detailed discussion of fundamental concepts of tire construction will be deferred to later papers.

The remaining step in fabricating the tire is the curing or vulcanization, in which the toroidal tire is heated to a temperature sufficient to vulcanize the elastomer while the tire is being forced against a mold by internal pressure.

This brief description of the tire fabrication process and of some of the tire constituents has introduced terminology and physical concepts which will be used throughout the following discussion.

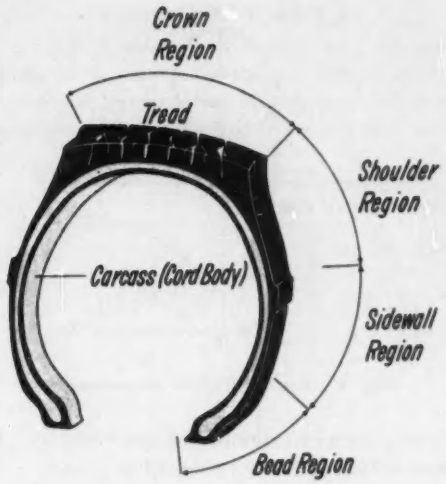

Fig. 1. Tire nomenclature.

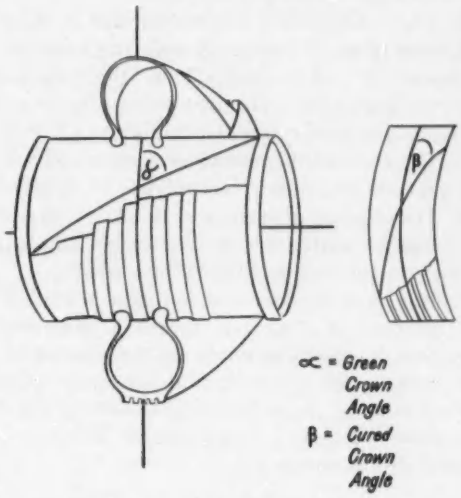

Fig. 2. Tire construction and expansion.

Specific Problem

The specific problem considered in this paper is the calculation of the stress distribution in an inflated but undeflected tire [3, 6, 8, 9, 11, 15]. To accomplish this, an idealization of the actual tire has been adopted. This "ideal" tire has been partially discussed in the literature. It has the following properties.

1. Since the tire carcass is the primary stress medium, the existence of the protective rubber layer is neglected. Measurements of dimensions are

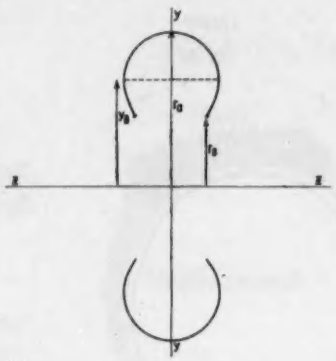

Fig. 3. Tire construction parameters.

made on a tire with sidewall and tread rubber. The thickness of the protective rubber layer is subtracted from the measurements to obtain the carcass dimensions used in the calculations.

2. The tire carcass is thin-walled, that is, the wall thickness is small compared with the over-all dimensions of the carcass. Thus the membrane theory of elasticity can be used to describe the stress configuration in the tire at equilibrium [8, 9, 11].

3. The cords all lie in the same plane. That is, the plies are assumed to be coplanar [8, 9, 12].

4. The physical properties of the matrix in which the cords are embedded are not specifically introduced into the mathematical formulation.

5. The cords are assumed to follow a variant of the "pantographic" action—that is, a network deformation in which the cords are flexibly linked at their intersection points and do not move relative to each other at those points as a result of the deformation [7, 9, 12]. Deformation between the hinge points is unrestrained.

The method selected [5, 10] involves a mathematical description of the tire surface (considered as a surface of revolution) in terms of basic tire construction parameters; the equations of equilibrium for this membrane; the equations for the force components in the principal directions; and the resulting stresses in the cords.

The solution of this problem in following the steps above is not difficult, except for the intractability of the description of the tire surface.

Symmetry of the inflated, undeflected tire makes it possible to reduce the description of the tire surface (torus) to the two-dimensional problem of mathematically characterizing the tire meridian. The meridian shape (Figure 3) of the inflated tire is given [9] as a mathematical expression involving such tire construction parameters as cord angle, cord extension ratio, and tire dimensions. The basic assumptions and derivations are completely described in the literature [9, 11]. We shall review them briefly, show their application and experimental check, derive general expressions for the principal stresses and the cord tensions, and present calculations and measurements of cord strains in expanded tires. Results are also discussed.

The Tire Meridian and Equilibrium Equations

The assumptions of the membrane theory of elasticity, for shells of revolution, were used by Martin [11] and Hofferberth [9]. The latter author found that the meridian shape of the inflated tire carcass (Figure 3) could be mathematically expressed as a hyperelliptic integral of the form

$$Z = \int f(y)dy = \int \left\{ \frac{(y^2 - y_B^2)\left[c_t^2 \frac{r_s^2}{\cos^2\alpha} - y^2\right]^{\frac{1}{2}} dy}{\left[(r_a^2 - y_B^2)^2\left(c_t^2 \frac{r_s^2}{\cos^2\alpha} - r_a^2\right) - (y^2 - y_B^2)^2\left(c_t^2 \frac{r_s^2}{\cos^2\alpha} - y^2\right)\right]^{\frac{1}{2}}} \right\} \quad (1)$$

where c_t = cord extension ratio as defined [6] (assumed constant in the derivation), y_B = height of maximum section width, r_a = maximum tire radius, r_s = drum radius, and α = green fabric cord angle (with the circumference).

From the theory of elasticity of this membrane, it is well known [5, 9, 10, 11] that the equations of equilibrium are

$$\left.\begin{aligned} \frac{1}{r_1}\frac{\partial(Ty)}{\partial\phi} + \frac{\partial N_\theta}{\partial\theta} + T\cos\phi + p_\theta y = 0 \\ \frac{1}{r_1}\frac{\partial(N_\phi y)}{\partial\phi} + \frac{\partial T}{\partial\theta} - N_\theta\cos\phi + p_\phi y = 0 \\ \frac{N_\theta}{r_2} + \frac{N_\phi}{r_1} = p_r \end{aligned}\right\} \quad (2)$$

where N_θ = force in the direction of the tangent to the parallels, N_ϕ = force in the direction of the

tangent to the meridians, $T = N_{\theta_\phi} = N_{\phi\theta}$ = shearing force, p_θ = load component in the direction of the parallel circle tangent, p_ϕ = load component in the direction of the meridian tangent, p_v = load component normal to the surface, and r_1, r_2 = radii of curvature in the meridian and parallel direction, respectively. Hofferberth [8] follows Flugge [5] and Love [10] in setting

$$\begin{aligned} \bar{N}_\theta &= (y'/y \cos\phi)\, N_\theta \\ \bar{N}_\phi &= (y \cos\phi/y')\, N_\phi \end{aligned} \tag{3}$$

and rewriting Equation 2 in terms of these "reduced" stresses as

$$\left.\begin{aligned} \frac{\partial \bar{N}_\theta}{\partial\theta} + \frac{\partial T}{\partial z} + 2\frac{y'}{y}T + \sqrt{1+(y')^2}\,p_\theta &= 0 \\ \frac{\partial T}{\partial\theta} + \frac{\partial \bar{N}_\phi}{\partial z} + p_\phi y - y\cdot y' p_v &= 0 \\ \bar{N}_\theta - \frac{y''}{y}\bar{N}_\phi - [1+(y')^2]p_v &= 0 \end{aligned}\right\} \tag{4}$$

which are more amenable to solution. Here we have used the standard notation

$$y' = \frac{dy}{dz} \qquad y'' = \frac{d^2y}{dz^2}$$

Computational Techniques

Equation 1, given in the literature, represents the desired expression for the tire carcass meridian in terms of construction variables. Other considerations of two-phase reinforced structures [1,

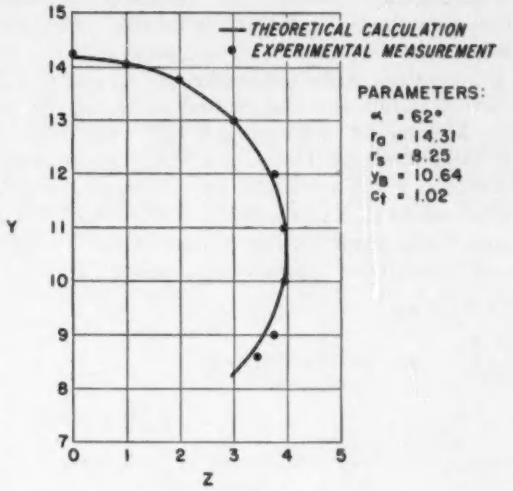

Fig. 5. Comparison of calculated and measured inflated tire contour. 8.00–15 nylon tire; 24 lb./sq. in. inflation pressure.

Tire Meridian Contour Case No. 330

8.00–15 Nylon
Height of max. width 10.639 Initial cord angle 62° Drum radius 8.250
Maximum tire radius 14.307 Extension ratio 1.02

Y	Z	0.0	0.5	1.0	1.5	2.0	2.5	3.0	3.5	4.0	4.5	5.0	5.5	6.0	6.5	7.0	7.5	8.0	8.5	9.0	9.5	10.
13.99465	1.45712	+			×																	+
13.69230	2.10723	+				×																+
13.38995	2.56734	+					×															+
13.08760	2.92131	+						×														+
12.78525	3.20252	+							×													+
12.48290	3.42823	+								×												+
12.18055	3.60867	+									×											+
11.87820	3.75035	+										×										+
11.57585	3.85756	+											×									+
11.27350	3.93315	+											×									+
10.97115	3.97895	+												×								+
10.66880	3.99597	+												×								+
10.36645	3.98454	+												×								+
10.06410	3.94432	+												×								+
9.76175	3.87425	+												×								+
9.45940	3.77239	+													×							+
9.15705	3.63567	+													×							+
8.85470	3.45929	+														×						+
8.55235	3.23570	+														×						+
8.25000	2.95220	+																				+
Y	Z	0.0	0.5	1.0	1.5	2.0	2.5	3.0	3.5	4.0	4.5	5.0	5.5	6.0	6.5	7.0	7.5	8.0	8.5	9.0	9.5	10.

Fig. 4. Computer plot of calculated tire contour.

2, 4, 11, 12, 13] have contributed very important knowledge to this field but have been restricted to inextensible cords. This inextensibility is obviously only an approximation for either rayon or nylon cords. Consequently, Equation 1 was programmed on a computer for numerical computation using the quadratic integration rule. Physical measurements of the cord carcass were taken to obtain values of the parameters y_B, r_a, and r_s and the calculation run and plotted on the computer for the standard cord angle $\alpha = 62°$. The interval of integration on y is $r_s < y < r_a$. Recognizing that at r_a, $z = 0$, we subdivided $r_a - r_s$ into twenty subdivisions each of length $\Delta y = (r_a - r_s)/20$ and applied the quadratic rule to each of the integrals over this interval. Specifically, we computed

$$z(r_a) = 0$$

$$z_1 = \int_{r_a-\Delta y}^{r_a} f(y)dy$$

$$\vdots$$

$$z_n = z_{n-1} + \int_{r_a-n\Delta y}^{r_a-(n-1)\Delta y} f(y)dy$$

This computation was iterated on c_t until a reasonable fit to the physical contour of the tire carcass was obtained. The resulting contour, as plotted on the computer, is presented in Figure 4. To compare this calculated contour with experimental data, the contour of an actual tire carcass was determined. The measurement was made on an actual tire and the known thickness of the rubber cover at each point was subtracted to obtain the dimensions of the fabric carcass. Figure 5 shows a replot of the numbers of Figure 4 compared to the actual tire contour. The theoretical curve (solid line) fitted the actual contour (experimental points shown as dots) extremely well. The parameters used for Figures 4 and 5 were $r_a = 14.31$ in., $r_s = 8.25$ in., $y_B = 10.64$ in., $\alpha = 62°$, and $c_t = 1.02$.

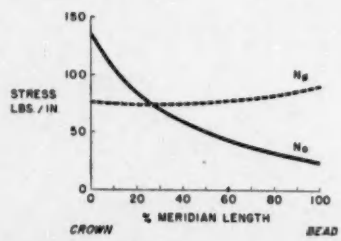

Fig. 6. Calculated tire stresses in the principal directions. 8.00–15 nylon tire; 24 lb./sq. in.; N_θ = circumferential direction; N_ϕ = meridian direction.

Since the meridian was now describable to a good approximation in terms of physical parameters of the tire it was possible to compute the stresses in the membrane and in the cords.

Principal Stresses and Cord Tensions

The stress levels in the membrane and the tensions in the cords for the equilibrium shape can be calculated from the equilibrium Equation 4 utilizing the meridian Equation 1. The derivation is shown below in terms of general $f(y)$ occurring in the tire meridian equation

$$z = \int f(y)dy$$

Thus the results obtained here can also be used when the form of the meridian is changed.

We have for the tire meridian

$$\frac{dz}{dy} = f(y) \tag{5}$$

Then

$$y' = \frac{dy}{dz} = \frac{1}{f(y)}$$

$$y'' = \frac{d^2y}{dz^2} = \frac{d}{dy}\left(\frac{dy}{dz}\right)\frac{dy}{dz} = -\frac{df}{dy}/f^3(y) \tag{6}$$

Hence

$$\sin\phi = \frac{1}{\sqrt{1 + (y')^2}} = \frac{f(y)}{\sqrt{1 + f^2(y)}} \tag{7}$$

$$\cos\phi = [1 + f^2(y)]^{-\frac{1}{2}} \tag{8}$$

$$\frac{1}{r_1} = -\frac{y''}{[1 + (y')^2]^{\frac{3}{2}}} = \frac{f'(y)}{[1 + f^2(y)]^{\frac{3}{2}}} \tag{9}$$

$$r_2 = \frac{y}{\sin\phi} = y\frac{[1 + f^2(y)]^{\frac{1}{2}}}{f(y)} \tag{10}$$

Under inflation, the load is symmetric, so that $T = 0$, $p_\theta = p_\phi = 0$, and $p_v = p$. From Equation 3 we then find

$$\frac{\partial \bar{N}_\phi}{\partial z} = y \cdot y' p \tag{11}$$

But

$$\frac{\partial \bar{N}_\phi}{\partial z} = \frac{\partial \bar{N}_\phi}{\partial y}\cdot\frac{dy}{dz} = \frac{d\bar{N}_\phi}{dy}\cdot y'$$

Hence

$$\frac{d\bar{N}_\phi}{dy} = py \tag{12}$$

or

$$\bar{N}_\phi = \frac{py^2}{2} + c = y\frac{\cos\phi}{y'}N_\phi$$
$$= yf(y)[1 + f^2(y)]^{-\frac{1}{2}}N_\phi$$

by integrating Equation 12 and substituting Equation 3 for N_ϕ. Since y_B is an extreme point, we have

$$\left.\frac{dz}{dy}\right|_{y = y_B} = f(y_B) = 0$$

so that

$$c = -p\frac{{y_B}^2}{2}$$

Hence

$$\bar{N}_\phi = \frac{p}{2}(y^2 - {y_B}^2) \tag{13}$$

and

$$N_\phi = \frac{p}{2y}\frac{(y^2 - {y_B}^2)\sqrt{1 + f^2(y)}}{f(y)} \tag{14}$$

In this calculation we have an indeterminate form at $y = y_B$ which must be avoided in the computer solution. Since

$$\frac{N_\phi}{r_1} + \frac{N_\theta}{r_2} = p$$

we can calculate

$$N_\theta = r_2\left(p - \frac{N_\phi}{r_1}\right)$$

and substituting for r_1 and r_2 from Equations 9 and 10, we have

$$N_\theta = \frac{py\sqrt{1 + f^2(y)}}{f(y)} \times \left[1 - \frac{1}{2y}\frac{(y^2 - {y_B}^2)f'(y)}{f(y)}\frac{1}{1 + f^2(y)}\right] \tag{15}$$

Figure 6 shows the comparison of the stresses N_θ, N_ϕ in the principal directions.

These stresses must be taken up by the cord carcass of the tire. Let $\beta = \beta(y)$ be the final cord angle (made with the circumference) and $n = n(y)$ be the number of cord ends per inch. Based on the assumptions of our ideal tire, we have for each unit length along the merdian circle a force

$$\frac{N_\phi}{4\sin\beta} \quad (4 \text{ plies})$$

If the cord density is $n(y)$ per unit length, then there are $n \cdot \sin\beta$ cords in the fabric of length 1 and width $\sin\beta$. Each cord supports the stress [8]

$$F_{N_\phi} = \frac{N_\phi}{4n\sin^2\beta} \tag{16}$$

Similarly

$$F_{N_\theta} = \frac{N_\theta}{4n\cos^2\beta} \tag{17}$$

Following Hofferberth [9], let c_a = extension ratio in the circumferential direction, c_b = extension ratio in the meridian direction, and c_t = extension ratio of the cord. With α = initial cord angle, Hofferberth shows that

$$c_a = c_t\frac{\cos\beta}{\cos\alpha} \tag{18a}$$

$$c_b = c_t\frac{\sin\beta}{\sin\alpha} \tag{18b}$$

Consequently

$${c_a}^2\cos^2\alpha + {c_b}^2\sin^2\alpha = {c_t}^2 \tag{19}$$

From these results we can see that since 1 in. of material, in the meridian direction with $n_0 \sin\alpha$ ends (n_0 = initial end count of the green ply material), goes into a meridian length c_a having $n \sin\beta$ ends per inch, we must have

$$c_a n\sin\beta = n_0\sin\alpha \tag{20}$$

$$n(y) = n_0\frac{\sin\alpha}{c_a\sin\beta} = n_0\frac{c_t}{c_a c_b}$$

from Equation 18.

Using this result and the fact that from Equation 18, $\sin^2\beta = 1 - {c_a}^2/{c_t}^2\cos^2\alpha$ and $c_a = y/r_s$, we have

$$F_{N_\phi} = \frac{N_\phi}{4n\sin^2\beta} = \frac{N_\phi}{\frac{\sin\alpha\sin^2\beta}{c_a\sin\beta}}\cdot\frac{1}{4n_0}$$

$$F_{N_\phi} = \frac{c_a N_\phi}{4n_0\sin\alpha\sin\beta}$$

$$= \frac{p}{8n_0 r_s\sin\alpha}\left[\frac{(y^2 - {y_B}^2)\sqrt{1 + f^2(y)}}{f(y)\sqrt{1 - \frac{y^2}{(r_s c_t)^2}\cos^2\alpha}}\right] \tag{21}$$

and

$$F_{N_\theta} = \frac{N_\theta}{4n\cos^2\beta} = \frac{c_a N_\theta\sin\beta}{4n_0\sin\alpha\cos^2\beta}$$

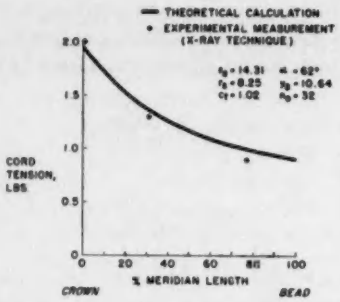

Fig. 7. Cord tensions in inflated tires. 8.00–15 nylon tire; 24 lb./sq. in. pressure.

$$F_{N_\theta} = \frac{y}{4n_0 r_s \sin\alpha}\left[\frac{\sqrt{1-\left(\frac{y}{r_s c_t}\right)^2\cos^2\alpha}}{\left(\frac{y}{r_s c_t}\right)^2\cos^2\alpha}\right] N_\theta \quad (22)$$

Equation 21 was adopted as an expression for the tire cord tension. Figure 7 shows the calculated cord tension for an 8.00–15 nylon tire. The stress is plotted against 100 times a nondimensional parameter

$$y^* = \frac{r_a - y}{r_a - r_s}$$

Determination of Cord Strain in Expanded Tires

The method is based on the simple network deformation theory as given by Rivlin [12] for inextensible cords and by Hofferberth [9] for extensible cords. Equations 18a, 18b, and 19 of Hofferberth are applied to a tire point by point. From the known green angle α and the measured cured angle β, a value of c_t can be calculated from Equation 18a if c_a is determined. Figure 2 illustrates the tire expansion process. The problem of finding c_a is handled in the following manner. A series of parallel lines is drawn on a mold drawing 1 in. apart. Their distance along the mold meridian is measured and the lines are transposed onto a master chart (Figure 8). A replica of the inside of the cured tire is made by painting a 2-in. strip with black wax pencil and tightly laying over it from bead to bead a #850 Scotch[3] brand Mylar[4] polyester film tape 1 in. wide. The device shown in Figure 9 is then used to determine the precise position of the meridian and circumference. The beads and the tire center line are marked on the tape.

The tape is pulled away from the tire and will have imprinted on its face an exact replica of the first ply cord network. Mylar polyester film is used because of its high strength and its dimensional stability. This tape is now placed on a master chart like that shown in Figure 8. The beads are located precisely and the center line is determined. The meridian marked on the tape is superimposed on the meridian line of Figure 8, assuring accurate alignment. In practice, Figure 8 need be set up for only ½ the tire meridian. Each vertical line now represents a value of c_a which is easily calculated from the drum dimensions. The value of c_a maximum at the center is determined from tire circumference, crown thickness, and drum diameter. It is now possible to measure the angle β at each of the positions 6, 5, 4, etc. The angle β at the bead is usually obscure and is assumed to be equal to α. The average value of c_a and of β between any two vertical lines is determined as the arithmetic mean of the c_a and β values at the two lines in question. It is always possible to make this assumption as nearly correct as desired by placing the lines as close together as necessary. In the interest of simplicity, six lines plus the center line are used. A table is now made of the known and measured values (Table I).

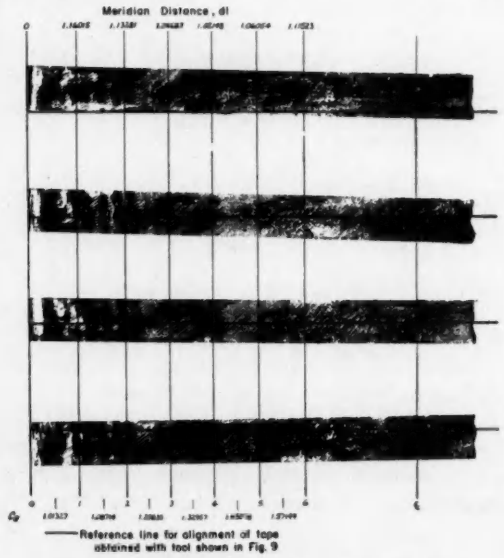

Fig. 8. Measurement of cord angles in cured tire.

[3] Minnesota Mining and Metallurgy Co. trademark.
[4] Du Pont trademark.

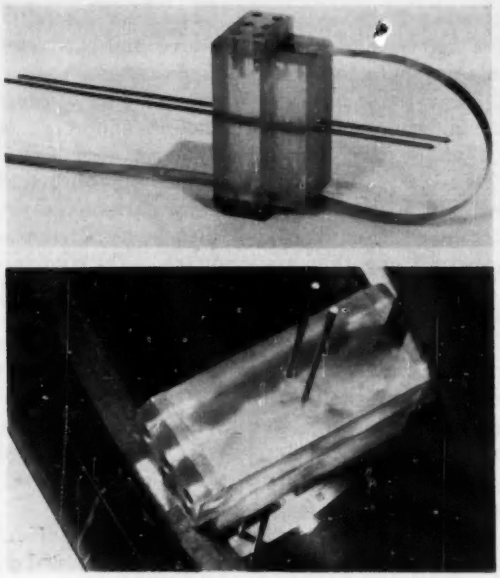

Fig. 9. Aligning tool for tire cord angle determination.

First c_t is calculated, using this table and Equation 18a. Next c_b is found from Equation 18b, and the appropriate values of β. The meridian distance between vertical lines is known (from the mold drawing, for instance). From the equation [9]

$$dS_w = dl/c_b \tag{23}$$

where S_w = drum width and l = meridian length the incremental drum width is found by dividing each meridian distance by the appropriate value of c_b. As a check, the sum total of incremental drum widths should equal the drum setting used to fabricate the tire. This usually has been found to be the case to within 2–3%.

The results are plotted as percent cord stretch vs. percent meridian length. A typical plot illustrating also the reproducibility of the measurements is shown in Figure 10. Another interesting use of the calculated c_t value is to determine the cumulative or over-all change in cord length. This is done by weighting each value of c_t by the length of cord over which it applies. (Cord length is found from meridian distance and cord angle.) Experimental values of over-all cord length change, as determined from the distance before and after expansion between knots sewed in the cord, agree quite well with the calculated cumulative values. The calculation of total cord length change is shown in Table I.

Further experimental evidence for the cord strain resulting from the tire expansion consists of x-ray measurements on metal shadowed cord [14]; Figure 11 illustrates this point. The agreement between measurements and calculations is good at the crown and near the beads; in the tire sidewall the measured values are lower than the calculated values. It should be noted, however, that the location of the sidewall x-ray measurement along the meridian length was not precisely determined. Apparently c_t, the cord strain, is not constant but varies from about 4% stretch at the crown to about 6% shrinkage at the bead. This results in cord nonuniformity and may partially offset the stretching treatment given the cord prior to tire building.

Discussion of Results

If it is assumed that the ideal tire carcass is thin-walled, that is, the wall thickness is small compared with the over-all dimensions of the carcass, the membrane theory of elasticity can be used to describe the stress configuration in the tire at equilibrium [8, 9, 11]. The assumptions of the membrane theory are only approximately true for the tire carcass but, for symmetric loading by inflation pressure only, give results which are in good agreement with experiment.

The hyperelliptic integral (Equation 1) which describes the tire meridian fits the physical meridian curve very well. The calculation of the stresses

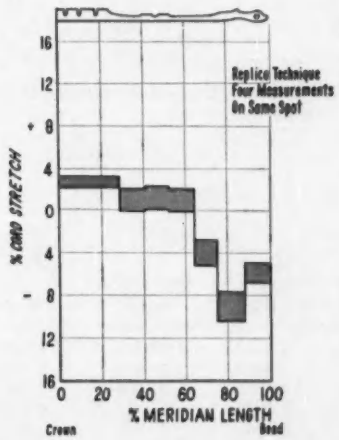

Fig. 10. Cord length changes resulting from tire expansion.

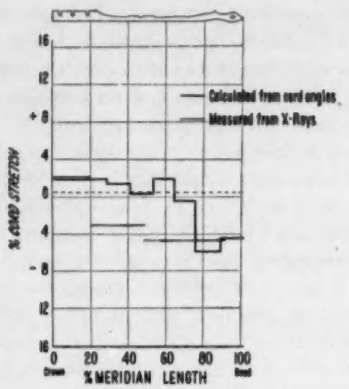

Fig. 11. Comparison of calculated and measured cord length changes.

N_ϕ, N_θ as they are shown in Figure 6 is based on the equilibrium conditions of the membrane and upon the network theory for an ideal tire as developed by Hofferberth [9] and Rivlin [12]. It is assumed that the cords are flexibly linked at their intersection points and, consequently, do not move relative to each other at those points as a result of the deformation. The hinge action is provided by the elastomer. This model represents the so-called pantographic expansion of the cord network.

In order to determine how closely the theoretical hinge theory corresponds to the actual physical situation, the calculated cured cord equilibrium angles of an ideal tire are compared to the measured cord angles of an actual tire. The equilibrium angles β are calculated using

$$\tan^2\beta = \frac{N_\phi}{N_\theta} \tag{24}$$

The results (y^* being the nondimensional parameter introduced previously) are shown in Table II. The agreement between measured and calculated angles is quite good.

The variable principal stresses (Figure 6) cause nonuniform cord tension; the nonuniform cord tension in turn causes nonuniform cord strain. This can be satisfactorily explained by noting that the cord structure is an integral part of the tire carcass. The cords cannot then be considered as lying on a smooth inelastic surface. The cord network forms a doubly curved surface which does not close on itself, being restrained at the beads. Consequently, more expansion is possible away from the beads, which results in lower end count per inch and smaller angles β. The cords bear a variable tension because the angles β are related to the variable principal stresses. The variable cord stresses may have an important effect on tire performance.

Some data exist in the literature for comparison with the results reported here. For a tire inflated to 29 lb./sq. in. with a 38° crown angle and 26 ends/in., Hofferberth [7] finds at the crown N_ϕ = 70.5 lb./in. and cord tension = 2.02 lb. In the work reported here for a tire of similar construction at an inflation pressure of 24 lb./sq. in., N_ϕ is found to be 76.7 lb./in. and the cord tension is 1.95 lb. at the crown.

Assuming that the stress distribution in the cords during the curing process is similar to that found in the inflated tire, it is possible to relate the observed cord stretch and cord shrinkage to the known elastic behavior of nylon tire cord at the temperatures usually prevailing in the tire curing process (about 300° F.). Wherever the cord experiences a tension less than its shrinkage tension, it will contract; wherever the tension exceeds the shrinkage tension,

TABLE I. Calculation of Total Cord Length Change

Line No.	Cured			Green		% Cumulative meridian distance	% Change	
	Cord length, in.	% Cumulative length	Cumulative length, in.	Cord length, in.	Cumulative length, in.		Incremental change in cord length	Cumulative cord length change
¢–6	4.1642	33.346	4.1642	4.0518	4.0518	28.893	2.78	2.78
6–5	1.6312	46.409	5.7954	1.6129	5.6647	41.023	1.13	2.31
5–4	1.4353	57.903	7.2307	1.4199	7.0846	52.558	1.07	2.06
4–3	1.3028	68.336	8.5335	1.2955	8.3801	63.669	0.56	1.83
3–2	1.3001	78.747	9.8336	1.3585	9.7386	75.056	−4.31	0.98
2–1	1.3704	89.217	11.1410	1.5112	11.2498	87.378	−9.32	−0.97
1–0	1.3465	100.000	12.4875	1.4370	12.6868	99.997	−6.27	−1.57

TABLE II. Comparison of Calculated and Measured Angles

y^*	β (Theoretical), ° and ′	β' (Measured on uninflated tire), °
1.0 (Bead)	62 36	62
.9	60 24	
.8	58 04	55
.7	55 49	
.6	53 27	52
.5	51	50
.4	48 27	
.3	45 48	46
.2	43 3	43
.1	40 4	
0 (Crown)	37 10	38

the cord will stretch. The shrinkage tension of nylon cord of normal denier is approximately 1.2 lb. Reference to Figure 7 shows that this tension occurs about halfway along the meridian. The cord in the lower half (towards the bead) should, therefore, shrink; the cord in the upper half (toward the crown) should stretch. Figure 10 shows that this does in fact occur.

A brief remark is in order concerning the comparison of calculated and experimental tensions. The calculations yield stresses in pounds per inch and tensions per cord in pounds. No direct measurements of stresses are possible. The x-ray technique (*cf.* Figures 7 and 11) yields a measure of strain. In order to make the comparison, the x-ray strain measurements [14] were converted to stresses using the known stress–strain relationship of nylon tire cord.

Summary of Results

The cord tension in an inflated nylon tire decreases from about 2.0 lb. at the crown to about 0.9 lb. at the bead after tire expansion. The cord strain in the expansion process is not constant, but increases from about 6% shrinkage at the beads to about 4% stretch at the crown. In an actual tire, where the plies are not coplanar, x-ray measurements [14] indicate that the cord stretch also increases from the inner to the outer plies.

Since the stresses in the tire cord are everywhere positive under expansion and inflation pressure, the existence of cord shrinkage or contraction in the lower sidewall and bead region is rather unexpected. It is suggested that this contraction occurs because of the stress–temperature conditions existing during tire expansion and curing. The shrinkage tension (the tension required to prevent contraction) of typical nylon tire cord at curing temperatures (about 300° F.) is approximately 1.2 lb. Therefore, wherever the cord is under a greater tension, it should elongate (stretch); wherever it is under a lesser tension, it should contract (shrink). A comparison of Figures 7 and 9 demonstrates this correspondence.

The correspondence between cord tension and cord strain suggests the further mathematical refinement of introducing a variable cord strain into the tire meridian Equation 6. The good fit of experimental data by use of a constant value for c_t indicates, however, that for purposes of calculating the stresses and the tire shape, the present scheme may be adequate.

This value of c_t might be found by relating the cord tension at the crown to the known stress–strain relation of the tire cord material. If the value of c_t used initially does not agree with the cord strain found on the stress–strain curve at the calculated stress, an iteration technique might be employed until agreement is obtained.

The concepts discussed here, although specific to a defined ideal tire, are in sufficient agreement with experiment so that it should be possible to use them as the basis for tire construction calcuations which would take into account the physical properties of the tire constituents as well as the physics of the tire as a whole.

Acknowledgments

The authors are grateful for encouragement of the work to Drs. J. M. Swanson and W. G. Mikell. They are indebted to H. H. McCrea, W. J. Schaffers, and L. A. Stone for valuable suggestions, discussions, and computer programming assistance, respectively. The work on x-ray strain measurements will be described in a separate paper by B. Weickert.

Literature Cited

1. Adkins, J. E., *Phil. Trans. Roy. Soc., London* **A249**, 125–150 (1956).
2. Adkins, J. E., *J. Rat. Mech. Anal.* **5**, 189–202 (1956).
3. Ariano, R., *L'Industria (Milan)* **49**, 151–160 (1935).
4. Ericksen, J. L. and Rivlin, R. S., *J. Rat. Mech. Anal.* **3**, 281–301 (1954).
5. Flugge, W., "Statik und Dynamik der Schalen," Berlin, Springer, 2nd ed. (1957).
6. Hencky, W., *Mech. Eng.* **57**, 149–153 (1935).
7. Hofferberth, W., *Kautschuk u. Gummi* **8**, Sonderheft "Der Reifen," 3–9 (1955).

8. Hofferberth, W., *Kautschuk u. Gummi* **8**, WT124–WT130 (1955).
9. Hofferberth, W., *Kautschuk u. Gummi* **9**, WT225–WT231 (1956).
10. Love, A. E. H., "Treatise on the Mathematical Theory of Elasticity," New York, Dover, 4th ed. (1944).
11. Martin, F., *Jahrbuch der deutschen Luftfahrtforschung* **1**, 470–96 (1939).
12. Rivlin, R. S., *J. Rat. Mech. Anal.* **4**, 951–974 (1955).
13. Rivlin, R. S. and Adkins, J. E., *Phil. Trans. Roy. Soc. London*, **A248**, 201–223 (1955).
14. Weickert, B., "An X-Ray Technique for Tire Strain Measurements," unpublished data.
15. Weihs, G., "Conditions of Stress and Distortion in Balloon Tires," Dissertation, Aachen (1911).
16. Woods, E. C., "Pneumatic Tire Design," Cambridge, W. Heffer (1955).

Manuscript received April 20, 1959.

Some Effects of Sheep Nutrition on the Mechanical Constants of Wool

V. D. Burgmann

C.S.I.R.O. Wool Research Laboratories, Division of Textile Physics, Ryde, N.S.W., Australia

Abstract

Results are reported of measurements on the mechanical constants of wool from sheep under closely controlled conditions of husbandry and nutrition. The experimental wool had a change of diameter along individual fibers which was due to a deliberate variation in food intake of the sheep during the growing period. Values for the yield region are given for a Merino and a Corriedale wool. The Merino showed no change due to diameter variation and the Corriedale only a slight change.

Introduction

Variations of cross-sectional area occur along the length of wool fibers. The variations are associated with changes in the food intake, age, environment, and health of the sheep. It would be useful to know the extent to which they are accompanied by changes in the mechanical constants of the wool and which, if any, of the causes of variation have a large effect on the constants. "Mechanical constants" are the intrinsic mechanical properties of the fiber substance, such as stress to produce a certain strain under specified conditions, or derivatives of these. In the Hookean and up to the beginning of the yield region the relationship between load and extension has been shown [6, 7, 16, 17, 20] to be greatly influenced by crimp. Crimp therefore makes it difficult to measure the constants in these regions. However, in the yield region fiber diameter appears to be the important parameter.

Studies [1, 3–8, 11–14, 16–23] of a variety of wools show that there are no great differences in the mechanical constants of wool fibers of widely different type and diameter. Nevertheless, small differences are being found which can be attributed to the origin of the fibers. Much of the work has been done at Textile Research Institute, Princeton, N. J., and the Western Regional Laboratory, Albany, California.

Some workers find a dependence of mechanical constants on fiber diameter; others do not. Recently, for example, Thorsen [24], using wool from 60 sheep of a number of breeds, has shown that there is an increase with diameter in the stress required to produce 30% extension in water. He also reported for a Lincoln wool sample a marked increase in this stress during the first twelve months of growth, followed by a relatively constant value up to the age of four years and then a slight decrease. On the other hand, Monfort [19], using five lots of wool with a mean diameter range 19.5 to 33 μ found that the stress for 20%, 25%, and 30% extension in air was independent of diameter. Dusenbury and Wakelin [6] also found no dependence of stress for 20% extension on fiber diameter.

All the above measurements were made on wool from sheep grazing in flocks. It is therefore difficult to decide the cause of diameter variations in the wool for which the mechanical constants were reported.

An experiment in Australia by the C.S.I.R.O. Division of Animal Health and Production has made available wool grown on two types of sheep under closely controlled conditions of husbandry and level of nutrition. Their experiment provided wool samples in which changes in the fiber diameter and mechanical constants could be attributed primarily to variations in the level of nutrition. This paper gives preliminary results and methods used to measure the mechanical constants in the yield region and shows that they were independent of diameter and hence level of nutrition for the particular Merino wool used, but some were slightly dependent for the Corriedale wool.

Experimental

Source of Wool

The wool came from the sheep used in the experiments by Ferguson, Carter, and Hardy [9] on comparative fleece growth in sheep. They used two types of sheep, 12 Merino and 12 Corriedale which were closely matched in general condition and in age, being two years old at the beginning of the experiment. The Merinos were particularly uniform in type because they were from a highly inbred flock which had been closed to outside blood for 60 or 70 years. The Corriedales were from a stud flock. Both lots of 12 after a conditioning period on uniform nutrition were further divided into three groups. The first group started the experimental growing period with a high level of nutrition and were later reduced to a low level. The second was on a uniform level throughout the experiment. The third was started on a low level and later raised to a high level. The food was of constant composition and good quality, but the range in daily ration from high to low was extreme, being from *ad lib* feeding to barely maintenance level. The sheep were kept in individual pens in a well-constructed and ventilated sheep house. They were thus protected from direct sunlight and rain. The experiments ran for 72 weeks and were very fully reported, including regular measurements of mean fiber diameter and rate of increase of wool weight. Variations in mean fiber diameter were attributed mainly to changes in food intake, but environmental temperature was also found to influence growth slightly. The preliminary results given here are for twelve months' growth of wool from both types of sheep, four of each being used.

Cross-Sectional Areas

Cross-sectional areas of the fibers were measured with a vibroscope. The vibroscope was specially constructed with a short gauge length and arranged so that the gauge could be moved along the fiber.

The vibroscope was operated at a constant driving frequency and gauge length. The fiber tension was adjusted until resonance was observed visually. The advantages of this arrangement were that all determinations were made at the same value of stress; also, the observed tension at resonance was directly proportional to the cross-sectional area of the fiber.

The resonant frequency of the fiber is given to a first approximation by

$$f = \frac{1}{2l}\sqrt{\frac{Tg}{\rho A}} \qquad (1)$$

where A = cross-sectional area (to be determined), f = driving frequency (a constant), l = gauge length (a constant), T = fiber tension (adjusted for resonance), and ρ = fiber density (a constant). The stress at resonance is

$$\frac{Tg}{A} = 4f^2l^2\rho$$

which is therefore a constant depending only on values chosen for f and l. Also the cross-sectional area

$$A = T\left(\frac{g}{4f^2l^2\rho}\right)$$
$$= T \times \text{constant}$$

The following values were used:

f = 5000 cycles/sec.
l = 0.865 cm.
ρ = 1.31 g./cm.^{3}
g = 981 cm./sec.^{2}

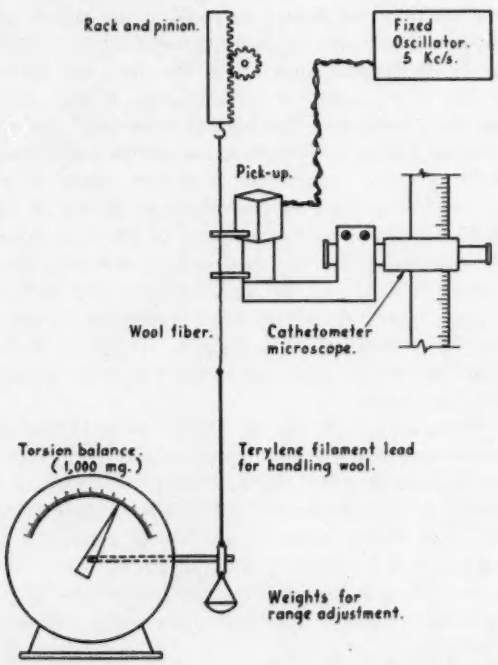

Fig. 1. Schematic of the vibroscope, showing the gauge mounted on the barrel of the microscope on the cathetometer used for traversing the length of the fiber.

With these values the stress at resonance is 1×10^5 g./cm.^{2}, which is just sufficient to decrimp the fibers. Also, the cross-sectional area in square microns is numerically equal to the tension in milligrams.

A schematic drawing of the vibroscope is shown in Figure 1. The fiber under test is connected between a torsion balance and a rack so that the tension in it can be adjusted for resonance and measured. The torsion balance had a range of 1000 mg. and could be read directly as microns squared. The gauge pins, one of which is in a phonograph pick-up, are carried on an extension arm from the microscope of a cathetometer which is traversed along the length

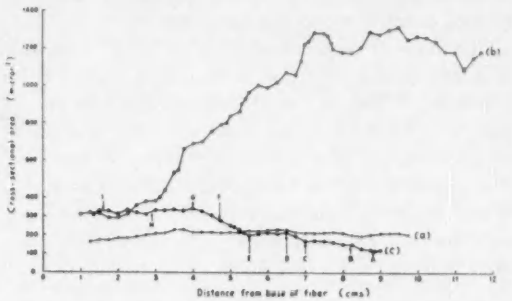

Fig. 2. Example of the actual vibroscope measurements of cross-sectional area along fibers at 2.5-mm. intervals. (a) Merino sheep on a uniform level of nutrition; (b) Corriedale sheep on a high level changing to a low level; (c) Merino on low level changing to a high level. The letters show where markers were tied for the load–extension tests on this particular fiber.

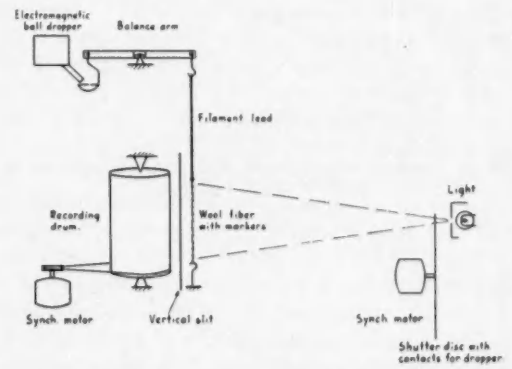

Fig. 3. Schematic of the extensometer with constant rate of loading showing recording drum for shadowgraphs with ball dropper which is synchronized by the light shutter. The drum has in front a vertical slit 1.6 mm. wide. The drum moves one slit width between ball drops, which are at 3-sec. intervals. The result is a series of shadowgraphs of the whole length of the fiber with markers for each increment in load.

of the fibers. Examples of the measurements made on fibers from sheep on a changing level and on a uniform level of nutrition are shown in Figure 2. Measurements of cross-sectional area were reproducible to about ± 0.5%, and were adjusted to the value expected at 65% relative humidity. The areas were measured at not less than 2.5-mm. intervals along the length of the fiber. No corrections [15] were applied to the vibroscope results; the absolute values may therefore be in error by about 1%. However, the relative value of cross-sectional area along and between fibers should not be seriously in error.

Extensometer

The load extension measurements were carried out in water at a constant rate of loading of 1 and 2 g./min. for the Merino and Corriedale wool respectively. The constant rate of loading was obtained by dropping ⅛-in. diameter ball bearings into the pan of a balance with unequal arms. The other arm was arranged to pull upwards on the fiber in increments of either 50 or 100 mg. at 3-sec. intervals. A schematic drawing of the extensometer is shown in Figure 3.

Extension of the fiber was recorded by a shadowgraph method. Before the fiber was mounted in the extensometer, points were selected and marked [2] along it by tying a terylene filament of 37 μ diameter around it with a single knot. After being tied the terylene was cut off close to the wool fiber; the knots were used as reference marks for extension measurements. Their positions were chosen from the record, as shown in Figure 2c, to be 0.5–2 cm. apart and so that in most cases the extreme range in cross-sectional area between any pair was not greater than ± 5%. The shadowgraphs of the fiber and knots were sufficiently well defined for the length between the knots to be measured to ± 0.01 mm. with a travelling microscope.

The above method allows all parts of the one fiber to be subjected to the same load while simultaneously recording their individual extensions. However, the measurement of lengths by travelling microscope is tedious. A set of load vs. length curves in Figure 4 shows the small scatter of points achieved. The fibers were not all extended until break, so observations of stress to break are not reported.

Results and Discussion

Load vs. length curves were plotted for the marked parts of each fiber tested, making a total of

61 curves from 9 Merino wool fibers and 47 curves from 8 Corriedale. In some tests the thicker parts were not extended beyond the yield region because other parts of the same fiber were too thin to sustain the necessary tension. Results in the post-yield region were therefore limited. As illustrated for part AB in Figure 4, the linear portions of the load–length curves were extended to determine the length at zero load, the beginning of the yield region, and the post-yield region.

The values of the stress at various extensions and the extension at the change from the yield to the post-yield region are shown in Table I. The mean values for Merino are slightly, but significantly, lower than Corriedale, both for stress at the beginning of the yield region and at 15% extension. There is no significant difference between the wools either for stress or strain values at the changeover from yield to post-yield. The mean values for stress at the beginning of the post-yield region agree well with the values reported by Thorsen [24] for 30% extension of his Merino wool samples. The Merino and Corriedale wools differ slightly in their mechanical constants, but only from the beginning of the yield region to a little over 15% extension. It is possible that some of the difference is due to crimp diameter relationship [7] not being the same for the Merino and Corriedale wools. However, no measurements of crimp were attempted, due to the large growth changes along the wool staple.

The tension required to produce 15% extension is shown in Figure 5 for Merino and Figure 6 for Corriedale. Tension at 15% extension was chosen because it is the point of inflexion [10] and might be expected to have a low coefficient of variation. The plotted points are individual results for each part of all the fibers; none was rejected. Those for sheep on a uniform level of nutrition are shown differently from those on a varying level. The scatter is small

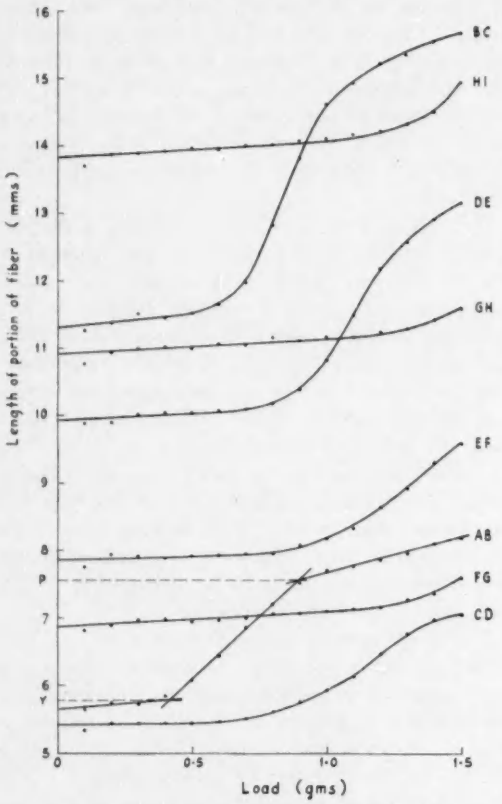

Fig. 4. Load vs. length curves for extension in water at 20° C. of the fiber shown in Figure 2c. Each length has letters corresponding to the marker knots and was measured from the shadowgraphs by a travelling microscope. The lines drawn on AB show how the beginning of the yield Y and post-yield P region was determined.

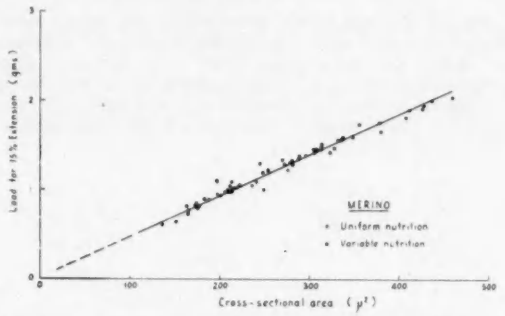

Fig. 5. Load vs. cross-sectional area for 15% extension in water at 20° C.—Merino.

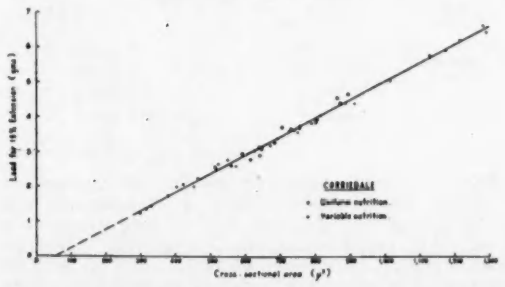

Fig. 6. Load vs. cross-sectional area for 15% extension in water at 20° C.—Corriedale.

TABLE I. Values for Points on the Stress–Strain Curves for the Two Wools in Water at 20° C.

		Mean value	Observations	CV, %	Significance
Stress at beginning of yield region	Merino	3.89×10^5 g./cm.^{2}	59	6.6	Difference of means significant at 0.1% level
	Corriedale	4.15×10^5 g./cm.^{2}	45	8.2	
Stress at 15% extension	Merino	4.70×10^5 g./cm.^{2}	61	4.8	Difference of means significant at 1% and almost at 0.1% level
	Corriedale	4.85×10^5 g./cm.^{2}	46	5.0	
Stress at change from yield to post-yield	Merino	5.66×10^5 g./cm.^{2}	41	5.8	Difference of means not significant at 5% level
	Corriedale	5.60×10^5 g./cm.^{2}	21	6.3	
Extension at change from yield to post-yield	Merino	30.2%	42	8.7	Difference of means not significant at 5% level
	Corriedale	29.6%	21	5.9	

for both. A straight line can be drawn through the points and the origin for the Merino, but for Corriedale it passes below the origin. This means that the stress to produce 15% extension is constant for the Merino wool, irrespective of cross-sectional area changes brought about by variations in wool growth, but for the Corriedale wool, the stress for 15% extension increases slightly with increase in cross-sectional area. Similarly, values for the stress at the beginning of the yield region and at the beginning of the post-yield region were found to be constant for Merino but area-dependent for Corriedale. Each stress constant for the Corriedale appeared to be increased equally by cross-sectional area. The stress for 15% extension was 4.65×10^5 g./cm.^{2} at 20 μ diameter and increased to 5.15×10^5 g./cm.^{2} at 40 μ diameter. This increase is equivalent to 0.02 g./tex/μ which compares well with 0.015 g./tex/μ obtained by Thorsen [24] as a grand average for stress at 30% extension for all the wools he tested. However, it is much lower than the value 0.073 g./tex/μ he obtained for changes in Lincoln wool over an age range of 5 years with accompanying changes in average diameter. Changes due to the sheep aging were not apparent in the present experiment, but might not be expected in the one year involved.

The results presented are for relatively few fibers from 8 out of the 24 experimental sheep. Nevertheless, these preliminary measurements show a definite trend for sheep on a varying quantity of good quality feed; the results for poor quality feed might well be different. The sheep were subjected to changing level of nutrition from *ad lib* feeding to barely maintenance level, which caused large variations in cross-sectional area along the fibers. In spite of these extreme conditions, changes in the mechanical constants of the wool, measured in water in the yield region, were only slight in the case of Corriedale and could not be detected in the Merino wool. Also, no difference could be found between Merino and Corriedale wool for the stress and extension at which the changeover from the yield to post-yield region occurs.

Acknowledgment

Thanks are due to Dr. K. A. Ferguson of the C.S.I.R.O. Sheep Biology Laboratory for supplying the wool samples.

Literature Cited

1. Anderson, S. L. and Cox, D. R., *J. Textile Inst.* **41**, T481 (1950).
2. Banky, E. C. and Sen, S. B., TEXTILE RESEARCH JOURNAL **25**, 358 (1955).
3. von Bergen, W. and Wakelin, J. H., TEXTILE RESEARCH JOURNAL **22**, 123 (1952).
4. von Bergen, W., in "Matthews Textile Fibres," ed. H. R. Mauersberger, New York, John Weber and Sons, 6th ed. 583 (1954).
5. Bosman, V., Waterson, E. A., and van Wyk, C. A., *Onderstepoort J. Vet. Sci. Animal Ind.* **15**, 313 (1940).
6. Dusenbury, J. H. and Wakelin, J. H., TEXTILE RESEARCH JOURNAL **28**, 989 (1958).
7. Evans, T. F., TEXTILE RESEARCH JOURNAL **24**, 637 (1954).
8. Evans, T. F. and Montgomery, D. J., TEXTILE RESEARCH JOURNAL **23**, 689 (1953).
9. Ferguson, K. A., Carter, H. B., and Hardy, Margaret H., *Aust. J. of Sci. Res.* **B2**, 42 (1949).
10. Feughelman, M., *J. Textile Inst.* **45**, T630 (1954).
11. Frishman, D., Smith, A. L., and Harris, M., TEXTILE RESEARCH JOURNAL **16**, 160 (1946).
12. Hardy, J. I., *J. Agr. Res.* **19**, 55 (1920).
13. Lindberg, J., TEXTILE RESEARCH JOURNAL **23**, 683 (1953).

14. Lecomte, J., Mazingue, G., and van Overbeke, M., *Bull. Inst. Textile de France* **69**, 8 (1957).
15. Mackay, B. H. and Downes, J. G., TEXTILE RESEARCH JOURNAL **28**, 467 (1958).
16. Menkart, J. and Detenbeck, Jeanne C., TEXTILE RESEARCH JOURNAL **27**, 665 (1957).
17. Meredith, R., *J. Textile Inst.* **36**, T107 (1945).
18. Meybeck, J. and Gianola, G., *Proc. Int. Wool Text. Res. Conf., Austr. 1955*, **D**, 135, C.S.I.R.O. Melbourne (1956).
19. Montfort, F., Franck, M., and Grignet, J., *Bull. Inst. Textile de France* **72**, 41 (1958).
20. O'Connell, R. A. and Yeiser, A. S., TEXTILE RESEARCH JOURNAL **24**, 629 (1954).
21. O'Connell, R. A. and Lundgren, H. P., TEXTILE RESEARCH JOURNAL **24**, 677 (1954).
22. Satlow, G., *Z. Ges. Textil-Ind.* **19**, 750 (1956).
23. Story, L. F. and Ross, D. A., N. Z. Woollen Mills Research Association (Inc.) Publication No. 65 (May 1957).
24. Thorsen, W. J., TEXTILE RESEARCH JOURNAL **28**, 185 (1958).

Manuscript received June 30, 1959.

Spectrophotometric Measurement of Color in Wool Fabrics

F. G. Lennox

Division of Protein Chemistry (Formerly Biochemistry Unit), C.S.I.R.O. Wool Research Laboratories, Parkville. N.2. (Melbourne), Victoria, Australia

Abstract

A method is described for measuring the differential absorption spectra of pale-colored fine-wool fabrics in the visible and ultraviolet regions. A strip of the fabric is immersed in a liquid having a refractive index close to that of wool and compared in an ultraviolet spectrophotometer with a similarly immersed uncolored or bleached strip of the same fabric.

The method is applied to the measurement of the absorption spectra of normal unbleached wool fabrics and to fabrics which have been yellowed either by heating at 97° C. in an aqueous buffer solution at pH 8 or by exposure to ultraviolet irradiation. Fabrics which have been dyed or treated with reagents producing colored derivatives of particular amino acid residues in the wool proteins have also been tested. Sizing and finishing agents in the fabric which absorb in the visible or ultraviolet regions are detected by the method.

When wool is yellowed by heating or exposing to ultraviolet irradiation, its absorption increases far more in the ultraviolet region of the spectrum, especially at 3100–3300 Å, than in the visible region above 3900 Å.

RESEARCH on the yellowing, bleaching, and dyeing of wool would be facilitated if better methods were available for measuring color in the intact fabric. Matching shades by eye, the commonly accepted method used in textile dyeing and dye fastness testing, is limited in scope, due to variations in acuity of vision among individuals and for the same individual at different times.

Surface reflectance measurements are free of subjective errors but are markedly affected by the structure of the fabric being tested. Some reflectance photometers are very insensitive to changes in shade which are easily detected by eye, and Graham and Statham [1] in a recent paper on the yellowing of wool fabric have stated that "attempts to assess the discoloration by means of a reflectance colorimeter were not successful."

In the present study it is shown that the differential absorption spectrum of modified wool fabric can be measured at wavelengths greater than 3000 Å by comparison with untreated fabric in an ultraviolet spectrophotometer of the type commonly used for

studying the absorption spectra of colored solutions. The method should also find application in studying some aspects of the structure and chemistry of intact wool.

Measurement of the Differential Absorption Spectrum

The standard fabric used in these investigations was made from 64's Merino wool in plain weave with 2/30's worsted yarn to give 30 ends and 30 picks/in. It weighed 5.0 oz./sq. yd. Samples measuring 53 × 23 mm. and weighing 0.2 g. were subjected to a coloring or bleaching treatment. Strips 44 mm. long and 10 mm. wide (11 threads) were cut from the colored and uncolored samples, and these were rinsed in distilled water to remove soluble materials where necessary, pressed between absorbent papers, and partly air-dried. They were then pressed with a warm electric iron to flatten and immersed in a liquid having the same refractive index as wool in silica cells 44 mm. high, 10 mm. wide, and having a 10-mm. light path. Each strip was pressed flat against the wall through which light entered the cell and its optical density d measured against the untreated strip over a range of wavelengths in a Beckman DU spectrophotometer.

Selection of Immersion Liquid

To compare various immersion liquids, the unbleached standard fabric was measured against the same fabric after bleaching. The samples were bleached by soaking in 0.5% wetting agent (Lissapol NX or Nonidet P40) for 30 min. at 45° C., transferring to 0.005 M sodium pyrophosphate containing 2% (vol./vol.) 100 vol. hydrogen peroxide for 3 hr. at 45° C. (pH 8.5), washing with distilled water, soaking in 0.5% sodium dithionite ($Na_2S_2O_4 \cdot H_2O$) for 2 hr. at 45° C., and rinsing several times in distilled water. A liquor:wool ratio of 30:1 was used throughout. Strips of bleached and unbleached fabric were immersed in a series of liquids placed in turn in the cells of the spectrophotometer and the differential absorption spectra measured. When the fabric was immersed in the following liquids with refractive indices ($n_D^{20°\,C.}$) not exceeding 1.4: water (1.33), ethanol (1.36), hexane (1.38), ethyl butyrate (1.39), heptane (1.39), and isobutanol (1.40), insufficient light was transmitted between 3100 Å and 4300 Å to permit measurement of the spectra. The curves for the unbleached fabric using Cellosolve (1.41), chloroform (1.45), dibutyl phthalate (1.49), xylene (1.50), benzene (1.50), ethylene dibromide (1.54), o-dichlorobenzene (1.55), and bromobenzene (1.56) all approximated in shape those shown for o-dichlorobenzene (Figure 1). Of the liquids having higher refractive indices than wool (1.55), quinoline (1.62) and carbon disulfide (1.63) failed to transmit enough radiation. Nitrobenzene (1.55), tricresyl phosphate (1.56), o-toluidine (1.57), aniline (1.59), 1-bromonaphthalene (1.66), and methylene iodide (1.74) were colored in the grades available and would be unsuitable for routine use. Because its refractive index approximates so closely that of wool, and since it has been used to reveal the presence of contaminants in wool [5], o-dichlorobenzene was chosen as the immersion liquid for the work described in this paper. Although the grade of o-dichlorobenzene used was pale yellow when viewed in thick layers, distillation to remove the color did not alter the differential spectral absorption curve of the unbleached wool fabric.

Spectral Absorption Curves of Various Unbleached Fabrics

To determine whether the method was generally applicable to different types of woven wool fabric, pieces measuring 380 × 160 mm. were cut from the cloths described in Table I and bleached together in the same flask using the peroxide-dithionite method already described. The absorption spectrum of each of the unbleached fabrics was determined by comparison with the corresponding bleached material.

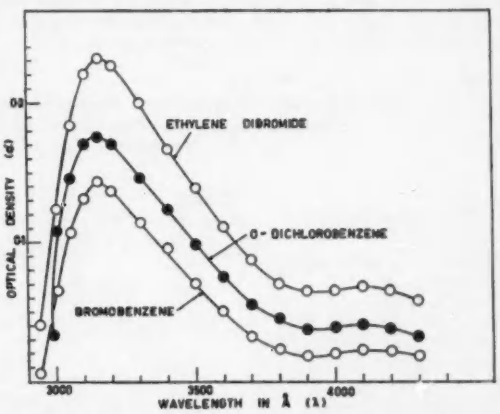

Fig. 1. Three immersion media used for measuring the differential absorption spectrum of unbleached 4.2 oz./sq. yd. light weight twill in a silica cell with 1-mm. light path.

A double thickness of fabric was used to increase the optical density readings.

The optical densities at different wavelengths for each fabric (Table I) show that the method should have wide application to cloths of various weights and constructions. The increase in the absorption by the 4.2-oz. light weight fabric to a maximum at 3700 Å is due to the presence of optical bleach. Besides being destroyed by the bleaching procedure, the absorption at 3700 Å was temporarily eliminated by soaking for 2 hr. at 50° C. in 2% soap solution containing ammonia, but it reappeared when the strips were examined again after standing in the laboratory for 2 days. High absorption by the 6.7-oz. plain weave woolen cloth at the higher wavelengths corresponds with a much deeper yellow shade than in the other cloths, and this color was not completely removed by bleaching. A slight peak in the absorption curve was detected about 4000 Å in several of the fabrics.

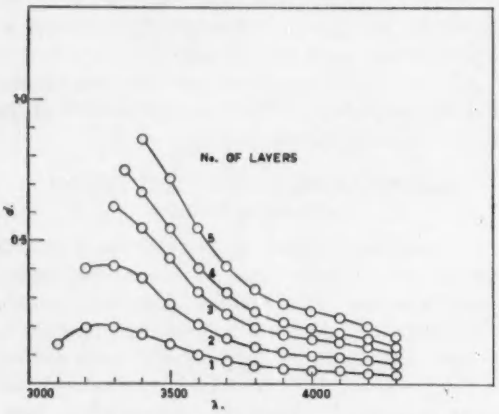

Fig. 2. Differential absorption spectra for multiple layers of unbleached standard wool fabric, using an equal number of layers of bleached fabric in the control cell. Silica cells with 10-mm. light path and *o*-dichlorobenzene immersion medium were used in this and subsequent experiments.

An attempt to measure the absorption spectrum of a plain weave fabric containing 85% wool and 15% nylon was unsuccessful, due to failure to transmit radiation at wavelengths below 3750 Å, even though the refractive index of nylon (1.52–1.58) is close to that of wool.

All-wool blanket material which had been yellowed by repeated boiling in an aqueous solution gave very variable results among samples, due to the presence of medullated fibers which could be clearly seen when the strips were immersed in the *o*-dichlorobenzene. Moreover, due to its thickness, radiation was not transmitted through this material below 3400 Å.

After the material was extracted with soap solution, the optical density of the 4.2-oz. 2/1 twill in the 10-mm. silica cells could be measured at wavelengths greater than 3060 Å, as compared with 3100 Å for the standard 5-oz. plain weave cloth. By use of silica cells having a 1-mm. light path the measurements could be extended to 2980 Å. By replacement of *o*-dichlorobenzene with ethylene dibromide or bromobenzene the sensitivity of the optical density measurements at low wavelengths was increased and the range of measurements on the lightweight twill in 1-mm. silica cells was extended further to 2940 Å (Figure 1). As shown in Figure 1, the optical densities above 3000 Å were reduced by replacing *o*-dichlorobenzene with bromobenzene; this was

TABLE I. Optical Density Measurements Obtained at Various Wavelengths with Two Layers of Unbleached Wool Fabric Measured Against the Same Fabric after Bleaching. The 2/2 Twill was Made from Merino 60's Wool and the Others from Merino 64's

Fabric construction	Weight, oz./sq. yd.	Wavelength, Å												
		3100	3200	3300	3400	3500	3600	3700	3800	3900	4000	4100	4200	4300
*Plain, 2/30's, worsted	5.0	—	0.33	0.32	0.29	0.23	0.17	0.13	0.10	0.09	0.08	0.09	0.08	0.07
2/1 Twill, 2/30's warp, 2/26's weft, worsted	7.9	—	—	0.22	0.18	0.14	0.11	0.08	0.06	0.06	0.07	0.07	0.07	0.05
Plain, 2/26's, worsted	6.8	—	—	0.19	0.14	0.10	0.07	0.04	0.03	0.02	0.03	0.04	0.06	0.04
2/2 Twill, 2/36's warp, 1/18's weft, worsted	7.3	—	—	0.37	0.31	0.25	0.20	0.16	0.14	0.12	0.12	0.12	0.10	0.09
2/1 Twill, 1/28's warp, 1/40's weft, worsted	4.2	0.54	0.53	0.50	0.58	0.71	0.75	0.82	0.80	0.69	0.46	0.22	0.10	0.09
Plain, 1/24's warp, 1/22's weft, Yorkshire skein	6.7	—	—	0.34	0.34	0.32	0.29	0.27	0.26	0.25	0.25	0.24	0.24	0.23

* Standard fabric.

confirmed in another experiment. However in the second experiment the optical densities for *o*-dichlorobenzene and ethylene dibromide were almost identical over the entire range of wavelengths. Thus the relative merits of these three immersion liquids have not yet been established with certainty.

Absorption in the ultraviolet region by the immersion liquids alone was such that, with the spectrophotometer slit fully open, the following lower limits were observed in 10-mm. and 1-mm. layers respectively: *o*-dichlorobenzene, 2990–2910 Å; bromobenzene, 2920–2830 Å; and ethylene dibromide, 2980–2750 Å.

Wool proteins extracted with dilute ammonia, following oxidation of the fiber with performic acid, and cast as a transparent film by evaporation on polished glass and examined in the spectrophotometer in the absence of any immersion liquid allowed measurements to be extended down to 2100 Å. Similarly a 0.1 *N* HCl solution of the partly-fractioned proteins extracted from wool with acid could be measured down to the same low wavelength.

Use of Multiple Layers of Fabric

By immersion of five layers of the standard fabric in the *o*-dichlorobenzene in one cell and five layers of bleached standard fabric in the comparison cell and measurement of the differential absorption spectrum repeatedly after removal of the layers one at a time from each cell, a series of curves was obtained (Figure 2).

For several different wavelengths, the optical densities when plotted against the number of layers of fabric show an approximately linear relationship, denoting close agreement with Beer's Law for the spectral absorption associated with yellowing.

Absorption Spectra of Wool Yellowed by Heat and by Ultraviolet Light

Samples of standard fabric, weighing 0.2 g. in equilibrium with the laboratory atmosphere, were heated at 97° C. for increasing periods of time in test tubes containing 12-ml. portions of 0.1 *M* H_3BO_3–NaOH buffer at pH 8.0. The pH fell to 7.9 after heating for 3 hr., but with the shorter periods of heating no change in pH could be observed. As shown in Figure 3, the spectral absorption in *o*-dichlorobenzene increased markedly with heating, especially in the ultraviolet region, and a progressive increase in yellowing could be detected by eye throughout the series. A rapid increase in absorption occurred during the initial 0.1 hr., the reaction slowing down considerably thereafter.

Yellowing and a corresponding increase in spectral absorption were also produced by heating 0.2 g. of the standard fabric for 20 min. at 97° C. in other alkaline solutions, for example in 12 ml. 0.1 *M* Na_2HPO_4, but the pH value fell during this treatment from 9.0 to 8.3.

Strips of standard fabric were yellowed by exposure for increasing periods of time 7 cm. from the arc of a 125-watt high pressure mercury vapor lamp from which the glass envelope had been removed. A water-filled silica cell was interposed between the lamp and the strip to shield the fabric

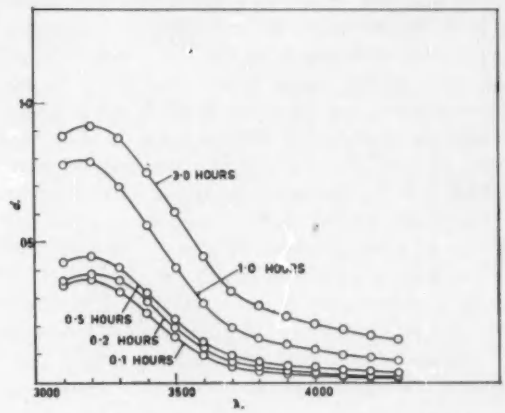

Fig. 3. Yellowing by heating for various periods at 97° C. in 0.1 *M* H_3BO_3 adjusted to pH 8.0 with NaOH; liquor:wool ratio 60:1.

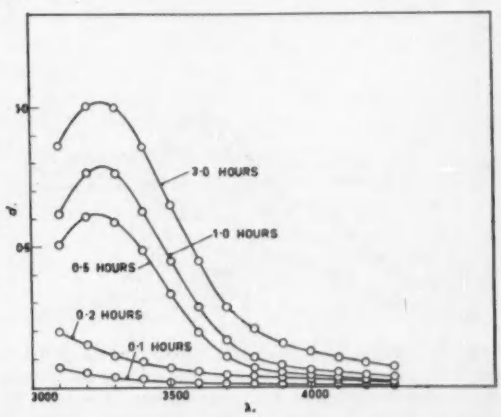

Fig. 4. Yellowing by UV irradiation at 7 cm. from 125-watt cooled Hg vapor street lamp with glass envelope removed.

from radiant heat and a cooling fan and water cooling coils were attached to the lamp housing. As shown in Figure 4, the differential spectral absorption curves obtained by comparison with a strip of untreated fabric resembled those for the samples heated in slightly alkaline buffer solution (Figure 3).

Spectral Absorption Curves for Dyes Attached to Wool Fabric

A strip of fabric 10 mm. wide was immersed at room temperature in 4.0 ml. of a solution (28 μequiv./l. of Orange II (CI Acid Orange 7) in 98–100% formic acid. Wool has been shown to absorb dyes from cold formic acid solution within 1 min. [3], but 18 hr. was allowed in this experiment to ensure equilibration. Spectral absorption curves were determined for the dye solution before and after dyeing, using formic acid alone in the comparison cell, and for the dyed fabric in *o*-dichlorobenzene compared with undyed fabric in the same liquid (Figure 5). Maximum absorption occurred at 5000 Å in the dye solutions and at 4900 Å in the fabric, which is close to the maximum observed for Orange II when dissolved in water. Although the optical density of the solutions of Orange II in formic acid increases as the wavelength falls below 3600 Å, the dyed fabric showed no absorption in this region. Apart from this region, a curve calculated by adding the optical densities corresponding

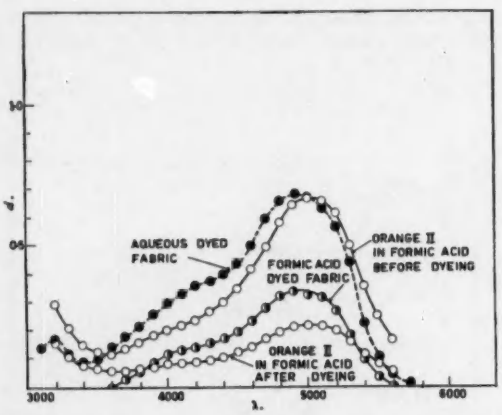

Fig. 5. Differential absorption spectra of wool fabric dyed with Orange II from formic acid solution and of the dye solution itself before and after dyeing, shown by the continuous lines. A curve for fabric dyed with Orange II from aqueous solution using 0.1% dye on weight of fabric is shown by the broken line.

to the dyed fabric and the formic acid solution of Orange II after dyeing lies only slightly below that for the original solution.

When the same dye was applied from aqueous solution to give 0.1% on the weight of fabric, a similar curve was obtained. This dyeing was effected by heating for 1 hr. at 97° C., the final pH of the liquor being 1.7. A small peak is observed in the curve at 3100 Å, which may be due to slight yellowing, but there is no evidence of extensive absorption in the ultraviolet region in spite of prolonged boiling.

The standard fabric was also dyed with the neutral dye, Irgalan Bordeaux 2BL (CI Acid Red 218), using 0.1% on the weight of wool in one instance and 0.5% in the other. The samples were heated to 70° C. during 20 min., then heated further to 97° C. in 40 min. and held at this temperature for 45 min. At this stage all the dye had been taken up from solution and the final pH value was approximately 7.5, but the dye uptake was uneven. The differential absorption spectra of these samples compared with the undyed fabric show a fairly broad band with maximum absorption at 5600 Å (Figure 6). The absorption also increases sharply with decreasing wavelength in the UV region, but the ratio of the absorption at say 3100 Å to that at 5600 Å is much the same for 0.1% dye uptake as for 0.5%, and no yellowing therefore occurred while heating in the dyebath.

Absorption Spectra Produced by Reaction with Specific Groups in Wool

When 44 × 10 mm. strips of the standard wool fabric were heated for 30 min. at 60° C. in 5 ml. of a 2% solution of *p*-dimethylaminobenzaldehyde in 20% HCl (Ehrlich's reagent), a purple color developed due to tryptophane in the wool. This and other color reactions with intact wool have been studied by McPhee [6], using reflectance spectrophotometry. In the present study it was examined by immersion in *o*-dichlorobenzene and comparison of the colored sample with untreated fabric as already described using transmitted light (Figure 7). Maximum absorption occurred about 5700 Å. Absorption curves corresponding to the colored solutions obtained for three different concentrations of tryptophane using the sulfuric acid procedure [2] are shown in the same figure. These give much broader peaks than the curve for wool itself, pos-

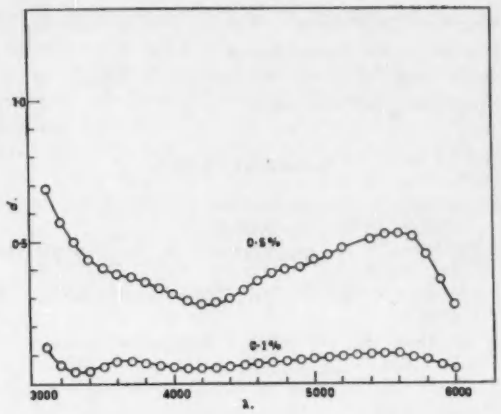

Fig. 6. Differential absorption spectra of wool fabric dyed with Irgalan Bordeaux 2BL from aqueous solution using 0.1% and 0.5% on weight of fabric.

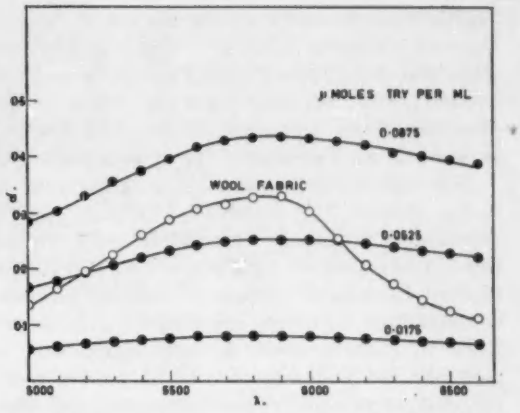

Fig. 7. Absorption spectra for wool fabric and standard tryptophane solutions after treatment with *p*-dimethylaminobenzaldehyde (Ehrlich reaction).

sibly because these colors were measured in aqueous solution, although maximum absorption occurs at about the same wavelength.

When the Pauly reaction, based on reaction of diazotized sulfanilic acid with the tyrosine in wool, was applied, the color produced was so intense that the absorption below 4000 Å could not be measured. A steeply rising curve was obtained between 5000 and 4000 Å. The Sakaguchi reaction for arginine was not applicable, due to the supercontraction produced when the fabric was immersed in 5% KOH solution. This caused the refraction index of the fabric to change to such an extent that it was no longer transparent when immersed in *o*-dichlorobenzene.

Discussion

Although color differences which are barely detectable by eye are easily distinguished by the method described when applied to the standard fabric, greater precision would be expected with cloths of closer weave and with those which had been milled or raised to smooth out variations in thickness due to the yarn structure. Also, decreasing the thickness of fabric examined and shortening the optical path through the layer of immersion liquid both extended the range of wavelength over which measurements can be made in the ultraviolet region. Scattering, due to slight differences in refractive index between the fiber surfaces and the immersion medium and among different histological components within the fibers, becomes more pronounced the lower the wavelength and in fact is generally believed to increase inversely with the fourth power of the wavelength.

The differential spectral absorption curves of unbleached wool fabric and of fabric yellowed by heating at 97° C. in a slightly alkaline buffer solution or by ultraviolet irradiation are essentially the same. All show maxima in the near ultraviolet at 3100–3300 Å and a steep drop in the absorption curve to much lower values at wavelengths above 3900 Å, extending into the visible spectrum. One remarkable feature of the differential absorption spectra for yellowed wool is that the absorption above 3900 Å is very small in comparison with the associated absorption in the ultraviolet region. Thus, although yellowing is apparent to the human eye, the major portion of the absorption peak responsible for this change is now shown to lie outside the range of human vision.

On the sheep, exposure of the fleece to ultraviolet light from the sun and to heat and moisture in the slightly alkaline environment provided by the suint would be expected to produce some yellowing and to increase absorption of ultraviolet light and thereby screen lower regions of the fleece and the sensitive skin of the animal against ultraviolet radiation. The same protective mechanism might operate in the hair and fur of other animals and in the epidermis of animals which have little natural covering (and man).

Comparison of the absorption curves of fabrics heated in buffer at pH 8.0 with those for UV irradiated fabrics shows that the former discolor more

rapidly than the latter during the initial stage of treatment (Figures 3 and 4). This may be due to protection of the interior of the fibers by the yellowed exterior or to an initial bleaching effect. Slight bleaching before yellowing was reported for wool exposed to the Fadeometer [4] or to sunlight [1].

The applications mentioned in this paper by no means exhaust the possibilities of this spectrophotometric technique. It could be used, for example, in studying the lightfastness and washfastness of dyed fabrics and perhaps to estimate particular chemical groups in wool quantitatively. It is proposed to examine some of these applications, in particular the yellowing of wool, in greater detail. A technique for enabling parallel assemblies of fibers to be examined would allow the method to be extended to the study of yellowing and other forms of discoloration in raw wool and in wool at various stages of processing. The method should be applicable to the measurement of color in textile fibers other than wool by immersion in liquids of appropriate refractive index.

Literature Cited

1. Graham, D. R. and Statham, K. W., *J. Soc. Dyers Colourists* **72**, 434 (1956).
2. Graham, D. R. and Statham, K. W., *Nature* **181**, 861 (1958).
3. Harrap, B. S., *J. Soc. Dyers Colourists* **75**, 106 (1959).
4. La Fleur, K. S., TEXTILE RESEARCH JOURNAL **18**, 39 (1948).
5. Lipson, M., *Proc. Roy. Soc. New South Wales* **76**, 225 (1943).
6. McPhee, J. R., TEXTILE RESEARCH JOURNAL **28**, 303 (1958).

Manuscript received April 27, 1959.

A New Replica Technique for the Study of Fabrics and Other Surfaces

W. Rhett Berry

Physical Research Department, Research and Engineering Division, American Enka Corporation, Enka, North Carolina

Abstract

The Silastic replica technique provides a new, unique, and simplified means for the replication and examination of fabric streaks, pile fabrics, and other surfaces. The basic technique is extremely simple and requires no special equipment. It depends on the properties of the silicone rubber, Silastic, produced by the Dow Corning Corporation. This material, received as a liquid, sets up at room temperature, upon the addition of a catalyst, to a smooth, rubbery, fine textured, nontacky film in approximately 30 min. The Silastic produces a replica of the sample fabric that will not only automatically classify the streak, but will also permit microscopical examination and photomicrography of the streak at a relatively high magnification. This material has also proved useful for replicating surfaces of other materials such as godets, draw pins, etc., which are inaccessible for microscopical examination of their surfaces.

Introduction

Streaks in fabrics, like many other problems of the textile industry, have been an ever plaguing condition to the weaving mills as well as the synthetic yarn producers. Textile technologists from producers of both yarns and fabrics have spent endless hours investigating streaks, determining their origin, seeking their correction, and attempting to camouflage their existence. This enormous profit eater in the textile trade has been the subject for a number of investigators who have described their classification and techniques for examination as well as

corrective measures for this seemingly endless condition.

Streaks primarily may be divided into two general classes: those caused by the internal variations within the fiber, such as luster, pigments, voids, skin thickness, etc.; and the external or mechanical streaks which occur due to physical changes brought about in the weaving or some mechanical operation involving the yarn or fiber.

A recent article by F. Schulze [4] gave a useful classification of streaks, including certain subdivisions.

A. Internal streaks
   1. Dye streaks
   2. Intrinsic luster streaks
B. External or physical streaks
   1. Yarn texture streaks
   2. Fabric configuration streaks
   3. Spacing streaks

A disconcerting characteristic of fabric streaks that has hampered the investigator is their virtual disappearance when viewed under even slight magnification. This, of course, leaves much to be desired when attempting to classify a streak as to type and causes. The well established techniques for the microscopical study of the individual yarns and filaments have been quite satisfactory for the investigation of the internal type streaks. Since all streaks do not fall in the internal classification, there existed a need for the development of a technique to aid in the classification and microscopical examination of the external type streaks. The Silastic replica technique developed in this laboratory has proved most adequate in classifying external type streaks as well as making possible their microscopical examination and photomicrography. Other authors, including Schulze, have described replicating techniques by the use of such plastics as polystyrene film, cellulose acetate, vinylite, and polymethyl methacrylate, which permit the investigator to see the detailed structure of the fabrics. This step is most helpful, since it is rather obvious that only external type streaks will replicate. However, the plastic replica techniques require special equipment, such as heated plates and presses, which are expensive and sometimes difficult to apply. Also, they are unsatisfactory for replicating pile fabrics.

Streaks are not necessarily limited to one particular classification. On occasions both classes of streaks may combine forces to produce a really complex streak. Such a condition was recently found in our laboratory in an investigation of fabrics involving spun yarns. Some of the fibers contained voids, causing a luster difference. In addition, the difference in filament shape resulted in nonuniformity of the threads, thus causing spacing difference in the fabric replica.

Pile fabrics, as well as flat goods, often contain streaks which likewise fall in the internal and external classification. Pile bloom and backing tensions are examples of causes for external streaks. Other investigators have experienced difficulties in the preparation of replicas of pile fabrics by previously published plastic replica techniques. The Silastic replica technique was found entirely satisfactory for the preparation of replicas of pile fabrics.

The replica techniques for the study of metal surfaces are well known to the electron microscopist. However, on occasions one may wish to examine larger areas of a metal surface of an object too large

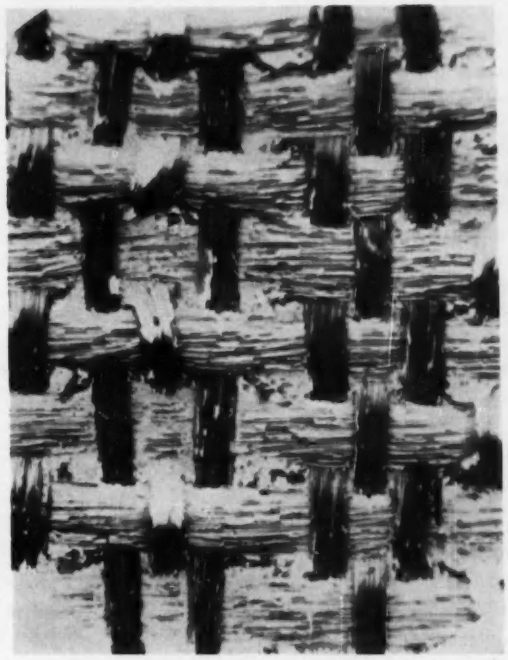

Fig. 1. Taffeta weave lining fabric with 100/60 bright yarn in warp streak. Magnification 27×; warp, vertical; filling, horizontal.

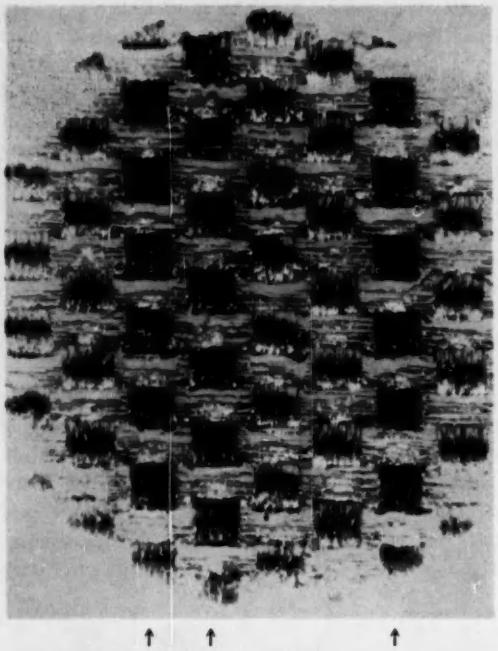

Fig. 2. Lining fabric with overstretched 100/40 bright yarn in filling streak. Magnification 21.5×; filling, vertical; warp, horizontal.

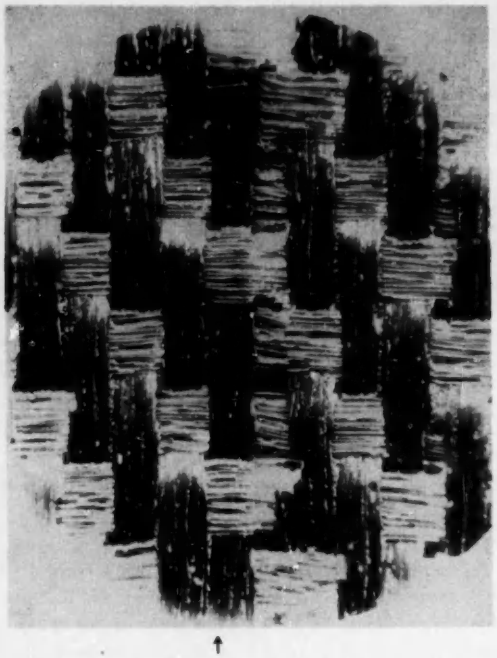

Fig. 3. Twill fabric with 100/60 bright yarn in warp streak. Magnification 23.5×; warp, vertical; filling, horizontal.

for the stage of the light microscope. A recent request of our laboratory was to furnish photomicrographs at a relatively high magnification of the corroded land portion of an extruder screw 3 ft. long and 2 in. in diameter. This, of course, necessitated the preparation of some type of surface replica. Since the silicone rubber had worked so well in the fabric replicas, it was tried on the metal surface. Again, the Silastic proved itself a unique and useful replicating media.

Experimental Procedure

The replica technique developed in this laboratory not only will distinguish between internal and external streaks, but will also permit microscopical examination and photomicrography of the streaks at relatively high magnification with excellent contrast.

The basic technique is extremely simple and requires no special equipment. It depends on the properties of the silicone rubber, Silastic, produced by the Dow Corning Corporation, Midland, Michigan. This material received as a liquid sets up, upon the addition of a catalyst, in about 30 min. at room temperature to a smooth, rubbery, fine textured, nontacky film.

For tight woven fabrics containing streaks, the fabric is taped to a glass surface, and the liquid is simply painted on the streaky portion to approximately 0.1-cm. thickness. After it is cured, the Silastic replica can be peeled from the fabric. If external streaks are present in the fabric, the replica will clearly show them plus any pencil marking or numbers that may have been present to identify the streaks. This, of course, completes the first phase of the investigation, since subsequent examinations will depend on the type of streak classification.

The photomicrographs in Figures 1, 2, and 3 show the negative Silastic replicas made from fabrics containing warp and filling streaks of the external type. Figure 1 was a 93 × 69 taffeta weave greige fabric with 100/60 bright yarn in the warp direction and 150/90 bright yarn in the filling direction. The two overstretched threads involved in the warp streak are marked. It is interesting to note that

there are two classes of external streaks involved in this particular fabric streak: a spacing streak (Classification 3 B) as well as the tension streak (Classification 2 B), shown in the variation in the height of the weaving crowns. This photomicrograph was made with a 2.5× objective and 10× eyepiece, using only transmitted light, and then enlarged photographically to 27×. Figure 2 shows tension streaks (shiners) from a lining fabric with overstretched 100/40 bright yarn in the filling direction. The photomicrograph was made with the same combination of objective and eyepiece as above, using both reflected and transmitted light. In this case, the photographic enlargement was 21.5× instead of 27. Figure 3 shows another warp streak in a lining twill fabric made with transmitted and reflected light.

For microscopical study and photomicrography, the additional step of evaporating a metal such as aluminum on the replica surface, in the direction of the streak, has been found useful to enhance the contrast. This shadowing phase of the technique is a modification of that used in the preparation of certain samples for the electron microscope. It has been found that the evaporation of 0.1 g. of aluminum at an angle of 19–23° to the plane of the sample and a distance of 11 cm. will produce good contrast when examined with transmitted and/or reflected light. All of the included photomicrographs except Figure 6 have been shadowed in the above manner.[1] Krammes and Maresh [2] also shadowed their methyl cellulose replicas with aluminum in the study of chintz fabrics.

For pile fabrics, loosely woven materials, and fabrics made from spun yarns, the procedure for making the replica has to be reversed. Instead of spreading the Silastic on the fabric, the Silastic is spread on a glass plate and allowed to cure for approximately 25–30 min. (The desired tacky feel of the Silastic is quickly learned from experience.) The sample fabric is then placed pile down on the partially cured film of Silastic with only sufficient pressure to smooth out the sample. After the silicone rubber has completely cured, the fabric is peeled off, leaving the pile replicated in the Silastic

[1] The shadow casting operation was done with the SC-3 Evaporator manufactured by the Vacuum Equipment Division, New York Air Brake Co., 1325 Wilson Blvd., Camden 11, New Jersey.

Fig. 4. Replica of 125/50 velvet pile. Magnification 23.5×; filling, vertical; warp, horizontal.

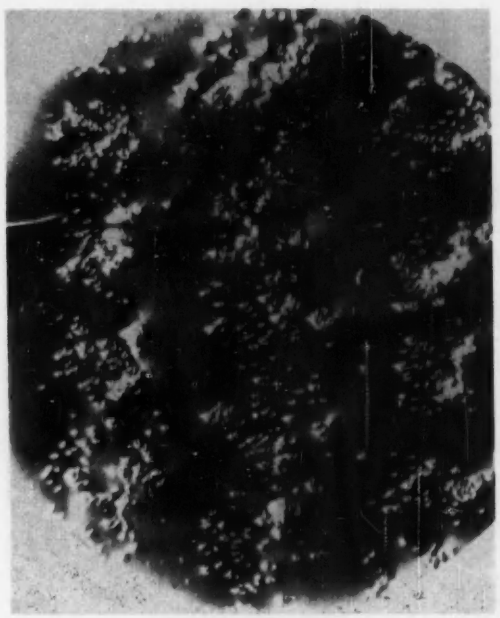

Fig. 5. Replica of 125/50 velvet pile. Magnification 23.5×; filling, vertical; warp, horizontal.

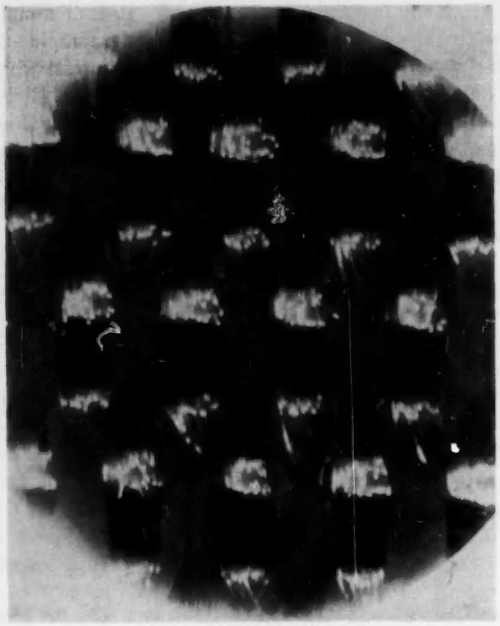

Fig. 6. Velvet pile with backing yarns removed. Magnification 23.5×; warp, vertical; filling, horizontal.

film. Figures 4 and 5 show the aluminum shadowed negative replicas of the pile from two different velvet samples. In each case, the pile yarn is 125/50 bright yarn, but was made by different producers. It is interesting to note that the bloom of the pile of the velvet replica shown in Figure 4 is greater than the one shown in Figure 5. This particular investigation was involved in finding the differences that existed between the two velvet yarns from different producers, in seeking the answer as to why one performed differently from the other.

If additional pressure is applied to the velvet fabric in the preparation of the replica, the pile can be sufficiently embedded so that the backing yarns can be completely removed, leaving only the pile tufts held in place. Figure 6 shows the pile yarns held by the Silastic with the backing yarn removed. This type of preparation may be helpful in the investigation of velvets when it is desired to look at the back of the pile yarn to determine what deformation may have occurred due to uneven backing tensions.

Aside from the study of streaky fabrics, this versatile Silastic has been extremely helpful in the

Fig. 7. Negative surface replica of the land portion of an extruder screw. Magnification 24×.

Fig. 8. Negative surface replica of step godet showing grooves. Magnification 200×.

examination of surfaces of glass, porcelain, and metal, particularly those that required the examination of a relatively large surface when the object itself was inaccessible to the microscope. Draw twister godets, extruder screws, and draw pins are some of the specimens used to illustrate this technique. After the necessary cleaning of the metal surface, the Silastic is painted on and allowed to cure. In some cases where the metal surface is curved, it is necessary to tape on a cardboard mold to hold the Silastic until cured. The negative replica can then be peeled off, shadowed, and examined microscopically. Figure 7 shows the negative replica of a pitted surface of the land portion of an extruder screw. Figure 8 is a replica of the surface of a stainless steel godet showing the grooves cut by nylon yarn. (The large object in the photograph is a foreign particle that landed on the replica just before shadowing.) Also note the well-defined detail of the metal surface outside of the grooved area.

The Dow Corning Corporation also produces a slower curing Silastic which sets up in approximately 10 hr. Both types have been tried and produce satisfactory replicas for both fabrics and metal surfaces.[2]

[2] The fast curing Silastic type is RTV 502, Lot No. 1050, while the slower curing Silastic is type RTV 501.

Conclusion

From the above discussion and the photomicrographs, it seems reasonable to conclude that the Silastic replica technique has been demonstrated to have unique and superior qualification for the classification, microscopical examination, and photomicrography of fabric streaks, as well as the examination of other surfaces. Its simplicity of use and application may make it attractive to mill technicians, as well as traveling textile trouble-shooters, since, for the classification of a streak, one needs only to spread the silicone rubber on and peel it off after 30 min.

Literature Cited

1. Handy, J. I., *J. Textile Inst.* **23**, T1–T5 (1952).
2. Krammes, R. and Maresh, C., *Am. Dyestuff Reptr.* **43**, 189 (1954).
3. Reumuth, H., *Melliand Textilber.* **36**, 533 (1955).
4. Schulze, F., *Modern Texiles Magazine* **39**, 69–74 (December 1958).

Manuscript received June 15, 1959.

Reaction of Epoxides with Cotton Cellulose in the Presence of Sodium Hydroxide

John B. McKelvey, Beverly G. Webre, and Elias Klein[1]

Southern Regional Research Laboratory,[2] *New Orleans, Louisiana*

Abstract

The reactions of various commercially available epoxides with cotton cellulose in the presence of sodium hydroxide have been investigated at 25°, 50°, and 95° C. The effects of solvents and alkali content of the yarn steep on the epoxy add-on have been studied.

Introduction

The present work is concerned with ascertaining the conditions under which epoxides in general react with cotton cellulose. The authors have been unable to find information in the literature which indicates that an uncatalyzed epoxide acts upon cotton, nor have they been able to bring about such a reaction, in spite of the fact that many epoxy compounds are exceedingly reactive with the functional groups (-OH) contained in cellulose. The reaction involved is that between the oxirane ring of the epoxide and the hydroxyl group of cellulose to form a primary or secondary hydroxy cellulose ether.

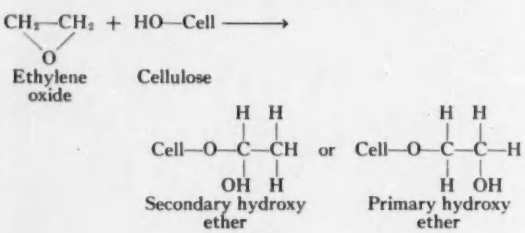

Significant is the fact that for every cellulose hydroxyl reacted, a new hydroxyl is formed on the entering group. Should an epoxide already containing a plurality of hydroxyl groups be joined to cellulose, one might expect enhancement of the hydrophilic properties of cellulose, while if the added epoxide were predominantly hydrophobic, it would be expected that some of the hydrophobic properties would be transferred to the cotton. Such changes in the properties of cotton have obvious commercial advantages.

Since it is well known that epoxides react easily with simple alcohols under conditions of acid and/or base catalysis [11, 24, 29–32] and even without catalysts [38, 39] in some instances, a study of catalysts required for the reaction of epoxides with cellulose was made.

Base Catalysis of Epoxides and Cellulose

As early as 1921, alkali cellulose was reported to react with epichlorohydrin [14], although it is doubtful if it was realized at that time that it was the epoxide group which reacted with the cellulose. Later Schorger [34, 35] reported the reaction of alkali carbohydrates (cellulose) with ethylene, propylene, and butylene oxides to form alpha-hydroxy ethers of the carbohydrate. Lawrie [20–22] also studied the action of ethylene oxide on alkali cellulose and patented the use of the substance for producing novel effects in dyeing and finishing. In 1940, Lawrie, Reynolds, and Ward [23] published the results of their work with ethylene oxide, propylene oxide, and glycidol. These workers showed that little or no reaction occurs between the cellulose and epoxide until the sodium hydroxide concentration reaches 9–11%, at which concentration good addition takes place. The reaction appears to be between alkali treated cellulose and the epoxide, and moisture is essential to the reaction. The favored sodium hydroxide concentration range was

[1] Present address: Courtaulds Incorporated, Mobile, Alabama.

[2] One of the laboratories of the Southern Utilization Research and Development Division, Agricultural Research Service, U. S. Department of Agriculture.

TABLE I. Reactivity of Epoxides and Cotton Cellulose in the Presence of Sodium Hydroxide

Epoxide	Source	Weight gain, % yarn	Temperature, °C.	Time, hr.
Butadiene monoxide	UCC*	15.7	25	22.0
Butadiene dioxide	UCC	226.0	25	16.0
Epichlorohydrin	Shell	57.8	25	20.0
Allyl glycidyl ether	Shell	20.7	95	2.0
Phenyl glycidyl ether	Shell	150.0	95	2.0
Butyl glycidyl ether	Ciba	153.0	95	4.0
Butylene oxides-S	Dow	10.0	62	11.5
Styrene oxide	Dow	42.0	95	2.0
Glycidyl methacrylate†	DuPont	22.0	55	16.0
Glycidol‡	Lab. prep.	8.0	25	16.0
Glycidol**	Lab. prep.	37.0	25	24.0

* Union Carbide and Chemical Corporation.
† 20% by volume solution in CCl_4.
‡ 20% by volume solution in H_2O.
** 20% by volume solution in $CHCl_3$.

9–22.5%, as above 22.5% the reactivity of the epoxides did not increase. The reaction will proceed out of brine solution, carbon tetrachloride, other organic solvents, and even out of water. In aqueous solutions, however, a self-condensation of the epoxide takes place within the cellulose, but the epoxide condensation products (glycol or polyglycols) are removed on washing. Organic solvents exert a catalytic effect on the ethylene oxide reaction, carbon tetrachloride being the best of a number tested. More recently a number of investigators have taken patents on the use of epoxides or prepolymer of epoxy resins [1, 5, 7, 8, 12, 13, 15, 26, 36, 37, 40, 43] for crease resistance of cotton or for other reasons.

Experimental

The following simple test procedure was used. A 1-g. skein of mercerized yarn (Linker Machines, Inc.)[3] was immersed in a solution of the alkali or other catalyst, degassed under a bell-jar for 0.5 hr., and centrifugally extracted to a 150–200% wet pickup. The wet yarn was placed in a small stoppered round-bottom flask containing 20–25 ml. of epoxide or epoxide solution. The flask was agitated by a wrist-action shaker in a thermostatically controlled bath at the desired temperature. After suitable time had elapsed, the yarn was drained; washed with methanol, chloroform, or ether (depending on solubility of the epoxide); acidified; and finally washed with distilled water. Drying was carried out at 100–105° C. or in a vacuum oven at 60–65° C.

The epoxides used, with the exception of glycidol, were research grade materials kindly furnished by the various sources listed[3] in Table I.

The glycidol was prepared by the thermal decomposition of glycerol carbonate [17]. Glycerol carbonate itself does not add to cotton cellulose in the presence of sodium hydroxide. A few epoxides were studied by varying the sodium hydroxide concentration from 0 to 35% in order to obtain information for optimum reaction conditions. A number of epoxides in solvents were tested against yarn containing optimum alkali content. Evidence of reaction was shown by excessive swelling and unwinding of yarn and weight gain. In some cases with very reactive materials the yarn resembled resin treated yarn or was glued to the flask. A further evidence of reaction was the inertness of treated material to hot solvent extraction with dimethylformamide. Little or no add-on was removed by the dimethylformamide.

[3] Trade names have been used to identify materials used in the work, and such use does not imply endorsement or recommendation by the U. S. Department of Agriculture over other products not mentioned.

Results

Pure Epoxides and Cotton Cellulose

No reaction between cotton yarn and the following epoxides in the absence of a catalyst occurred either at room temperature or at 95° C. for 24 hr.: epichlorohydrin, butadiene diepoxide, styrene oxide, phenyl glycidyl ether, and glycidol. Phenyl glycidyl ether did not react at 180° C. in an atmosphere of nitrogen in 2 hr., even though this epoxide reacts

TABLE II. Epichlorohydrin and Cotton Cellulose* Reaction

Time, min.	Weight gains, % 25° C. Pure	25° C. Solution†	50° C. Pure	50° C. Solution†	65° C. Solution†
15	0	0	5.3	2.0	4.2
30	1.9	0	12.3	11.5	12.8
45	2.3	0	17.2	9.1	19.3
60	1.6	0.1	21.3	11.9	22.9
90	2.1	0.8	25.1	17.8	26.2
120	5.0	2.8	26.3	19.9	27.5
180	7.9	3.2	26.8	32.5	31.6
240	11.2	6.8	29.1	37.0	28.5

* 200% wet pickup from 13.5% NaOH.
† 20% by volume of epichlorohydrin in CCl_4.

with simpler alcohols [38, 39]. Butadiene monoepoxide and butylene oxides-S did not react at reflux temperatures. A similar series was run with cotton which had been treated overnight with ethylamine in a Dewar flask and subsequently washed with chloroform. In all cases except with butadiene diepoxide, there was no weight gain. The latter diepoxide apparently reacted with residual amine in the yarn to form a visible solid which was water soluble.

Epoxides and Cotton Cellulose in the Presence of Sodium Hydroxide

A summary is given in Table I of the reactive epoxides tested and the temperatures at which reactions with cellulose occurred, as evidenced by weight gain after methanol, acid, and water washes. Optimum alkali concentration was that concentration where greatest add-on was obtained in the shortest time; 13–15% at room temperature. There were shifts in the optimum to higher concentrations at higher temperatures for epoxides that react both at low and high temperatures. Each epoxide was tested at 25°, 50°, and 95°, except butadiene monoepoxide and butylene oxides-S, which boil below 95°.

In cases where no gain was observed, slight weight losses were experienced. Those epoxides which did not react at temperatures up to 95° were the following: vinylcyclohexene monoepoxide, vinylcyclohexene diepoxide, 3,4-epoxy-6-methylcyclohexylmethyl-3,4-epoxy-6-methylcyclohexanecarboxylate (E.P. 201), 1,2,di-isobutylene epoxide, 1,4,di-chloro 2,3, epoxy butane, limonene diepoxide, 1,2,-epoxy decane, and the sodium salt of 9,10-epoxy-undecylenic acid, all furnished by the Union Carbide Chemical Company; 1,2-epoxy octane, 1,2-epoxy-dodecane, and dipentene monoxide, all furnished by Becco Division of Food Machinery and Chemical Corporation; and butyl epoxy stearate and alpha pinene oxide, prepared in the U. S. Department of Agriculture Laboratory.

Data in Table II show variations of weight gains with temperature and time for the reactions between cotton cellulose of 200% wet pickup from 13.5% NaOH solution and pure epichlorohydrin as well as 20% by volume solutions of epichlorohydrin in CCl_4.

Data in Table III show the effect of alkali concentration used in the yarn steep on the epoxy add-on from chlorinated solvents.

Since several of the epoxides react only at elevated temperatures, alkali concentrations were varied for styrene oxide and phenyl glycidyl ether at 95° C. These results are given in Table IV.

Although a complete study was not made, experiments on the loss in tensile strength of a number of yarns tested after various percentages of epoxide add-ons showed that only 50–70% of the breaking strength was retained.

Effect of Water on Alkali Treated Cellulose—Epoxide Reaction

After cotton cellulose had been treated with sodium hydroxide solution, the water was removed from it by extraction with absolute ethanol, diethylamine, dioxane, etc. without much loss of caustic. When such extracted yarns were reacted with butylene oxides-S, phenyl glycidyl ether, or styrene oxide at reflux temperatures or at 95° C., either very low weight gains or no reactions were obtained. The cellulose became bright yellow, then brown. These same epoxides gave high add-on when water was present.

TABLE III. Effect of Alkali Content of Yarn Steep on Epoxy Add-On from Chlorinated Solvents

	Reaction conditions		Weight gains, %					
			% NaOH used in yarn steep					
Epoxide	Time, hr.	Temperature, ° C.	5.0	10.5	15.0	17.3	30.0	50.0
Epichlorohydrin*	21	25	3.2	16.9	26.5	37.8	7.5	loss
Epichlorohydrin*	21	50	6.1	20.2	46.0	54.6	61.6	26.0
Butadiene diepoxide†	16.5	25	15.0	58.0	76.0	73.0	24.0	—

* 20% by volume in CCl_4.
† 20% by volume in $CHCl_3$.

Effect of High Boiling Solvents on Epoxy Addition to Alkali Treated Cellulose

The common low boiling organic solvents did not permit working at very elevated temperatures; hence some higher boiling liquids were selected as solvents for the phenyl glycidyl ether and styrene oxide addition reactions with cotton cellulose. The epoxides were made up to 20% by volume in the solvent and heated for 6 hr. at 95° C. with cellulose prepared from 13–15% NaOH solution and 200% wet pickup. These results are in Table V.

Epoxylated Yarn and Substantive Dyeing

When cellulose ethers are formed *in situ* in cotton, the yarn eventually should commence to take up dyes such as Celliton Red which untreated cellulose rejects. This has been realized after the reaction of butylene oxides-S with cotton cellulose in the presence of sodium hydroxide. Some of the properties of the yarn after the addition of the butylene oxides-S at 62° C. are recorded in Table VI. However, it might be expected from the structure of some epoxides that there is the possibility of introducing a plurality of hydroxyl groups on the surface of cotton. Thus, each glycidol molecule added to the cellulose introduces two hydroxyl groups and each butadiene diepoxide introduces at least two and possibly more hydroxyl groups. This should cause an assist in direct dying, while if more hydrophobic groups, such as aromatic or other rings, were introduced, dye resists should be possible. A number of epoxylated yarns containing 20–30% add-on and a mercerized yarn control were dyed simultaneously in a 0.5% Calcomine Blue NR solution for 15 min. at the boiling point.

TABLE IV. Effect of Alkali Concentration on Cotton Cellulose Weight Gains

% NaOH	Add-on from 100% styrene oxide (3 hr. at 95° C.)	Add-on from 100% phenyl glycidyl ether (1.5 hr. at 95° C.)
1.0	slight loss	—
2.0	5.3	—
4.0	14.1	76.6
9.7	30.5	160.3
14.3	59.2	228.0
17.0	38.6	—
20.0	14.7	9.0
25.0	loss	10.7
30.0	—	4.2

Yarns treated with glycidol, epichlorohydrin, and butadiene diepoxide dyed black; yarns treated with butadiene monoepoxide and butylene oxides-S dyed blue, as did the mercerized yarn control. The yarns treated with styrene oxide and phenyl glycidyl ether dyed grey and unevenly.

Discussion

It can be noted from the weight gains recorded in Table I that only 10 of the 23 epoxides added to cotton cellulose in the presence of sodium hydroxide. Of the reactive epoxides, it is believed that three (glycidol, epichlorohydrin, and glycidyl methacrylate) gave the same end-product. Yarn reacted with the glycidyl methacrylate showed no bromine absorption. This indicates that glycidyl methacrylate did not add *per se* because an ester is unstable under conditions of alkaline hydrolysis. In the case of epichlorohydrin, Ross [33] proved that the chloride group is rapidly hydrolyzed in alkaline solution. In

TABLE V. Effect of Solvents on Cotton Cellulose–Epoxide Reaction*

Solvent†	Dielectric constant	Weight gain from phenyl glycidyl ether, %	Weight gain from styrene oxide, %
Xylene	2.4	92.0	—
Toluene	2.6	94.0	0
Chlorobenzene	5.6	36.8	loss
o-dichlorobenzene	7.5	47.9	—
p-dichlorobenzene	2.9	−4.0	−14.0
Trichlorobenzene	—	54.5	0
Dioxane	2.2	4.2	0
s-tetrachloroethane	2.3	−4.6	small loss
1,1,2 trichloroethane	3.6	32.0	loss
1-nitropropane	23.2	−5.0	loss
Nitrobenzene	34.8	10.4**	—
Mineral spirits	1.9	(insoluble)	30.2
Ethanol‡	24.3	0	−1.0
t-butyl alcohol	17.0	−4.6	−8.1
70% ethanol / 30% water	—	0	0
Cyclohexanone	18.3	1.4	1.0
Mesityl oxide	15.1	9.3	—
Benzonitrile	25.2	20.5	—
Isophorone	—	73.5	—
Allyl ether	—	29.3	—
Dimethylformamide	—	−3.5	−5.0

* Reaction for 6 hr. at 95° C. with cotton cellulose prepared from 13–15% NaOH and 200% wet pickup.

† Epoxide solution was 20% by volume in commercial solvent.

‡ Same conditions except temperature was 76–78° C.

** Reacts with NaOH.

TABLE VI. Properties of Yarn* after Treatment with Butylene Oxide S at Reflux (62° C.)

Reaction time, hr.	Weight gain, %	Cuene solubility†	Staining with Celliton Red	Action of organic solvents	Condition of yarn
3	12.7	soluble	negative	no action	stiff
6	32.5	swollen	positive	no action	very stiff
23	100.0	insoluble	strongly positive	yarn swells in MeOH or $CHCl_3$	waxy

* 200% wet pickup from 13.5% NaOH.

† As determined microscopically in a solution which is 1 *M* with respect to cupric hydroxide and 1.9 *M* with respect to ethylene diamine.

the case of epichlorohydrin in carbon tetrachloride solvent, however, where an add-on of 19.3% was obtained, the purified yarn showed 0.19–0.22% chlorine content, indicating the chlorine is not all hydrolyzed. Other samples tested showed chlorine contents varying from 0 to 0.23%, indicating that the chlorine is largely removed from the molecule by the basic solution. Had the chlorine in epichlorohydrin remained intact, about 38% of the weight gain would have been chlorine. A control yarn averages about 0.03–0.05% chlorine.

That the reaction under consideration is ionic and catalytic is easily shown by the facts that no reaction between pure epoxides and cellulose was observed and that when water was extracted from the system, the reaction rate decreased and approached zero as the water was removed completely. However, what is not so clear is why the amount of epoxy add-on (Tables III and IV) is dependent on the alkali content of the cellulose, especially so when it is remembered that the caustic is not consumed.

The simplest explanation of the phenomenon is that maximum add-on occurs in the region of maximum alkali swelling of the cellulose [27]. Hence, more surface is presented to the entering epoxide in the heterogeneous reaction. It is not, however, the whole consideration because, as has been shown, when the cellulose is swollen to a maximum and the water removed, little or no reaction occurs. Under these optimum conditions there are good indications that either a loose coordination complex of cellulose, water, and caustic is formed [9, 10, 28] or, under some extreme conditions, sodium cellulosate [41] is present. Solvents such as absolute alcohols upset the cellulose complex by removing water. It would appear, therefore, that caustic solutions serve a dual purpose in the reaction; first, by swelling the cellulose or "activating" it for a complex formation and second, by opening the epoxide ring, which Ross [33] has shown is more easily opened by hydroxide ions than was formerly believed [6]. The earlier belief probably arose from the fact that many epoxides had been prepared by using strong alkali on a chlorohydrin to form the ring in the first place.

It has also occurred to the writers that active hydroxyl groups in cellulose as in simpler polyols [18] are analogous to but differ in degree of activity from the hydroxyl groups of phenols in regard to the epoxide reaction. In fact, Boyd and Marle [2, 3] showed that ethylene oxide reacted only slightly with various phenols (1% conversion), but when the phenol was neutralized with alkali a high conversion to the phenol hydroxy ether occurred. This analogy was strengthened by Guss [16], who showed that a high yield of mixed hydroxy ethers resulted in the alkaline catalysis of styrene oxide and phenol. The "acidity" of cellulose [27] is very small as evidenced by the ionization constant, $K = 1.84 \times 10^{-14}$, while that for phenol is $K = 1.3 \times 10^{-10}$.

However, as has been pointed out, more than half of the epoxides tested fall into the inert category towards alkali cellulose. Schorger [34, 35] made the statement that with 1-2 epoxides, the reactivity with cellulose ended at about a five carbon atom chain in the aliphatic series of epoxides. There is no literature on the activity of the aromatic epoxides with cellulose.

One might say the inertness of some epoxides is due to the nucleophilic nature, which in turn is due to the type of group substituted adjacent to the epoxide ring. The sole effect of the substituted group is an inductive one; that is, if it acts as an electron attracting group, the attack of the anion on the epoxy ring would be facilitated. Since styrene oxide and 1,2-epoxydecane react very differently with cellulose under conditions of alkaline catalysis, the in-

ductive effects of the aryl and decyl groups must differ. The aryl epoxy reacts with cellulose in a few hours at 95° C., while the epoxydecane does not react under the same conditions. Therefore, in the case of the epoxy compounds, the phenyl group is acting as an electron attracting group.

In the reaction between olefins and peracetic acid [42], the phenyl group acts as an electron repelling group since there is unsaturation in the compound. Swern [42] found that the specific reaction rate constant for styrene ($k = 11.2 \times 10^{-3}$) is larger than that for 1-decene ($k = 4.7 \times 10^{-3}$) at 25° C. This indicates that the phenyl group is a more electron releasing group than is the octyl group; therefore the electron density at the double bond is greater in the aryl olefin. Swern [42], aware of this apparent anomaly, stated that the phenyl group can act as an electron release group, though frequently the reverse is true.

The most interesting observation encountered in this investigation was the effect of solvents on the base catalyzed epoxide-cellulose reaction (Tables II, III, and V). Solvents were thought to be desirable for economic reasons, but it is by no means certain that an epoxide reacts out of a solvent with cotton cellulose in the presence of sodium hydroxide in the same manner as does the pure epoxide. The solvents changed the reaction rates, as indicated by the data in Table V. Some of the results are readily explained. For instance, dioxane and absolute ethanol remove water from the alkali cellulose, thus stopping the reaction. On the other hand, a 30% water–70% ethanol mixture which is also a solvent for the epoxide, phenyl glycidyl ether, did not permit a reaction to occur. Possibly such a mixture removes alkali from the cellulose, thus breaking up the complex of water, caustic, and cellulose. The dielectric constant of the reaction medium does not appear to give a clue to the reaction mechanism. Furthermore, if the dielectric constant gave a clue, styrene oxide should react in toluene nearly as well as in mineral spirits, but no reaction occurred in the former solvent.

A further peculiarity is the very weak yarn produced when solvents are used for phenyl glycidyl ether and styrene oxide. It was established in the beginning of this investigation that the epoxide add-on caused strength losses in all yarns tested. Only 50–70% strength was retained after the reaction. When styrene oxide 100% was reacted with cotton cellulose in the presence of sodium hydroxide, a strength retention of 53% was observed in the yarn at 100% add-on. Yet when only 30% add-on was obtained from a mineral spirit solution of styrene oxide (20% by volume), the strength retention was only 27%. If more concentrated solutions of styrene oxide were used, for example, 40% and 60% by volume solutions, the strength retention of the yarn dropped to 14% or values too low to measure; the yarn literally fell apart. Samples of yarn containing phenyl glycidyl ether add-on from solvents also showed very low strength retentions.

This striking anomaly may be explained on the basis of different types of reactions occurring in the two systems. Without solvents, linear polymers of the epoxide are formed by self-polymerization. These polymers can be shown to exist by heating a 13% caustic solution with styrene oxide or phenyl glycidyl ether in the absence of cellulose at 95° C. for a few hours, during which time the epoxide layer becomes highly viscous. Solutions of the epoxides in solvents do not thicken; in a solvent in the presence of cellulose, however, the reaction is largely between random cellulose hydroxyl groups and epoxy rings. The net result is that a greater number of the hydroxyl groups of cellulose are substituted, and the yarn strength is decreased. That linear graft polymers do occur when 100% epoxide is reacted with cotton cellulose in the presence of sodium hydroxide is evidenced by the observations in two cases at least, namely, with phenyl glycidyl ether and butadiene diepoxide. In these instances, the calculated DS is greater than 3. Such a value is not reasonable in a heterogeneous reaction of this nature, when the reactants at best are only partially in contact. The plausible explanation is that in either case some epoxy groups react with the hydroxyl groups of the cellulose; they may in one case or may not in another form linear graft polymers.

The weight gains obtained with a carbon tetrachloride or chloroform solution of butadiene diepoxide (Table III) were explained by the writers [19] as due to the effect of the activity of the hydroxide ion. The degree of ring opening was directly proportional to the activity of the hydroxide ion. However, the epoxide is less soluble in the alkali as the concentration of NaOH increases, thus accounting for low add-on at high caustic concentrations.

Recently, the elegant research of Long and Pritchard [24, 31] has proved that epoxy ring opening

with base catalysis is a typical S_N2 mechanism, proceeding as follows

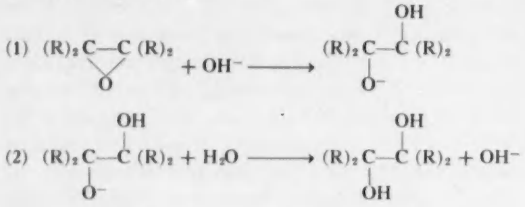

where R = H or other substituent. Equation 1 is the slow, rate-determining reaction, and Equation 2 is the fast, concluding reaction.

If the reasonable assumption of the formation of the cellulosate ion, $\overline{A}$, in alkali is permitted, it follows, according to a similar mechanism in which the $\overline{A}$ ion is substituted for the $\overline{OH}$ ion in Equation 1, that cellulose hydroxy ethers, $R_2—\underset{OH}{\overset{A}{C}}—C—R_2$, are formed. This is essentially the Lowry mechanism [4, 25]. Since both cellulosate ions and hydroxide ions are present in the reaction mixture, both enter competitive reactions with the epoxides. The reaction can stop after the monomer ether of cellulose is formed, or linear graft polymers can be formed by either of two mechanisms. If the hydroxide ions remove protons from the cellulose hydroxy ethers, the latter can add epoxide units. Alternately, the epoxide units can add to the anion product of Equation 1. Either of these processes results in a stepwise growth.

Conclusions

In general summation, it may be said that certain epoxides, those in which the ring is strained but unhindered by adjacent substituents, will react with cotton cellulose in the presence of sodium hydroxide. The derivatives prepared may be single cellulose hydroxy ethers formed from solvents, or linear graft polymers of the epoxide formed randomly and unevenly in the yarn in absence of solvents. The reactivity of the epoxides with cellulose is not dependent upon their solubility in water, since such water-insoluble epoxides as phenyl glycidyl ether and styrene oxide react as easily as some water-soluble epoxides.

Any reaction mechanism has to take into account the maximum add-on obtained when the sodium hydroxide concentration of the yarn steep is varied, the necessity of the presence of water, and the solubility of the epoxide in the caustic solution. It is suggested that the reaction is an S_N2 mechanism probably similar to the mechanism proposed by Lowry [4, 25] and that the properties of the cellulose derivatives are greatly dependent on the hydrophilic–hydrophobic balance of the reacting epoxide.

Literature Cited

1. Balassa, L., U. S. Pat. 2,588,463 (March 11, 1952).
2. Boyd, D. R. and Marle, E. R., *J. Chem. Soc.* **97**, 1788–1790 (1910).
3. Boyd, D. R. and Marle, E. R., *J. Chem. Soc.* **105**, 2117–2139 (1914).
4. Branch, G. E. K. and Calvin, M., "The Theory of Organic Chemistry" New York, Prentice-Hall, 403 (1941).
5. Broderick, A. E. (to Union Carbide and Carbon Corp.), U. S. Pat. 2,682,535 (June 29, 1954).
6. Brönsted, J. N., Kilpatrick, Mary, and Kilpatrick, M., *J. Am. Chem. Soc.* **51**, 428–461 (1929).
7. Castan, P., U. S. Pat. 2,324,483 (July 20, 1943).
8. Castan, P. (to De Trey Freres S.A.), U. S. Pat. 2,444,333 (June 29, 1948).
9. Champetier, G. and Neel, J., *Bull. Soc. Chim. France* [5] **16**, 930–937 (1949).
10. Chédin, J. and Marsaudon, A., *Makromol. Chem.* **20**, 57–82 (1956).
11. Chitwood, H. C. and Freure, B. T., *J. Am. Chem. Soc.* **68**, 680–683 (1946).
12. Cohen, S. G. and Haas, H. C., *J. Am. Chem. Soc.* **72**, 3954–3958 (1950).
13. Condo, F. E. and Schroeder, C. W. (to Shell Chemical Co.), U. S. Pat. 2,752,269 (June 26, 1956).
14. Dreyfus, H., Brit. Pat. 166,767 (July 28, 1921).
15. Greenlee, S. O. (to Devoe & Reynolds Co., Inc.), U. S. Pat. 2,668,805 and 2,668,807 (February 9, 1954).
16. Guss, C. O., *J. Am. Chem. Soc.* **71**, 3460–3462 (1949).
17. Jefferson Chemical Co., "Preparation of Glycidol from Glyceryl Carbonate," personal communication.
18. Karrer, P., *Cellulosechemie* **2**, 125–128 (1921).
19. Klein, E., McKelvey, J. B., and Webre, Beverly G., *J. Phys. Chem.* **62**, 286–288 (1958).
20. Imperial Chemical Industries, Ltd., Lawrie, L. G., Reynolds, R. J. W., and Piggott, H. A., Brit. Pat. 439,880 (December 17, 1935).
21. Lawrie, L. G., Reynolds, R. J. W., and Piggott, H. A. (to Imperial Chemical Industries, Ltd.), U. S. Pat. 2,109,295 (February 22, 1938).
22. Lawrie, L. G., Reynolds, R. J. W., and Walker, E. E. (to Imperial Chemical Industries, Ltd.), U. S. Pat. 2,164,248 (June 27, 1939).
23. Lawrie, L. G., Reynolds, R. J. W., and Ward, D. J., *J. Soc. Dyers Colourists* **56**, 6–17 (1940).

24. Long, F. A. and Pritchard, J. G., *J. Am. Chem. Soc.* **78**, 2663–2667 (1956).
25. Lowry, T. M., *J. Chem. Soc.* **127**, 1371–1385 (1925).
26. Musser, D. M. (to Pacific Mills), U. S. Pat. 2,455,083 (November 30, 1948).
27. Neale, S. M., *J. Textile Inst.* **21**, T225–230 (1930).
28. Percival, E. G. V., Cuthbertson, A. C., and Hibbert, H., *J. Am. Chem. Soc.* **52**, 3257–3269 (1930).
29. Petrov, A. A., *J. Gen. Chem. (U.S.S.R.)* **14**, 1038–1043 (1944); through *Chem. Abstr.* **40**, 7153 (1946).
30. Petrov, A. A., *J. Gen. Chem. (U.S.S.R.)* **16**, 1206–1212 (1946); through *Chem. Abstr.* **41**, 3051 (1947).
31. Pritchard, J. G. and Long, F. A., *J. Am. Chem. Soc.* **78**, 6008–6013 (1956).
32. Reeve, W. and Christoffel, I., *J. Am. Chem. Soc.* **72**, 1480–1483 (1950).
33. Ross, W. C. J., *J. Chem. Soc.* **1950**, 2257–2272.
34. Schorger, A. W. (to C. F. Burgess Laboratories, Inc.), U. S. Pat. 1,863,208 (June 14, 1932).
35. Schorger, A. W. (to C. F. Burgess Laboratories, Inc.), U. S. Pat. 1,941,278 (December 26, 1933).
36. Schroeder, C. W. and Sumers, R. W. (to Shell Chemical Co.), U. S. Pat. 2,774, 691 (December 18, 1956).
37. Schroeder, C. W. and Condo, F. E., TEXTILE RESEARCH JOURNAL **27**, 135–145 (1957).
38. Shechter, L. and Wynstra, J., *Ind. Eng. Chem.* **48**, 86–93 (1956).
39. Shechter, L., Wynstra, J., and Kurkjy, R. P., *Ind. Eng. Chem.* **48**, 94–97 (1956).
40. Suen, T. J. (to American Cyanamid Co.), U. S. Pat. 2,730,427 (January 10, 1956).
41. Sugihara, J. M. and Wolfrom, M. L., *J. Am. Chem. Soc.* **71**, 3509–3510 (1949).
42. Swern, D., *J. Am. Chem. Soc.* **69**, 1692–1698 (1947).
43. Tasker, C. W. (to American Viscose Corp.), U. S. Pat. 2,667,481 (January 26, 1954).

Manuscript received February 16, 1959.

Stress Relaxation and the Transition Temperature of Wool

B. J. Rigby

C.S.I.R.O. Wool Research Laboratories, Division of Textile Physics, Ryde, N.S.W., Australia

Abstract

The stress–relaxation behavior of a number of chemically and physically modified wool fibers has been examined and shown to correlate with the temperature of transition of the particular modified wool. The transition temperature has been discussed previously by Feughelman, Haly, and Rigby. Below the transition temperature the stress decays in 1 hr. by 33%, and above the transition temperature by 73%, of its initial value. These quantities are independent of the particular modification and appear to be associated with reversible and nonreversible transformations of native keratin.

Introduction

In some recent papers [1, 2, 3] it has been shown that normal wool fibers when stretched in water show a second-order transition in the temperature range 60°–70° C. This transition is most conveniently observed by measuring the strain at the turnover point between the yield and post-yield regions. Below the transition temperature this turnover value is about 30% and is independent of temperature, while above this temperature the strain at turnover increases with increase of temperature. The transition temperature has a different value for various chemically modified fibers, but the behavior above and below the transition temperature is the same as with the normal fiber.

The second-order transition is shown up in other ways, as reported in the above references, e.g., change in birefringence and change in nature of remanent stress. In particular the relation between transition temperature and the ability to permanently set is reported for a number of chemically modified fibers by Feughelman, Haly, and Rigby [2].

In this paper are reported some stress–relaxation experiments on chemically modified fibers and their correlation with the above observations on transition temperatures.

Experimental

In all the experiments the fiber was extended by the fiber motor of a standard Cambridge Textile Extensometer, but the load was measured with a Statham electrical transducer, the output of which was fed into a potentiometric recorder. The transducer was mounted on the extensometer in the position normally occupied by the vibrating arm used to link the fiber and spring. The fibers were strained at a constant rate of 41%/min. to an extension of 20%, at which extension they were allowed to relax for 1 hr. All the experiments were carried out in distilled water adjusted to the required temperature. The rate of straining, and the strain of 20%, at which the experiments were carried out, were chosen as being values of these parameters allowing reproducible results at room temperature, provided the fiber is suitably relaxed in water at 53° C. between tests. This kind of test, in which the strain and rate of straining become parameters when examining stress–relaxation, has been discussed fully elsewhere [7].

All the wool used was from penned Corriedale sheep hand-fed for uniformity of growth of the fibers, as specified in previous work [2]. The wool type number is SW13.

The experiments involved the measurement of stress–relaxation for 1 hr. at both 20° C. and 80° C. for untreated fibers and a number of chemically modified fibers; these included Van Slyke's reagent treated fibers (34 cc. water, 8.69 g. $NaNO_2$, and 7.2 cc. glacial acetic acid at 20° C. for 27 hr.), iodinated (Richards and Speakman [6]), ultraviolet

irradiated (Mitchell and Feughelman [5]), treatment in 1 *N* thioglycollic acid at PH 5 for 21 hr. at 37° C., and treatment in 0.1 *M* mercuric acetate in 0.1 *N* acetic acid for 10 hr. at 25° C. The last treatment is claimed to cross-link wool [4].

Results

A typical stress–strain curve, together with the stress–relaxation when the fiber is held at a given strain, is shown in Figure 1. The quantities F_0 and F_{60}, which are used later, are defined in this figure. F_0 is the stress corresponding to the strain at which the relaxation curve is obtained and F_{60} is the stress in the fiber after 60 min., extended, by 20%. The rate of relaxation has become very slow after this time and the stress F_{60} (and $(F_0 - F_{60})/F_0$) have been chosen as arbitrary, convenient measures with which to compare results of different fibers. Figures 2 and 3 give stress relaxation data plotted against logarithm of time. Figure 2 gives the data at 20° C. and Figure 3 data for similarly treated fibers at 80° C. Each curve is the average of at least four experiments. The initial decay of stress is rapid, and the time taken (relaxation time) for the stress to decay by 50% of the total decay in 60 min. $(F_0 - F_{60})$ is less than a minute in each case. Some more accurate determinations of the relaxation time at 20° C. for normal, Van Slyke's reagent, iodinated, ultraviolet irradiated, and mercuric acetate treated fibers gave 17, 10, 15, 20, and 25 sec. respectively, with an error of ± 2 sec. in each case. Owing to this error, there is probably no difference between normal and iodinated fibers. However, the Van Slyke's reagent treated fibers appear to decay more rapidly, and the mercuric acetate treated fibers more slowly, than the normal. As an auxiliary experiment the transition temperature of mercuric acetate treated fibers was determined [2]; this temperature was between 50° and 60° C. Table I lists the two stresses F_0, F_{60}, the percentage drop in stress in 1 hr. $(F_0 - F_{60})/F_0$, the relaxation time as defined above, and the transition temperature for each modified wool.

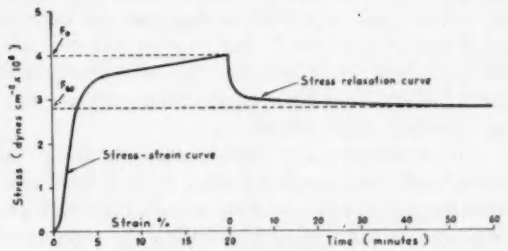

Fig. 1. A plot of the stress–strain curve and subsequent stress–relaxation behavior of a normal Corriedale fiber stretched in water at 20° C., to a strain of 20% and at a rate of 41%/min. The fiber diameter (wet) was 47μ. The plot shows the meaning of F_0 and F_{60}.

No particular physical significance can be attached to the numerical value of the quantity $(F_0 - F_{60})/F_0$ and to the relaxation time, as they are dependent upon the rate of straining, and to a lesser extent strain. It is shown [7], in fact, that $(F_0 - F_{60})$ is independent of strain (at a fixed rate of straining) between the limits 5–25%. It is also shown that $(F_0 - F_{60})$ varies as the logarithm of the rate of straining; thus $(F_0 - F_{60})/F_0$ may be predicted for any rate once it has been measured at a known rate. However, the constancy of these values above and below the transition tempera-

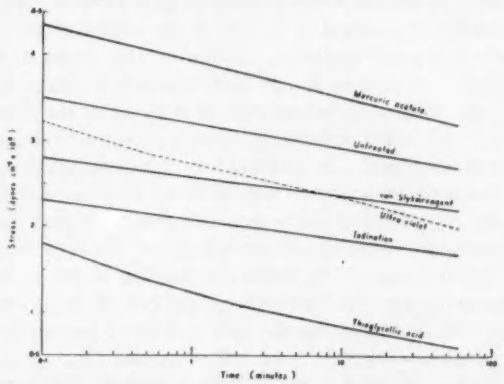

Fig. 2. A plot of stress–relaxation against logarithm of time for normal and treated Corriedale fibers stretched in water to a strain of 20%. The temperature was 20° C. and the rate of straining 41%/min. Each curve is drawn from the average results of at least four experiments.

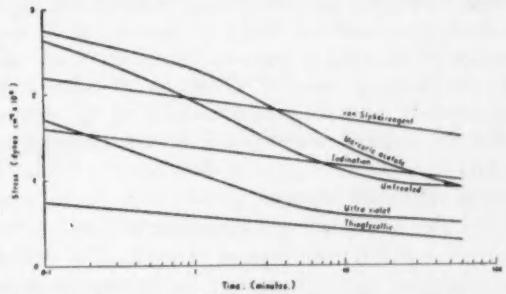

Fig. 3. A plot of stress–relaxation against logarithm of time for normal and treated Corriedale fibers stretched in water to a strain of 20%. The temperature was 80° C. and the rate of straining 41%/min. Each curve is drawn from the average results of at least four experiments.

TABLE I

	Untreated		Van Slyke		Iodinated		Ultra-violet		Thioglycollic acid		Mercuric acetate	
	20°	80°	20°	80°	20°	80°	20°	80°	20°	80°	20°	80°
F_0, dynes cm.$^{-2}$ × 10^8	4.0	2.9	3.2	2.2	2.6	1.6	3.6	2.0	2.1	1.1	4.9	3.1
F_{60}, dynes cm.$^{-2}$ × 10^8	2.7	0.9	2.2	1.5	1.7	1.0	2.0	0.5	0.6	0.3	3.2	0.9
$\frac{F_0 - F_{60}}{F_0}$, %	33	70	31	32	35	37	45	75	72	73	34	71
Relaxation time* (sec.) at 20° C.	17		10		15		20				25	
Transition temperature, ° C.	~60		>80		>80		~20		<20		~60	

* The time for the stress to drop by a value of 1/2 ($F_0 - F_{60}$).

tures, independent of the particular modification, and the large difference between the value of $(F_0 - F_{60})/F_0$ above and below is significant and will be discussed in the next section.

Discussion

The bottom line in Table I lists the approximate transition temperatures as reported in a previous paper [2], and it is immediately clear from the values of $(F_0 - F_{60})/F_0$ and Figures 2 and 3 that two distinct types of relaxation behavior occur depending on whether the transition temperature has been exceeded or not. Below the transition temperature the stress decays by about 33% of its initial value, while above it decays by about 73%.[1] Further, as the figures show, the relaxation curve shape is independent of chemical treatment below the transition temperature. Only the initial stress has been altered, and only in the case of mercuric acetate treated fiber has it become greater than that of the unmodified fiber. All these results agree with the contention [2] that the transition temperature should not be exceeded if the α x-ray pattern is to be recovered upon unloading a stretched fiber. A fiber would be expected to show an increase in stress–relaxation due to the breaking down of the organized material, if structurally altered upon stretching to the extent that its original organization is not recoverable. Thus it might be suggested that the two kinds of stress–relaxation reported above (decay of 33% or 73%) are associated with reversible and nonreversible structural transformations in wool. This notion is supported by the nature of the stress–relaxation curves. In all cases where fibers are below their transition temperature, the stress–relaxation vs. log time curves are linear, suggesting that the process of relaxation is the same, independent of chemical modification; i.e., the basic molecular structure is unaltered. The only differences are the rate at which the initial rapid relaxation occurs and the slope of the stress vs. log time in the case of mercuric acetate treatment; these could be due to viscous effects caused by the alteration of side chain structure during chemical modification.

Some treatments, e.g., thioglycollic acid and ultraviolet irradiation, are able to alter the transition temperature, perhaps by breaking certain cross-linkages or groups of linkages, thus reducing the stability of native material and allowing it to break down more easily under load. Van Slyke's reagent and iodination are on the other hand able to stabilize the structure, giving the reverse effect. The behavior of the mercury treated fibers is interesting, as definite cross-linking is claimed [5], which the increase in F_0 above normal supports. However the increase in relaxation time to 25 sec. indicates that the large F_0 could be due to viscous effects and that if the fiber were extended sufficiently slowly, F_0 would not appear abnormal. In addition the transition temperature is the same as for normal wool, whereas if definite cross-linking had occurred we might expect the transition temperature to increase. Whatever has happened due to this treatment, heating to 80° C. in water returns the fiber to a normal condition, as can be seen by comparing the data in Table I for normal and mercury treated wool. F_0, F_{60}, and $(F_0 - F_{60})/F_0$ are identical at 80° C. If cross-links had been formed they are entirely ruptured by the hot water and the fiber behaves normally. It should be remembered that the behavior described in this paper occurs

[1] Actually Table I shows a decay of 45% at 20° C. for ultraviolet treated fibers, showing that transformation has already begun at this temperature.

only for wool in water. Wool may be heated to greater than 100° C. in the dry state with no adverse effects upon stretching.

Summarizing, we can say that two types of stress–relaxation can occur in stretched wet wool. Below the transition temperature the relaxation process appears to involve the reversible transformation of keratin resulting in a decay of stress of about 33% of the initial value. Above the transition temperature, the native keratin breaks down (transforms) irreversibly, resulting in a decay in stress of about 73%. Certain chemical treatments alter this temperature of transition, but do not greatly affect the stress–relaxation behavior, indicating that the basic molecular structure is unaffected by treatment and that the effects are due to breakage of cross-links which make the basic structure more vulnerable, or in some cases more stable, and to viscous effects due to the alteration of side chain structure.

Literature Cited

1. Feughelman, M., Haly, A. R., and Mitchell, T. W., TEXTILE RESEARCH JOURNAL **28**, 655 (1958).
2. Feughelman, M., Haly, A. R., and Rigby, B. J., TEXTILE RESEARCH JOURNAL **29**, 311 (1959).
3. Feughelman, M. and Mitchell, T. W., TEXTILE RESEARCH JOURNAL **29**, 404 (1959).
4. Menkart, J. and Speakman, J. B., *J. Soc. Dyers Colourists* **63**, 322 (1947).
5. Mitchell, T. W. and Feughelman, M., TEXTILE RESEARCH JOURNAL **28**, 453 (1958).
6. Richards, H. R. and Speakman, J. T., *Proc. Int. Wool Conf. Austr. 1955*, **C**, 308 (1956).
7. Rigby, B. J., *Aust. J. Phys.* **8**, 176 (1955).

Manuscript received May 4, 1959.

Correction

The review of "Handbook of Chemical Microscopy" (Vol. I, 3rd ed., Wiley, 1958) which appeared in the September issue unintentionally omitted the name of the senior author, Emile M. Chamot.

Information for Contributors

Requirements for copy submitted to TEXTILE RESEARCH JOURNAL conform, in general, with those for other scientific publications. This outline is intended to point out several differences in content and style.

Subject Matter

The JOURNAL covers the broad field of textile research with papers on pure science, engineering, and technology; it includes studies relating to chemistry, physics, and physical chemistry.

Types of Papers.—There are five principal classes of contributions suitable for the JOURNAL. *Fundamental research articles* should present new information and data and should represent distinct contributions to science. *Technical papers* may describe development work, engineering advances, and innovations in manufacture and processing. *Laboratory techniques* should include brief descriptions of practical methods developed which may be helpful to workers in other laboratories. In describing new instruments or modifications of existing apparatus, experimental data illustrating the utility of the instrument should be included. *Letters to the Editor* are intended for prompt publication of new discoveries and observations, or for informative comment on papers previously published in the JOURNAL; rarely should they exceed 1,000 words. *Review articles* of an authoritative and critical nature are occasionally published when judged to be of sufficient interest and importance.

Acceptance.—Papers are submitted to qualified persons for review, critical comment, and suggestions. Names of reviewers are not disclosed except with their consent.

Preparation of Manuscripts

Arrangement.—Any logical arrangement of the subject matter is acceptable. The order used by many authors is *Abstract, Introduction, Experimental Procedure, Results, Discussion, Conclusion, Acknowledgment,* and *Literature Cited,* with variations suitable to the particular subject. Subheadings are an aid in following the exposition.

Style.—The JOURNAL's style guides are "Webster's Unabridged Dictionary" and the "Government Printing Office Style Manual," with few exceptions. For situations not covered in these references, consult a recent issue.

Authors' Names and Affiliations.—This information should be given exactly as it is to appear in print. If the author is no longer with the company where the work was done, his new affiliation should be given in a footnote.

Typing.—Manuscripts should be typed, double-spaced; two copies should be submitted. They should be in *final form* and *checked for accuracy* to eliminate changes after the article is set in type.

Abstract.—A brief abstract (about 150 words) should accompany each paper. The abstract serves as an editorial lead and should give a simply worded preview of the paper.

Equations and Formulas.—All equations should be checked carefully by the author to avoid costly alterations which require hand-setting of type. Exponents should be legible and properly positioned. There should be a clear distinction between small and capital letters, between 1 (one) and l (el), and between the letter O and zero. Fairly simple structural formulas can be set in type; complicated ones should be lettered in India ink on a separate sheet of paper, from which a plate will be made. Greek letters should be written clearly; it is helpful to spell out the name of the symbol in the margin (lightly, in pencil) if an unfamiliar one is used. Equations are numbered in parentheses to the right; they are referred to in the text as Equation 2, Equation 11a, etc. (no parentheses).

Description of Experiments.—The apparatus and procedures used should be described in sufficient detail to enable other investigators to repeat the experiments. Data should be included to substantiate conclusions drawn. To show a trend, graphical presentation may be best; to point out small differences, tabulation may be preferred; do not use both forms for the same data unless essential to the exposition.

Illustrations.—Drawings should be made in India ink on white paper or blue tracing cloth. Coordinate paper must be ruled in blue if the lines are not to show in the finished illustration. Clear photographic prints of drawings are also acceptable. The ultimate size of the illustration should be kept in mind when the originals are made; the table below gives a lettering guide for reduction to the usual 3-in. column width. Lettering in all capital letters usually is more legible than caps and lower case.

Size of Original	Height of Letters
4×5	2–3 mm.
8×10	4–5 mm.
10×16	8+ mm.

Letters and figures made by stencils are preferable; they should *never* be typewritten. Captions should not appear on the drawings; they are set in type below the figures and should be submitted together on a separate sheet. Blueprints, Verifax or Thermofax copies, or other reproductions may accompany the carbon copy.

Photographs.—Photographs should be glossy prints, clear, sharp, and as contrasty as possible without loss of detail. Identification of the figures should be made very lightly on the back with a soft pencil, as heavy writing or typing will appear on the printed figure; paper clips should be avoided or used on a part of the photo that will not be reproduced. To avoid cracks and creases, photos should be mailed flat, protected by heavy cardboard.

Tables.—Every table should have a caption above it and be identified with Roman numerals. For arrangement, see tables in current issues of the JOURNAL.

Literature Cited.—Data should be given in the following order: authors' names followed by initials (comma), name of publication (in quotes for a book, underlined for a journal, no punctuation following), volume number (comma), place and publisher for a book, (commas), inclusive page numbers (no punctuation following), and year of publication (in parentheses). If pagination is not consecutive throughout the volume, issue number and complete date of publication should also be given. Abbreviations of journal titles follow those used by *Chemical Abstracts.* Items are arranged alphabetically by author and numbered. Patent references include patent number, date, and assignee.

Galley Proofs–Reprints

Galley proofs are sent to the author for checking before publication. He is responsible for the accuracy of all text and tabular matter as well as numbering of figures, references, etc. It is urgently requested that the author confine his changes to corrections of errors and that he does not insert additions or make alterations, unless such material radically affects the conclusions drawn in the original work. If such alterations are extensive the paper may, at the editor's discretion, be again subject to review, and additional typesetting costs may be chargeable to the author.

A reprint order form is sent with galley proofs; it should be returned with them. Orders received after publication cannot always be filled, as type is destroyed after each issue and no extra reprints are made.

CHEMSTRAND RESEARCH . . .

is writing a new story. A story in the field of Research. Soon Chemstrand Research Center, Inc., will occupy its new facilities, now under construction at the Research Triangle in North Carolina. The Triangle is formed by three well-known cities: Raleigh, Durham and Chapel Hill, North Carolina. With these new facilities, Chemstrand Research Center, Inc., will expand its staff and research activities.

Obviously, the success of future fibers will depend upon their chemical and physical properties. Yet much research will be required in order to relate these characteristics to the composition of polymers, structure of fibers, and behavior of end products.

A new section will be established in the Chemstrand Research Center which will have responsibility for the study of these relationships. Men with all levels of experience and trained in several scientific disciplines will be required in order to properly staff this section. The Section Leader should have a PhD degree or equivalent experience in the physics, physical chemistry or mechanics of fiber forming materials. Experience in research in the area related to fiber characterization is especially important. For group leaders and other research men, less background of training and experience will be needed. Salary for these openings will be commensurate with experience and training.

For further information concerning these openings write to:

Manager-Employment Recruitment, Box R-7
CHEMSTRAND RESEARCH CENTER, INC.
(a wholly owned subsidiary of The Chemstrand Corporation)
DECATUR, ALABAMA